Alexander Knebe, *Universidad Autonoma de Madrid*

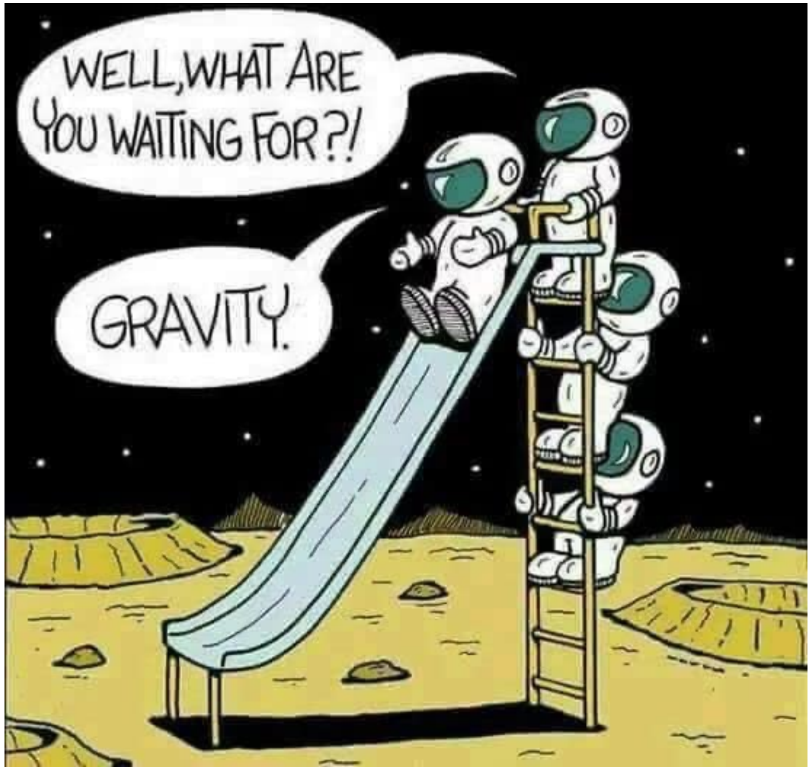

…subtle differences of the same underlying phenomenon!

- **strong lensing**
  - lensing of background sources by foreground galaxies, clusters, …
    (→ strong distortion, magnification, and multiple images)

- **microlensing**
  - mainly referred to as lensing by objects of stellar (point) masses
    (→ no distortion, mainly magnification)

- **weak lensing**
  - lensing via large-scale structure
    (→ weak distortion and magnification)

similar in nature!

- strong lensing
  - lensing of background
    (→ strong distortion,
- microlensing
  - mainly referred to as lensing by objects of stellar (point) masses
    (→ no distortion, mainly magnification)
- weak lensing
  - lensing via large-scale structure
    (→ weak distortion and magnification)

> "Gravitational microlensing can be thought of as a version of strong gravitational lensing where the image separation is too small to be resolved."
> (Wambsganss, *Living Review*)

- strong lensing:
  - macrolensing > 0.1 arcsec
  - millilensing ~ 10^{-3} arcsec
  - microlensing ~ 10^{-6} arcsec
  - nanolensing ~ 10^{-9} arcsec
  - …

- concept
- theory
- applications

- **concept**
- theory
- applications

- images from strong lenses depend on...

  1. lens mass distribution

  2. source location

- images from strong lenses depend on...

1. lens mass distribution
determines type of images

2. source location
determines position of images
(and their number)

α_1

- images from strong lenses depend on...

1. lens mass distribution
determines type of images

2. source location
determines position of images
(and their number)

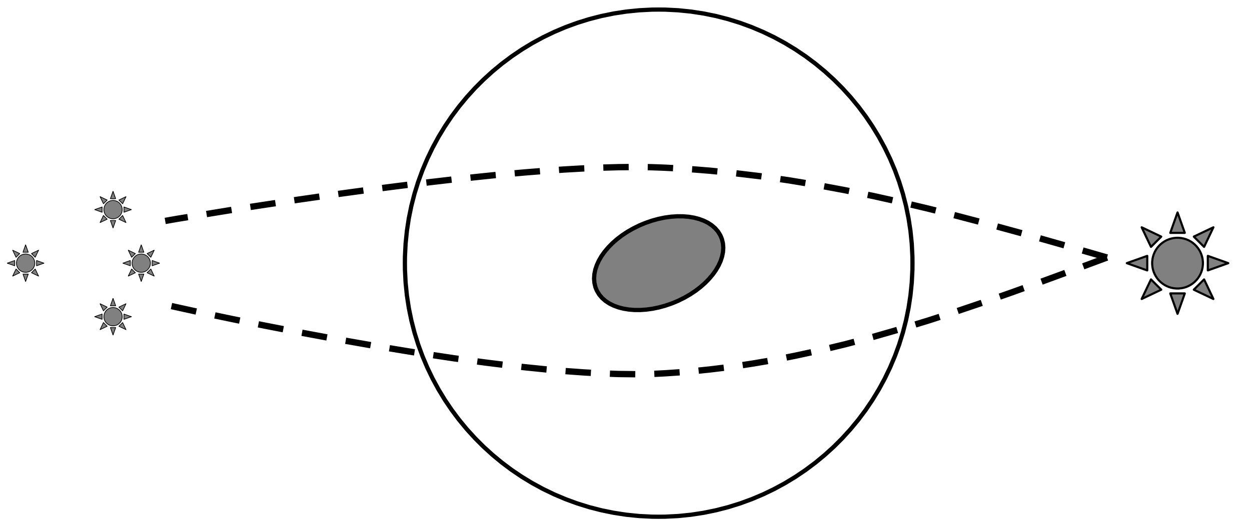

- images from strong lenses depend on...

1. lens mass distribution
determines type of images

2. source location
determines position of images
(and their number)

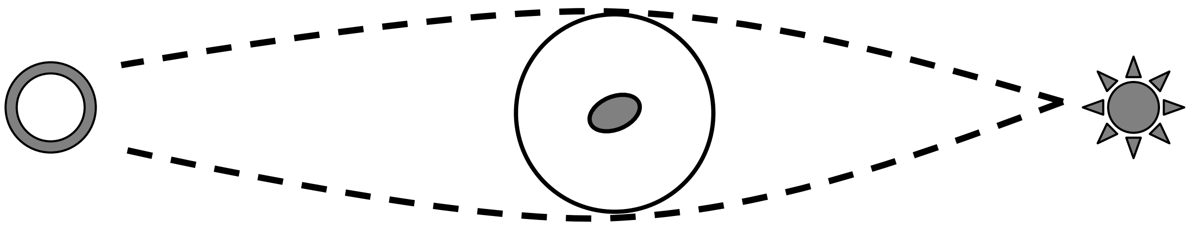

- images from strong lenses

1. lens mass distribution
determines type of images

2. source location
determines position of images
(and their number)

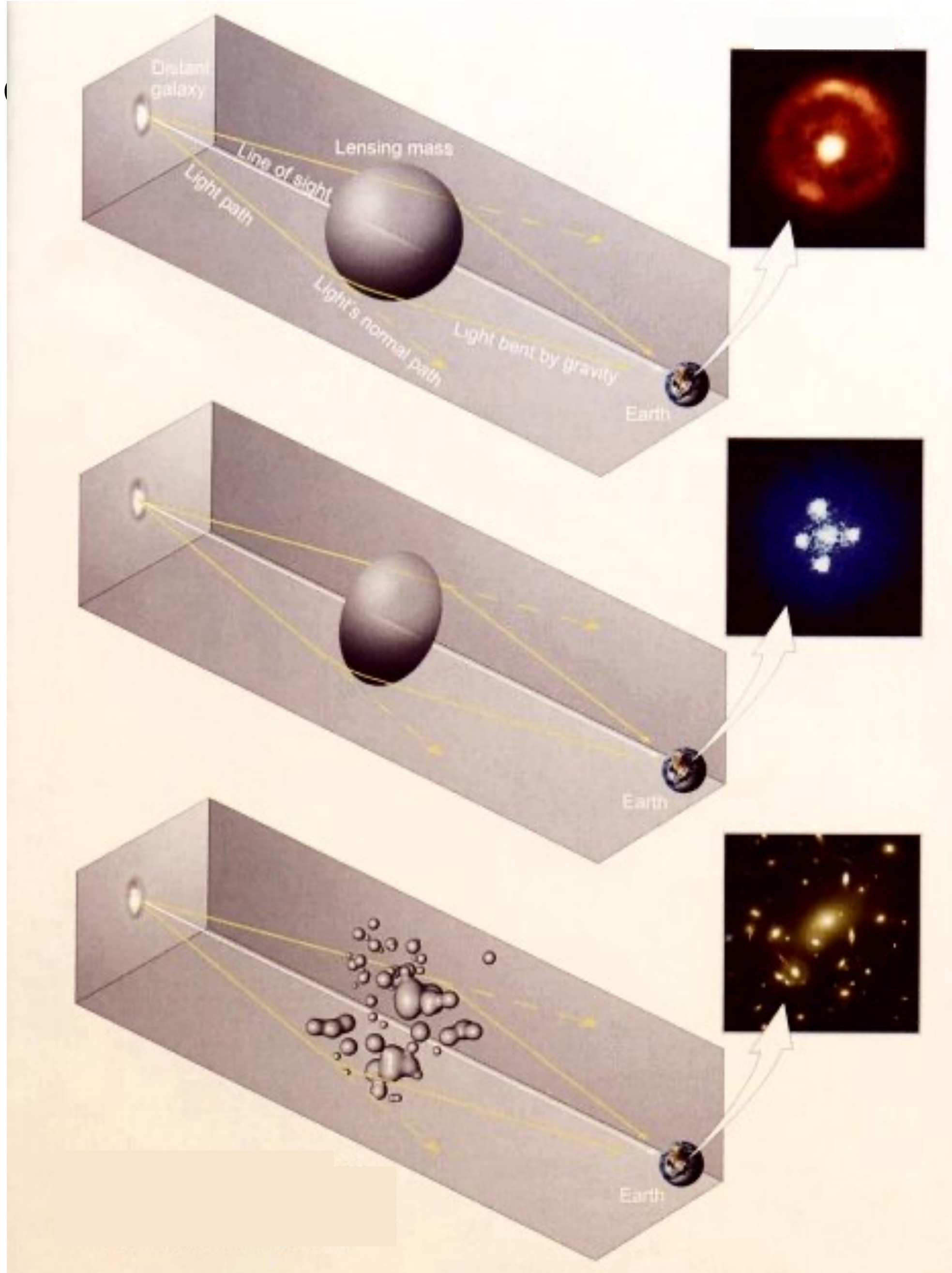

- images from strong lenses depend on...

1. lens mass distribution
determines type of images

2. source location
determines position of images (and their number)

caustics
(source plane)

critical curves
(lens plane)

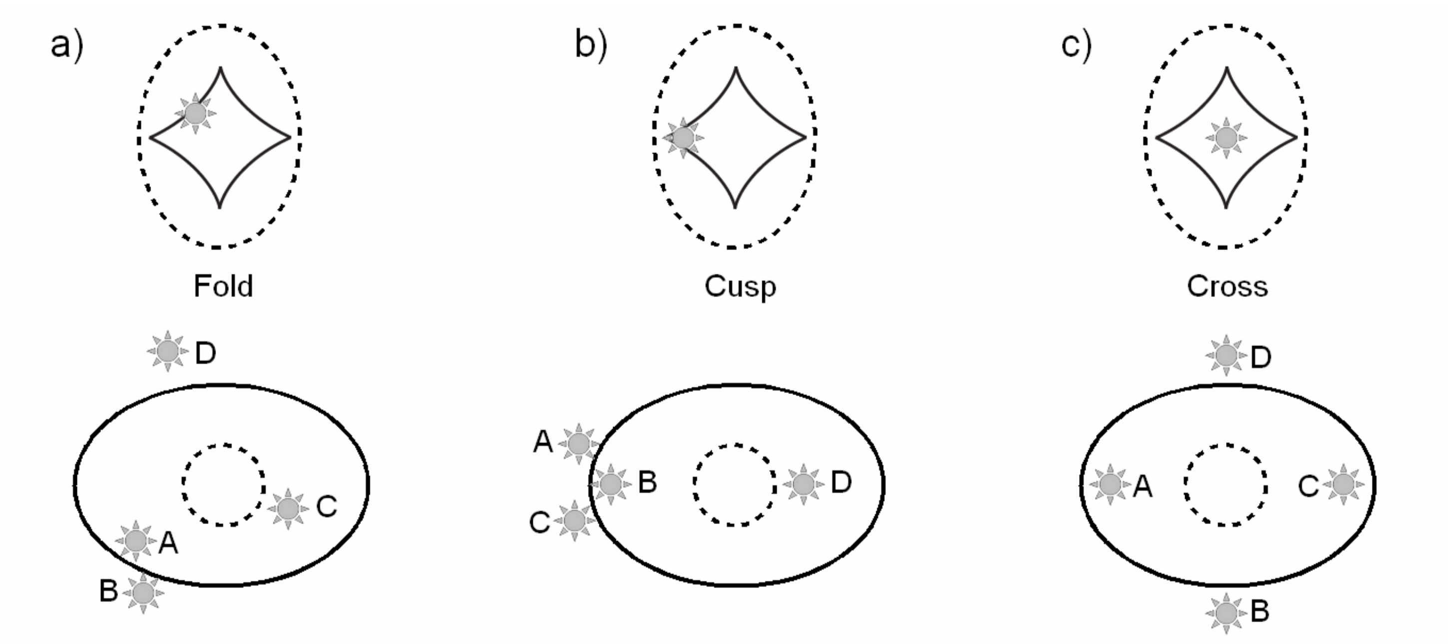

- concept
- **theory***
- applications

skip theory...

*just a repetition of results presented in the lecture "The Basics of Gravitational Lensing"

$\hat{\alpha} << 1$

$|\Phi| << c^2$

$v_{lens} << c$

- in general

  - deflection angle

$$\vec{\alpha}(\vec{\theta}) = \nabla_\theta \varphi(\vec{\theta}) \quad \text{with} \quad \nabla_\theta^2 \varphi(\vec{\theta}) = 2\frac{\Sigma(\vec{\theta})}{\Sigma_{crit}}$$

and $\Sigma_{crit} = \frac{c^2}{4\pi G}\frac{D_S}{D_{LS}D_L}$

$$\Sigma(\theta) = \int \rho(\theta, z)dz$$

  - lens (ray-tracing) equation

$$\vec{\beta}\left(\vec{\theta}\right) = \vec{\theta} - \vec{\alpha}\left(\vec{\theta}\right)$$

$\hat{\alpha} << 1$

$|\Phi| << c^2$

$v_{lens} << c$

- in general

  - deflection angle

$$\vec{\alpha}(\vec{\theta}) = \nabla_\theta \varphi(\vec{\theta}) \quad \text{with} \quad \nabla_\theta^2 \varphi(\vec{\theta}) = 2\frac{\Sigma(\vec{\theta})}{\Sigma_{crit}}$$

and $\Sigma_{crit} = \frac{c^2}{4\pi G} \frac{D_S}{D_{LS} D_L}$

$$\Sigma(\theta) = \int \rho(\theta, z) dz$$

  - lens (ray-tracing) equation

$$\vec{\beta}\left(\vec{\theta}\right) = \vec{\theta} - \vec{\alpha}\left(\vec{\theta}\right)$$

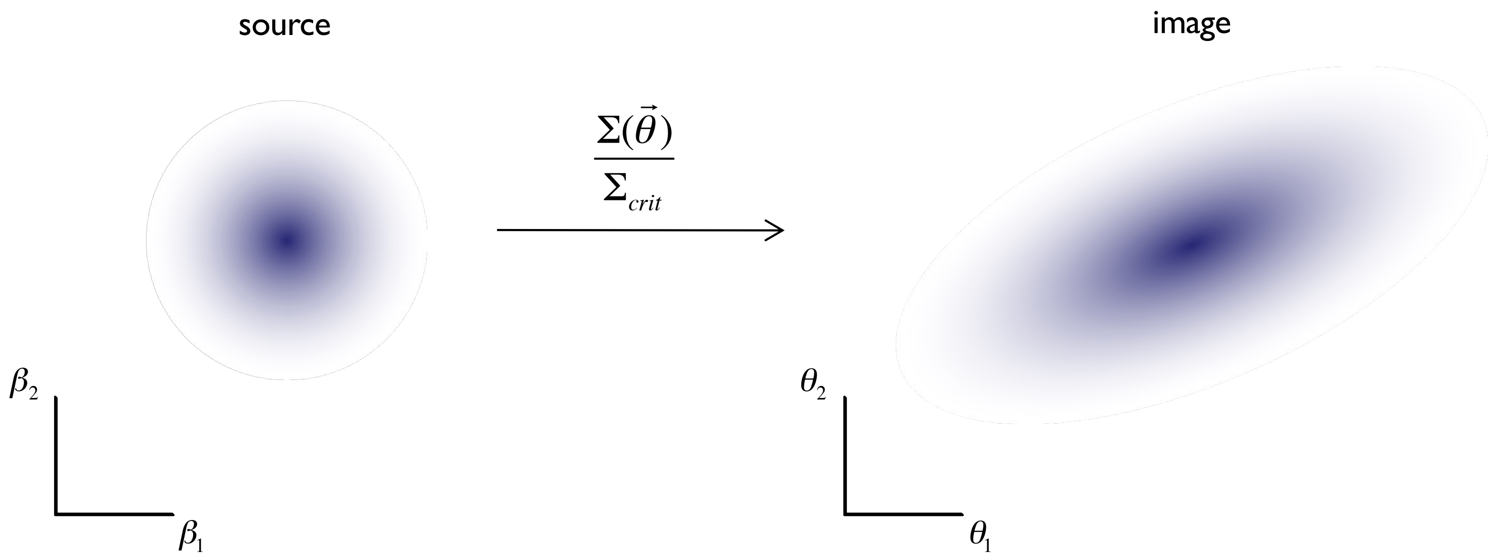

$\hat{\alpha} << 1$

$|\Phi| << c^2$

$v_{lens} << c$

▪ in general

- deflection angle

$$\vec{\alpha}(\vec{\theta}) = \nabla_\theta \varphi(\vec{\theta}) \quad \text{with} \quad \nabla_\theta^2 \varphi(\vec{\theta}) = 2\frac{\Sigma(\vec{\theta})}{\Sigma_{crit}}$$

and $\Sigma_{crit} = \frac{c^2}{4\pi G}\frac{D_S}{D_{LS}D_L}$

$$\Sigma(\theta) = \int \rho(\theta, z)dz$$

- lens (ray-tracing) equation

$$\vec{\beta}\left(\vec{\theta}\right) = \vec{\theta} - \vec{\alpha}\left(\vec{\theta}\right)$$

- magnification

$$\mu = \left|\det\left(\frac{\partial\vec{\beta}}{\partial\vec{\theta}}\right)\right|^{-1}$$

- distortion

$$A_{ij} = (1-\kappa)\begin{pmatrix} 1 & 0 \\ 0 & 1 \end{pmatrix} - \gamma\begin{pmatrix} \cos 2\varphi & \sin 2\varphi \\ \sin 2\varphi & -\cos 2\varphi \end{pmatrix}$$

▪ lensing by point masses

- deflection angle

$$\alpha = \frac{D_{LS}}{D_S D_L} \frac{4GM}{c^2 \theta}$$

- lens (ray-tracing) equation

$$\theta_{\pm} = \frac{1}{2}\left(\beta \pm \sqrt{\beta^2 + 4\theta_E^2}\right)$$

$$\theta_E = \sqrt{\frac{D_{LS}}{D_S D_L} \frac{4GM}{c^2}}$$

θ_E: Einstein radius

- magnification

$$\mu = |\mu_+| + |\mu_-| = \frac{u^2 + 2}{u\sqrt{u^2 + 4}}$$

$$u = \frac{\beta}{\theta_E}$$

▪ lensing by point masses

- deflection angle

$$\alpha = \frac{D_{LS}}{D_S D_L} \frac{4GM}{c^2 \theta}$$

- lens (ray-tracing) equation

$$\begin{pmatrix} \theta_{1,\pm} \\ \theta_{2,\pm} \end{pmatrix} = \frac{1}{2}\left(\beta \pm \sqrt{\beta^2 + 4\theta_E^2}\right) \begin{pmatrix} \frac{\beta_1}{\beta} \\ \frac{\beta_2}{\beta} \end{pmatrix}$$

(θ_E: *Einstein radius*)

$$\theta_E = \sqrt{\frac{D_{LS}}{D_S D_L} \frac{4GM}{c^2}}$$

$$\beta = \sqrt{\beta_1^2 + \beta_2^2}$$

- magnification

$$\mu = |\mu_+| + |\mu_-| = \frac{u^2 + 2}{u\sqrt{u^2 + 4}}$$

$$u = \frac{\beta}{\theta_E}$$

▪ lensing by extended masses

- surface mass density:

$$\Sigma\left(\vec{\xi}\right) = \int \rho\left(\vec{\xi}, z\right) dz$$

$$dM\left(\vec{\xi}\right) = \Sigma\left(\vec{\xi}\right) d^2\xi$$

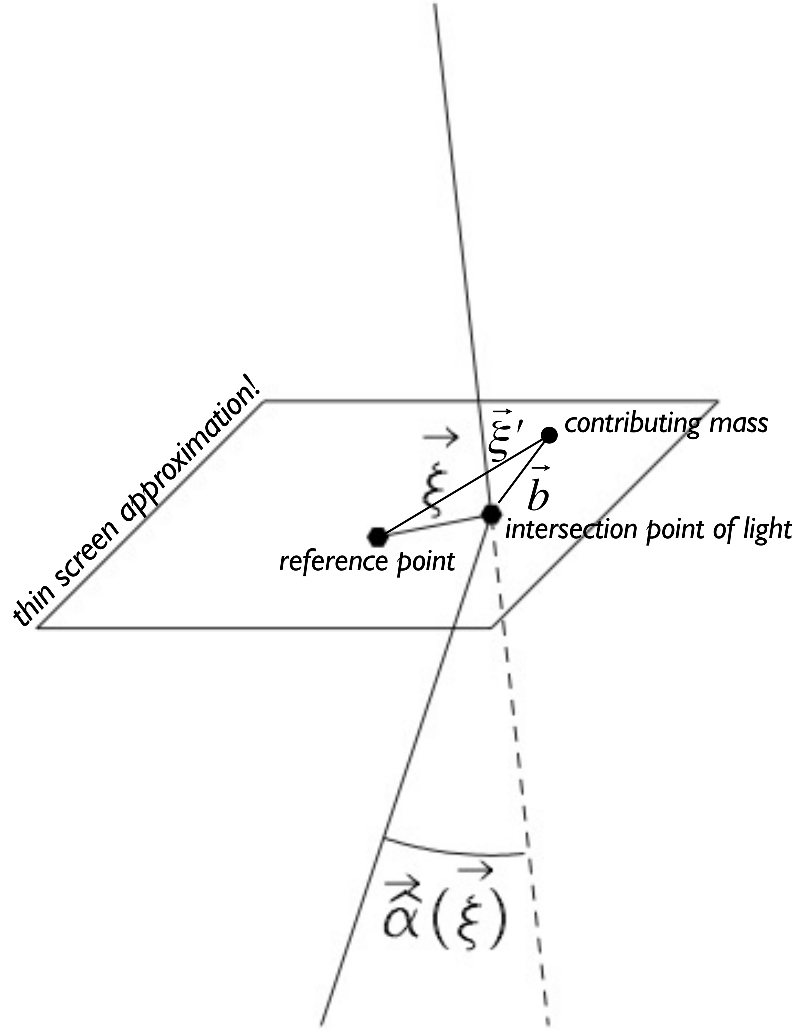

- deflection angles are additive:

$$\vec{\hat{\alpha}}(\vec{\xi}) = \frac{4G}{c^2} \int \frac{\vec{b}}{b^2} dM = \frac{4G}{c^2} \int \frac{\left(\vec{\xi} - \vec{\xi}'\right)}{\left(\vec{\xi} - \vec{\xi}'\right)^2} \Sigma\left(\vec{\xi}'\right) d^2\xi'$$

figure adapted from Narayan & Bartelmann (1995)

▪ lensing by extended masses: *circular lens*

- deflection angle

$$\alpha = \frac{D_{LS}}{D_S}\frac{4GM(<\xi)}{c^2\xi} \quad \text{with} \quad M(<\xi) = 2\pi\int \Sigma(\xi')\xi' d\xi'$$

- lens (ray-tracing) equation

$$\beta(\theta) = \theta - \frac{D_{LS}}{D_S D_L}\frac{4GM(<\theta)}{c^2\theta}$$

- magnification

$$\mu = \frac{\theta}{\beta}\frac{d\theta}{d\beta}$$

▪ lensing by extended masses: *lens with constant surface mass density*

- deflection angle

$$\alpha = \frac{\Sigma}{\Sigma_{crit}} \theta$$

- critical surface mass density

$$\Sigma_{crit} = \frac{c^2}{4\pi G} \frac{D_S}{D_{LS} D_L}$$

- lens with critical surface mass density

$$\Rightarrow \quad \alpha(\theta) = \theta$$

perfectly focusing lens!

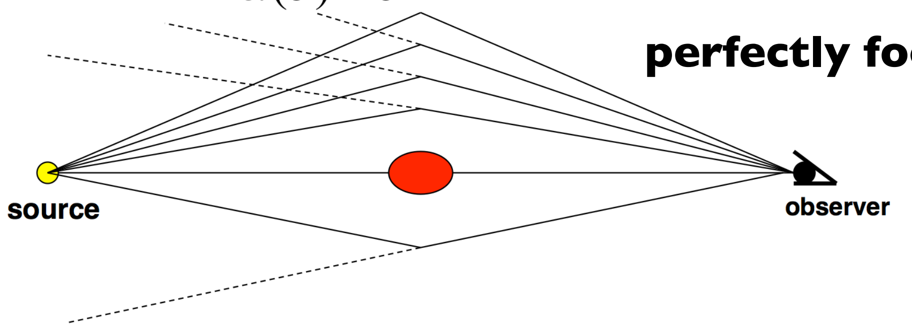

▪ lensing by extended masses:

singular isothermal sphere

$$\rho(r) = \frac{\sigma_v^2}{2\pi G}\frac{1}{r^2}$$

- deflection angle

$$\alpha = \frac{D_{LS}}{D_S}\frac{4\pi\sigma_v^2}{c^2}$$

- lens (ray-tracing) equation

$$\beta(\theta) = \theta - \alpha = \theta \pm \theta_E$$

- magnification

$$\mu = \frac{\theta}{\beta}\frac{d\theta}{d\beta} = \frac{\theta}{\beta} = \frac{\theta}{\theta \pm \theta_E} = \frac{1}{1 \pm \frac{\theta_E}{\theta}}$$

- concept
- theory
- **applications**

- concept
- theory
- **applications:**
    - micro-lensing
    - strong lensing

- concept
- theory
- **applications:**
    - **micro-lensing:**
        - planet detection
        - dark matter detection
    - strong lensing

- concept
- theory
- **applications:**
  - **micro-lensing:**
    - **planet detection**
    - dark matter detection
  - strong lensing

- **microlensing** - planet detection

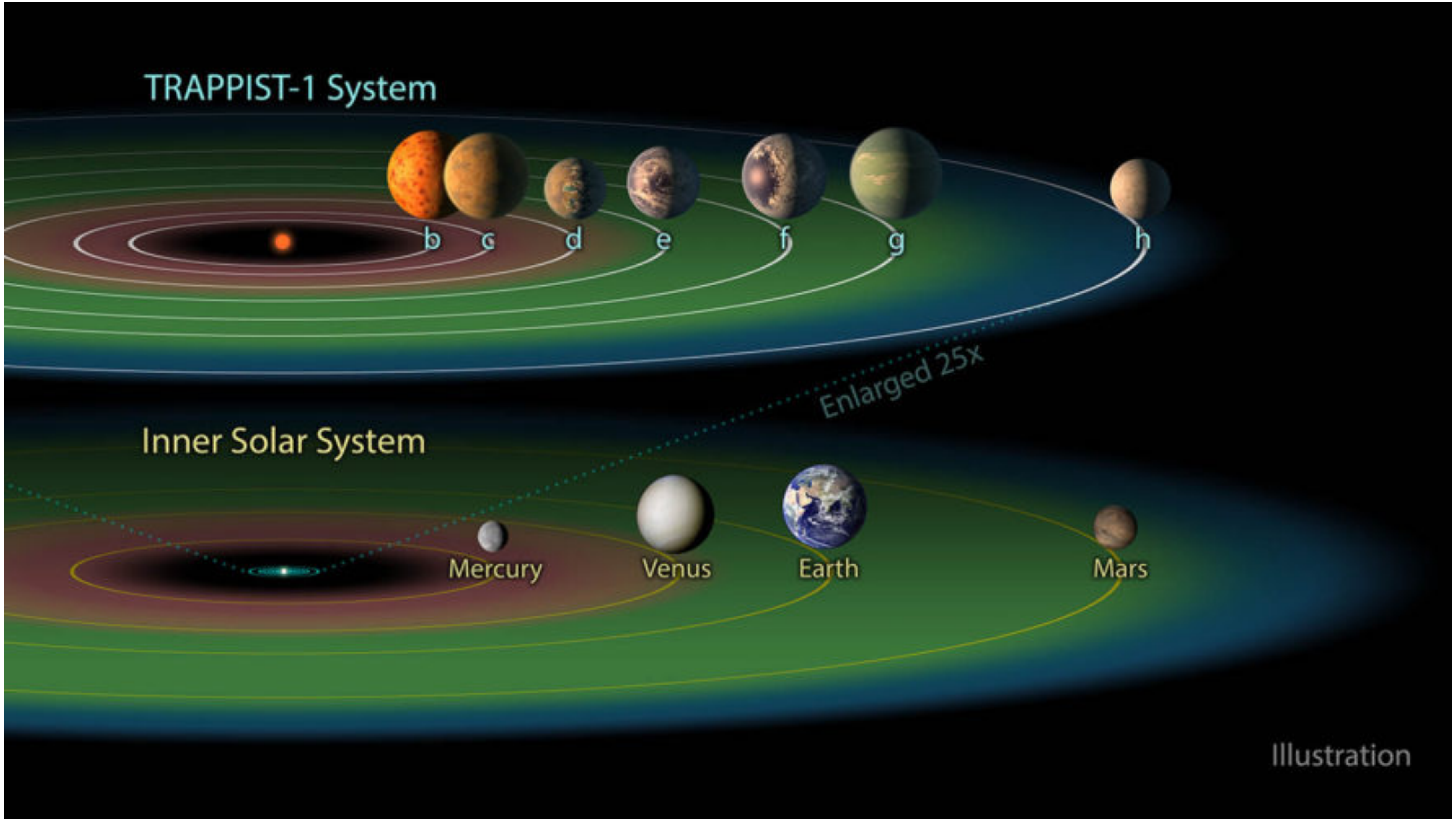

- **microlensing** - planet detection

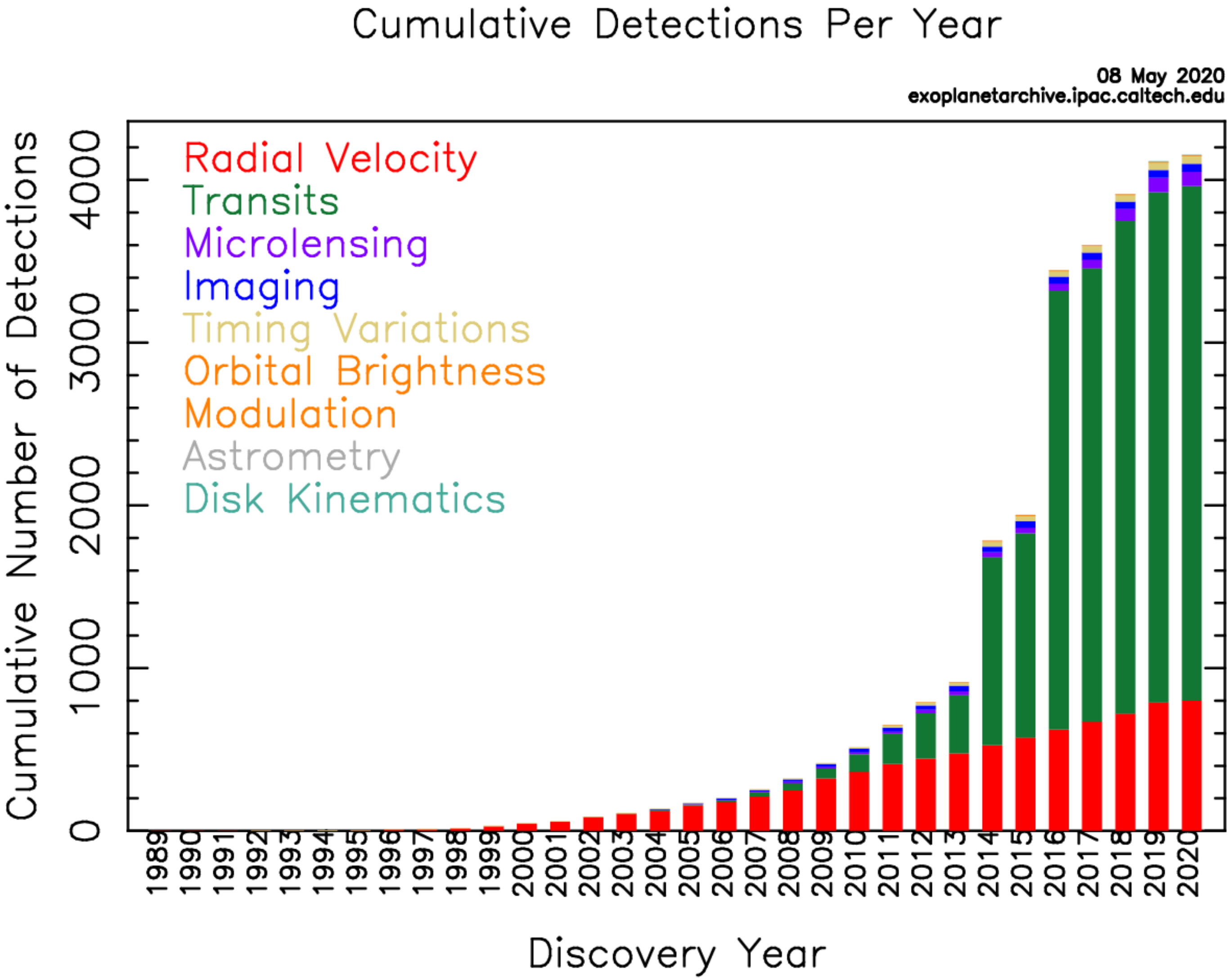

2020: more than 4000 confirmed exoplanets

- **microlensing** - planet detection

double feature in microlensing lightcurve

- **microlensing** - planet detection

double feature in microlensing lightcurve

- **microlensing** - planet detection

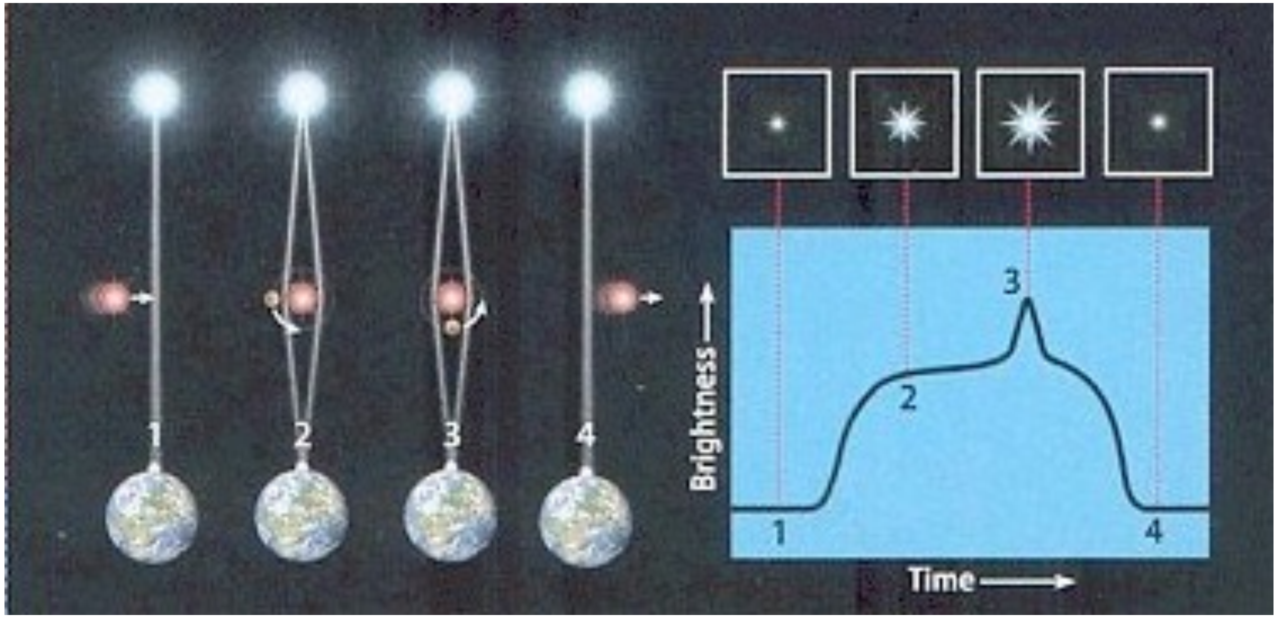

double feature in microlensing lightcurve

- **microlensing** - planet detection

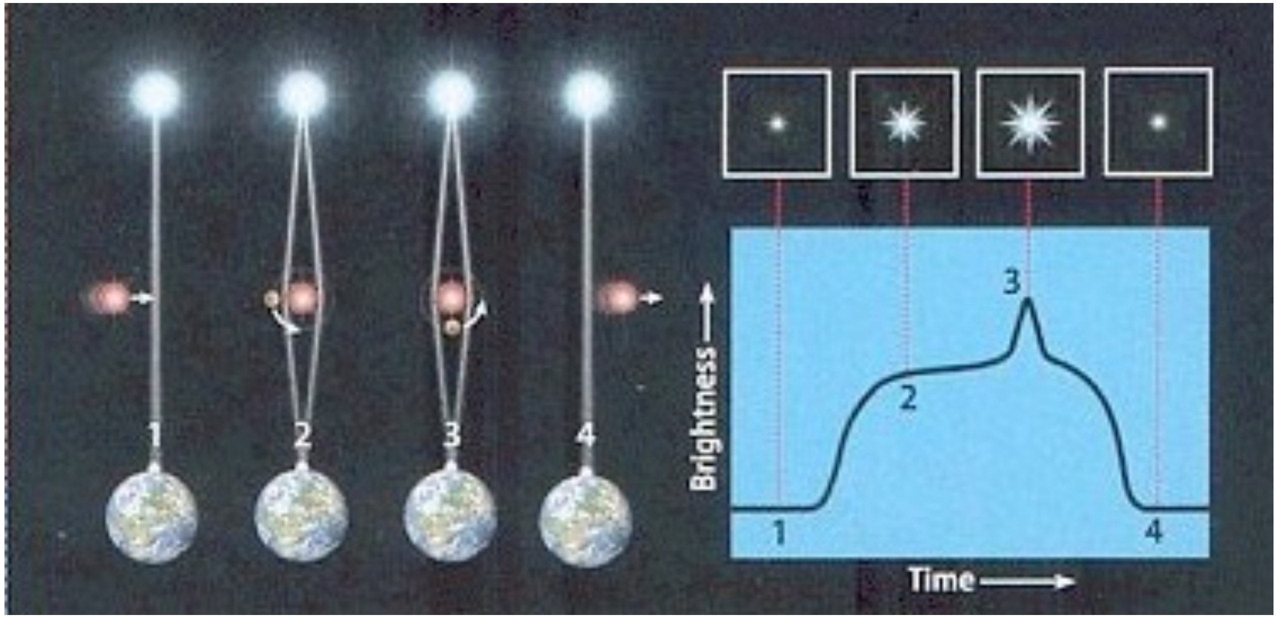

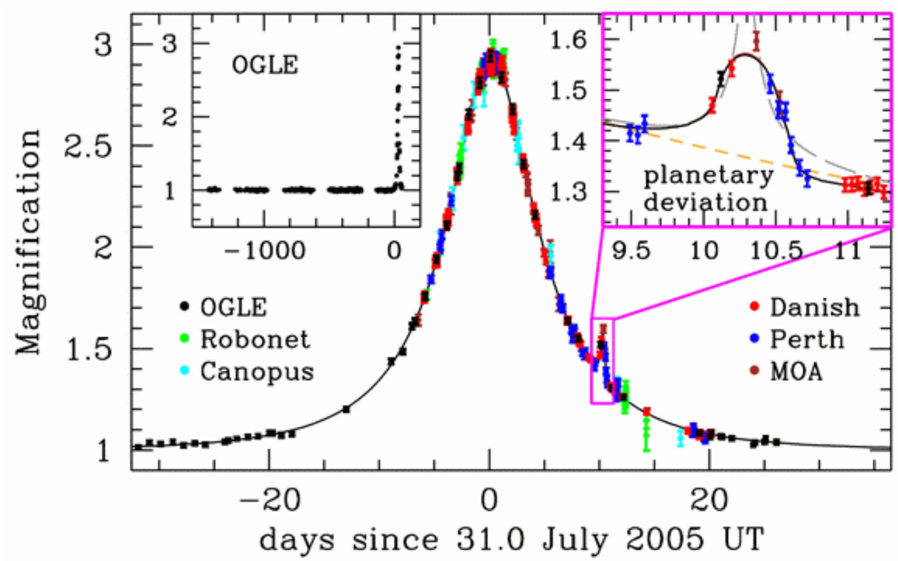

- concept
- theory
- **applications:**
  - **micro-lensing:**
    - planet detection
    - **dark matter detection**
  - strong lensing

- **microlensing** – dark matter detection

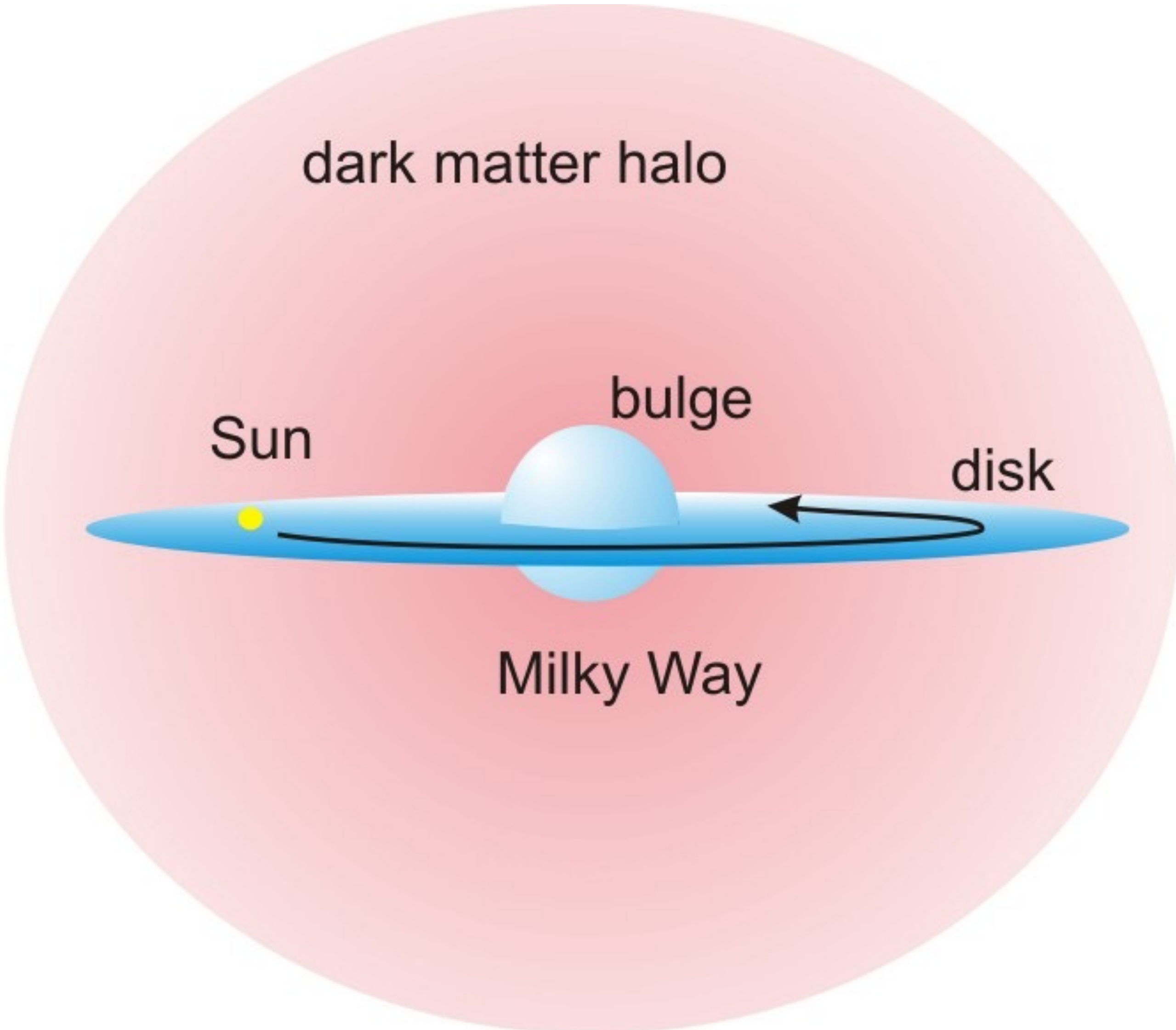

- **microlensing** – dark matter detection

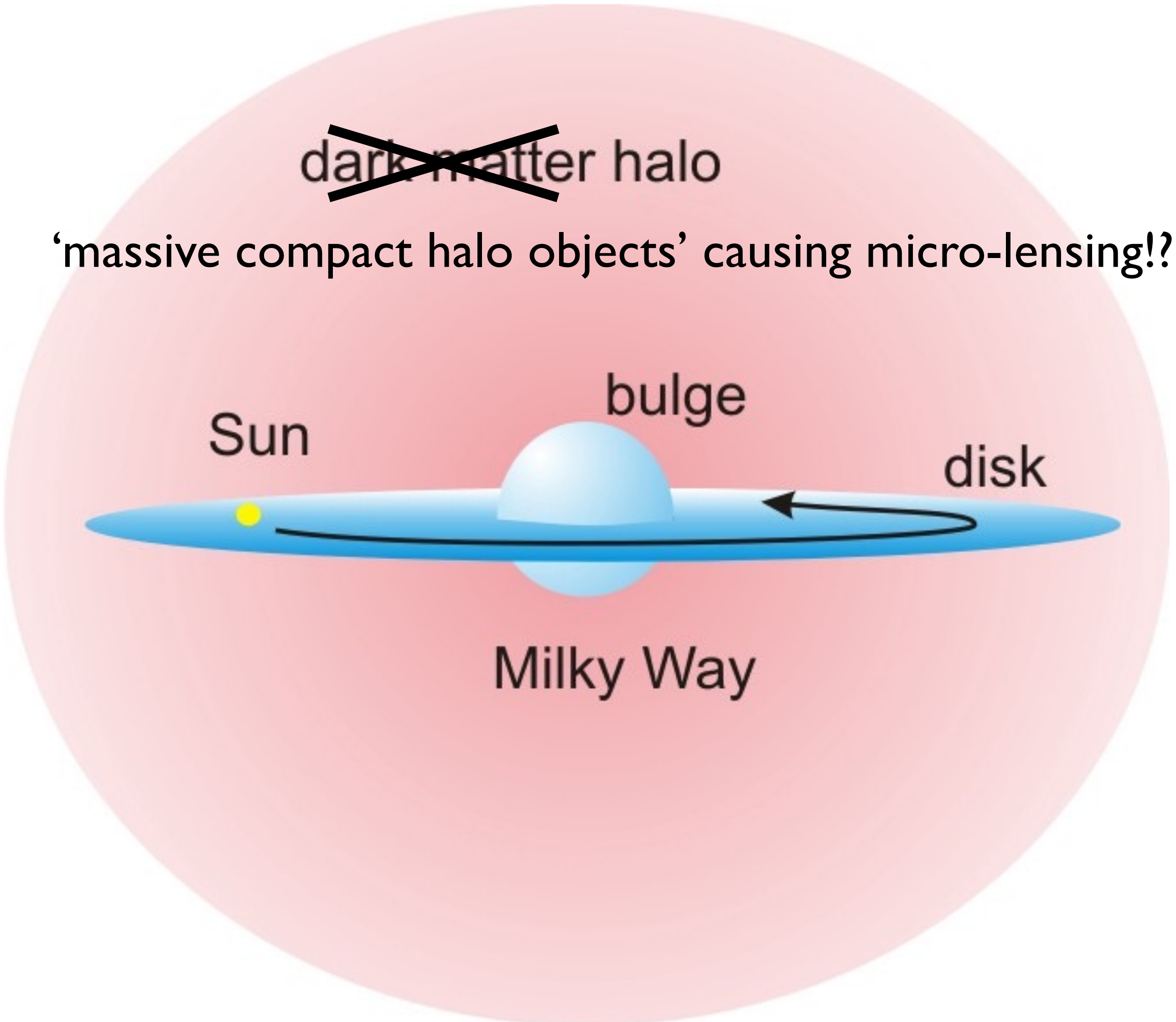

- **microlensing** – dark matter detection

OGLE experiment (Udalski et al. 1992)
(Optical Gravitational Lensing Experiment)

PLANET collaboration (Albrow et al. 1998)
(Probing Lensing Anomalies Network)

MOA collaboration (Muraki et al. 1999)
(Microlensing Observations in Astrophysics)

MACHO collaboration (Alcock et al. 2000)
(Massive Compact Halo Object)

POINT-AGAPE experiment (Kerins et al. 2001)
(Pixel-lensing Observations with the Isaac Newton Telescope - Andromeda Galaxy Amplified Pixels Experiment)

EROS experiment (Afonso et al. 2003)
(Expérience pour la Recherche d'Objets Sombres)

- **microlensing** – dark matter detection

OGLE experiment (Udalski et al. 1992)
(Optical Gravitational Lensing Experiment)

PLANET collaboration (Albrow et al. 1998)
(Probing Lensing Anomalies Network)

MOA collaboration (Muraki et al. 1999)
(Microlensing Observations in Astrophysics)

MACHO collaboration towards LMC (Alcock et al. 2000)
(Massive Compact Halo Object)

POINT-AGAPE experiment towards M31 (Kerins et al. 2001)
(Pixel-lensing Observations with the Isaac Newton Telescope - Andromeda Galaxy Amplified Pixels Experiment)

EROS experiment towards SMC (Afonso et al. 2003)
(Expérience pour la Recherche d'Objets Sombres)

- **microlensing** – MACHO experiment

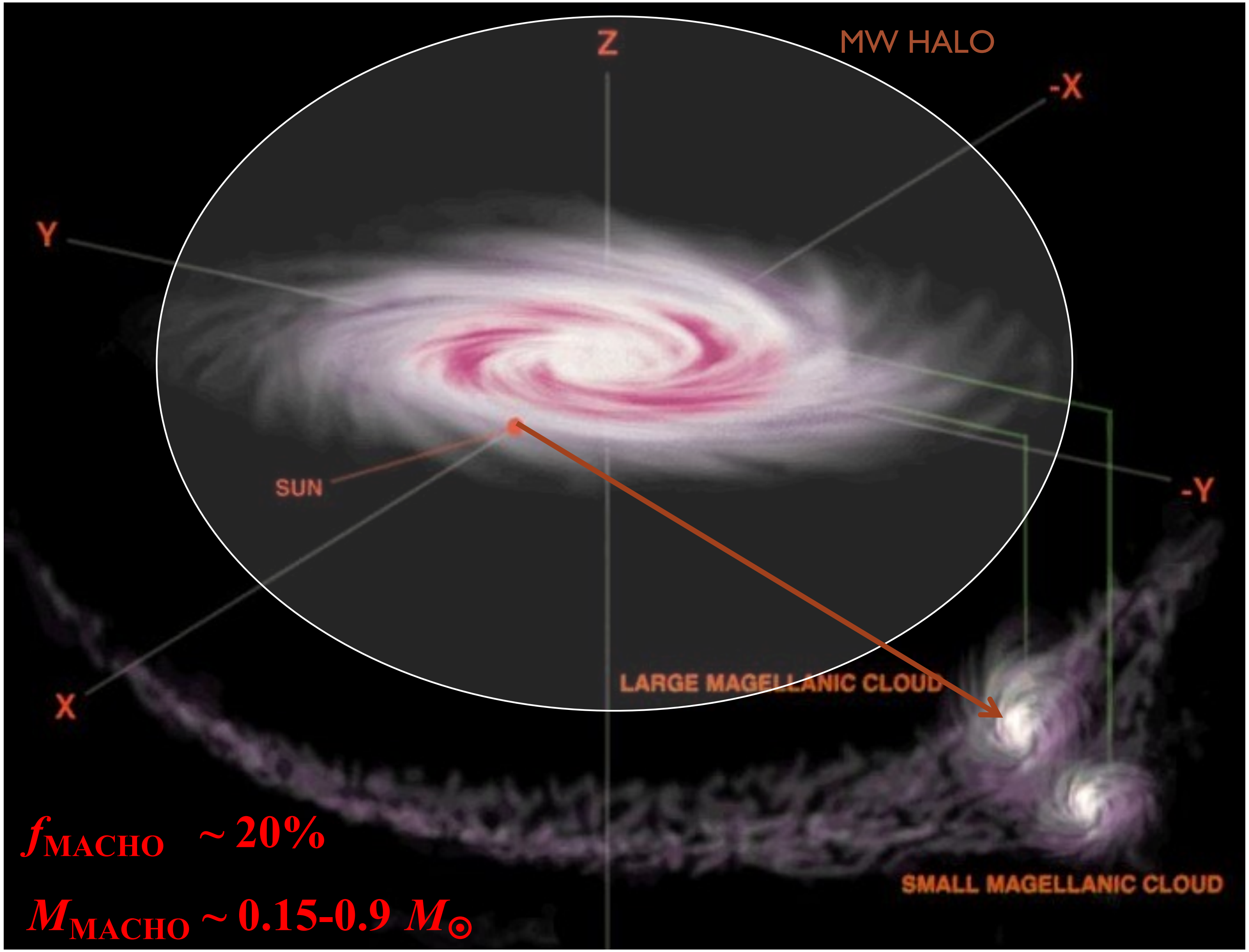

- **microlensing** – EROS experiment

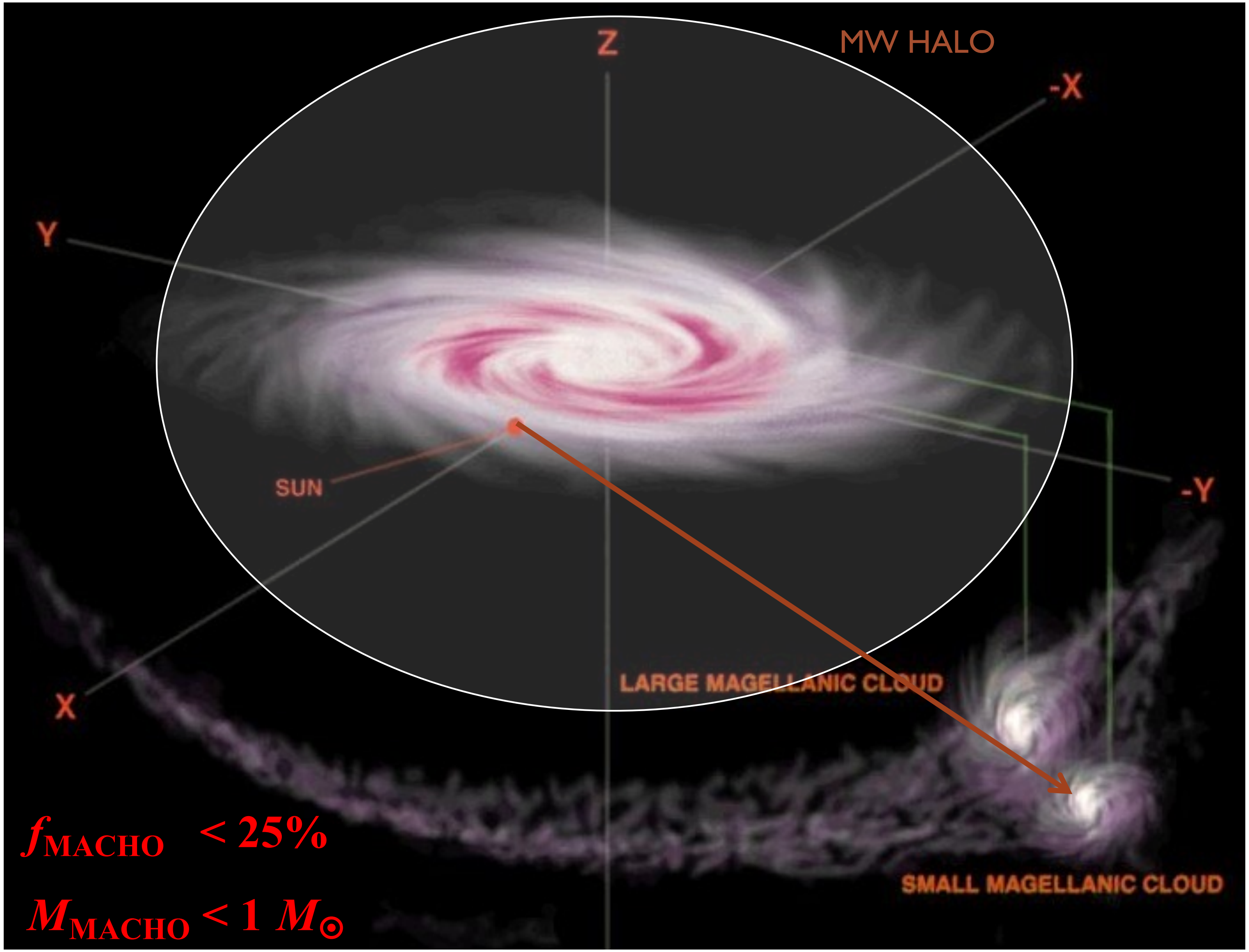

$f_{\rm MACHO} < 25\%$

$M_{\rm MACHO} < 1\ M_\odot$

- **microlensing** – POINT-AGAPE survey

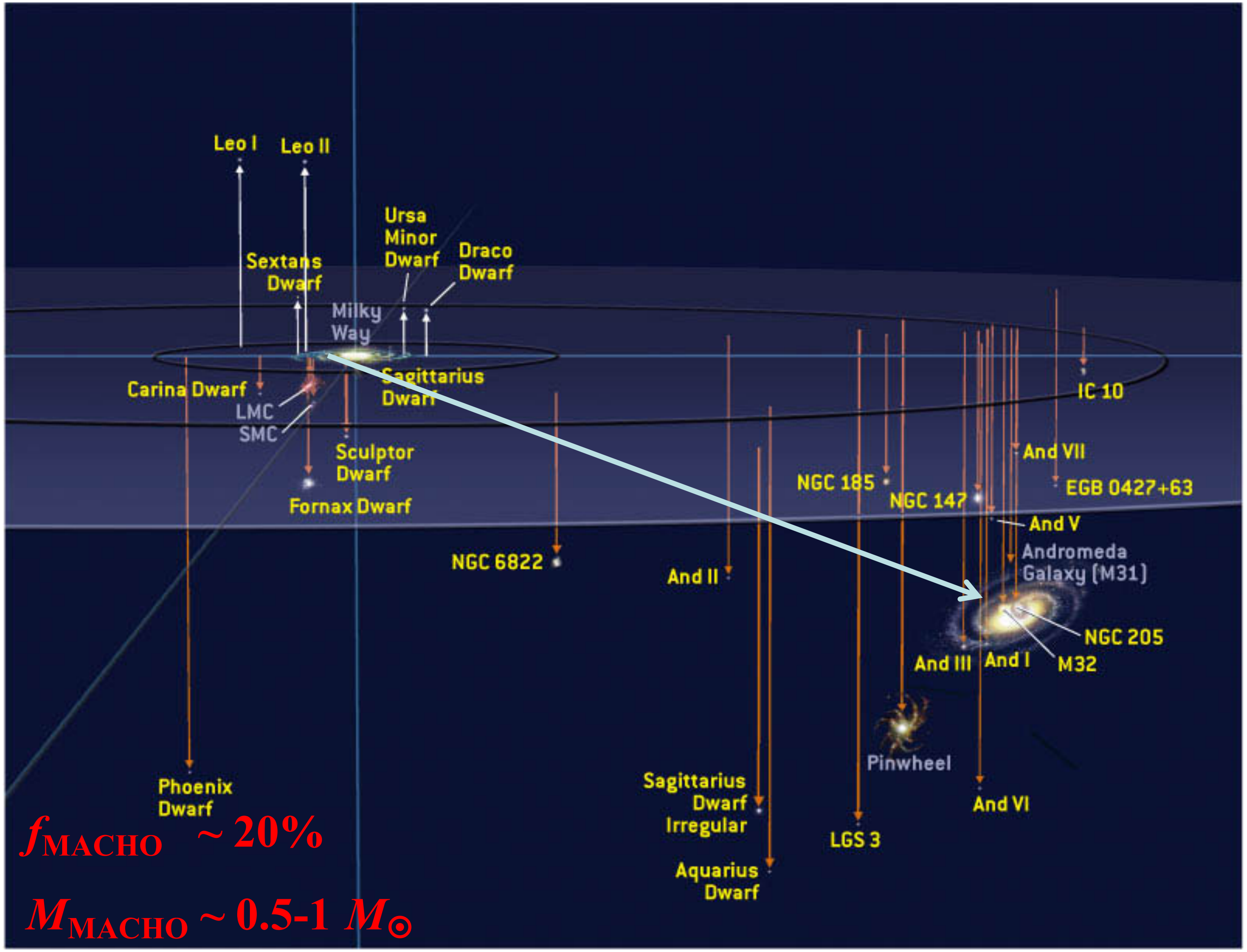

- **microlensing** – results

MACHO	(LMC)	$f_{\text{MACHO}} \sim 16\%$	(Bennett 2005)
POINT-AGAPE	(M31)	$f_{\text{MACHO}} > 20\%$	(Calchi Novati et al. 2005)
EROS-2	(SMC)	$f_{\text{MACHO}} \sim 8\%$	(Tisserand et al. 2007)
OGLE-II	(LMC)	$f_{\text{MACHO}} \sim 8\%$	(Wyrzykowski et al. 2009)

=> consistent with self-lensing!?

=> MACHO's are not the sought after dark matter…

- concept
- theory
- **applications:**
    - micro-lensing
    - **strong lensing**

- **strong lensing**

CASTLES project (Munoz et al. 1999)
(CfA-Arizona Space Telescope Lens Survey)

LSD survey (Koopmans & Treu 2002)
(Lenses, Structures & Dynamics)

CLASS survey (Browne et al. 2003)
(Cosmic Lens All-Sky Survey)

ANGLES network (Browne et al. 2004)
(Astrophysics Network for Galaxy Lensing Studies)

COSMOGRAIL (Eigenbrod et al. 2005)
(Cosmological Monitoring of Gravitational Lenses)

SLACS survey (Bolton et al. 2006)
(Sloan Lens ACS Survey)

OMEGA mission (Moustakas et al. 2008)
(Observatory for Multi-Epoch Gravitational Lens Astrophysics)

Note: this list does not claim to be complete!

- concept
- theory
- **applications:**
  - micro-lensing
  - **strong lensing:**
    - cosmic telescopes
    - H_0 determination
    - missing satellite problem

- concept
- theory
- **applications:**
  - micro-lensing
  - **strong lensing:**
    - **cosmic telescopes**
    - H_0 determination
    - missing satellite problem

- **strong lensing** – cosmic telescopes

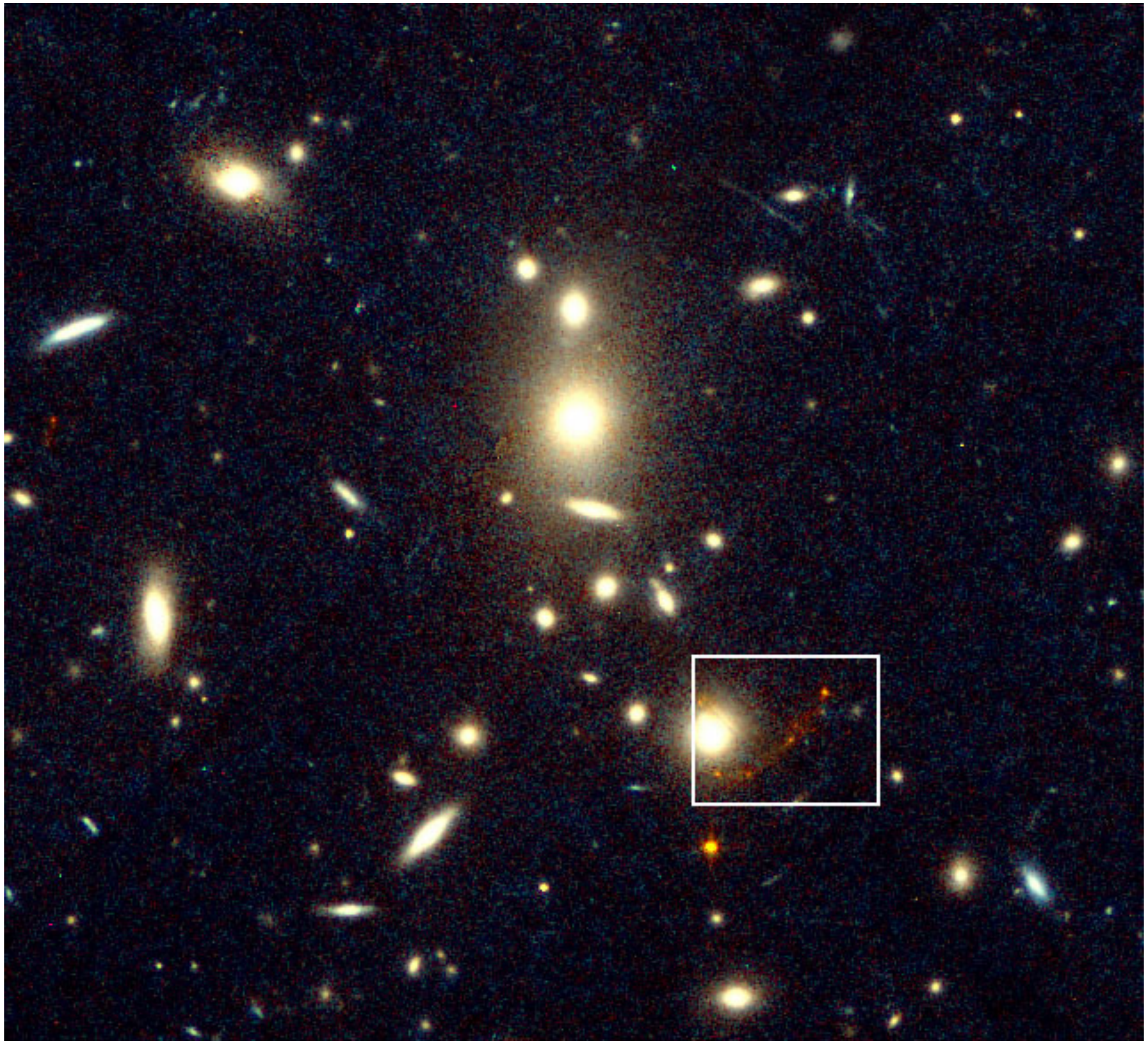

(a galaxy at redshift z=5.34, behind CL1358+62)

- **strong lensing** – cosmic telescopes

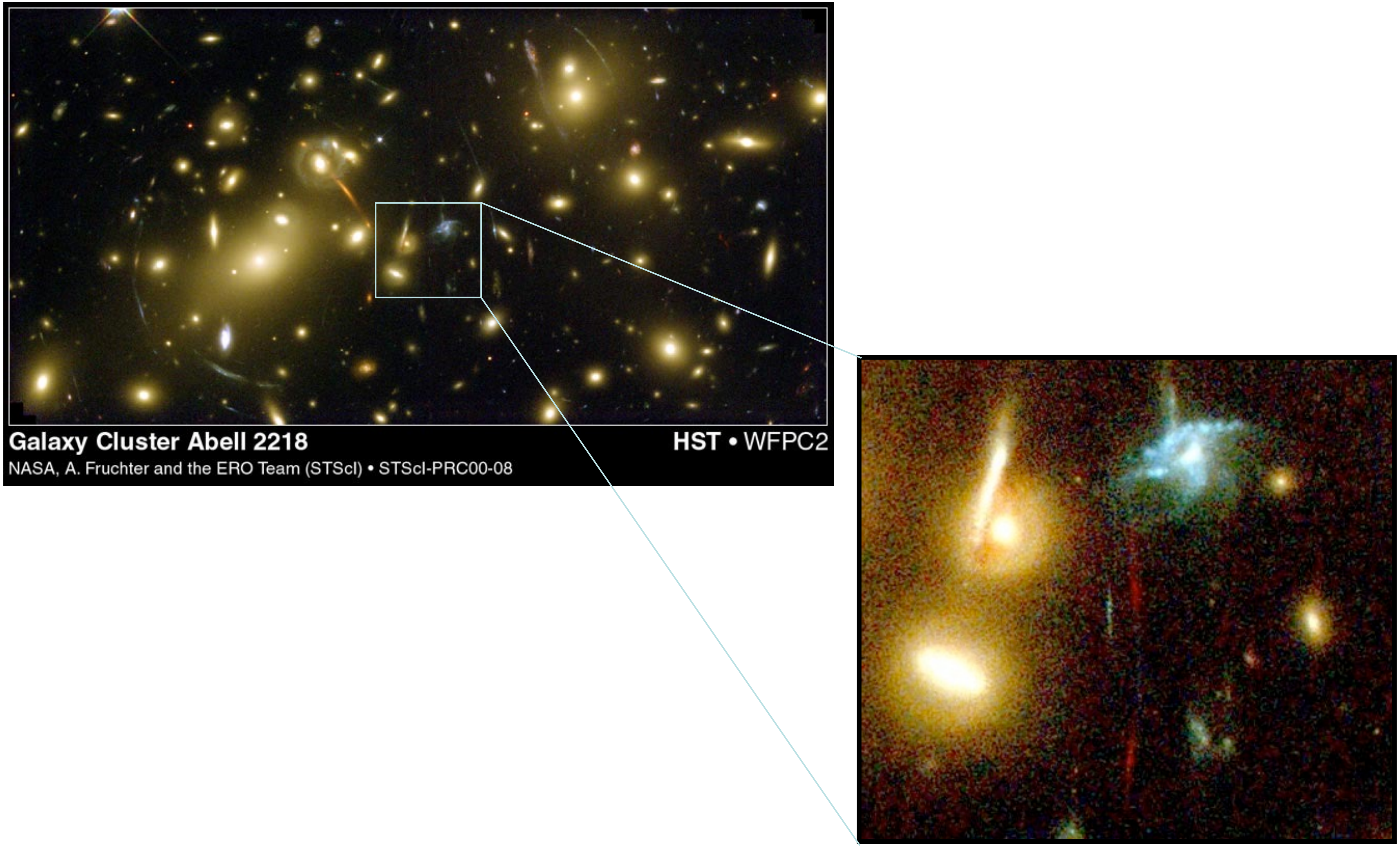

- **strong lensing** – cosmic telescopes

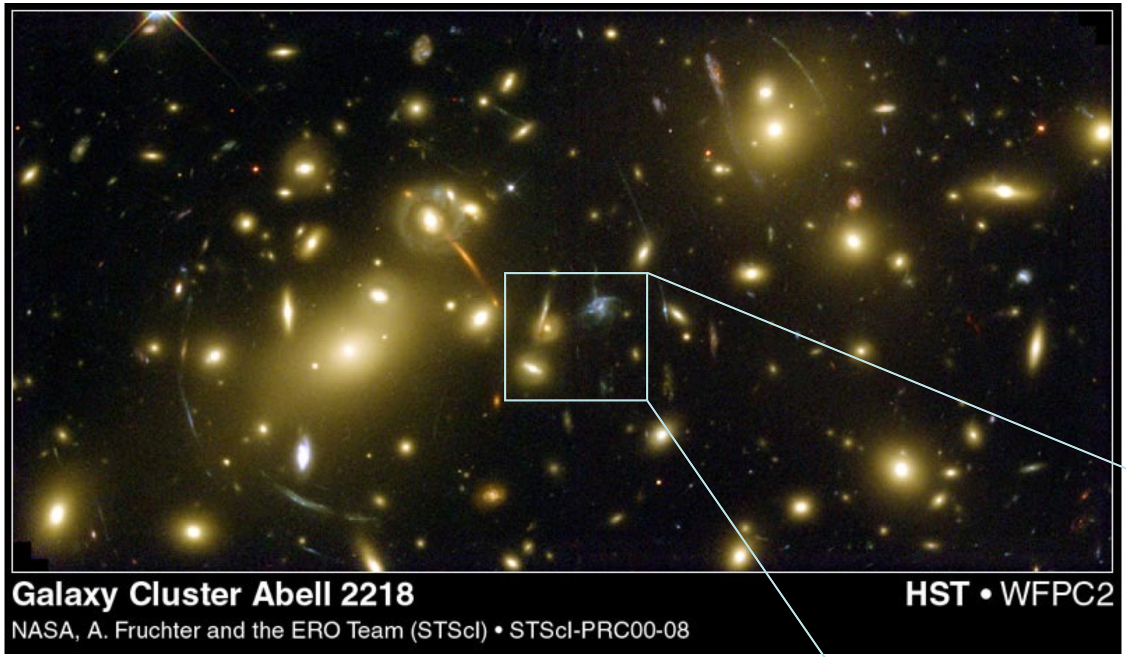

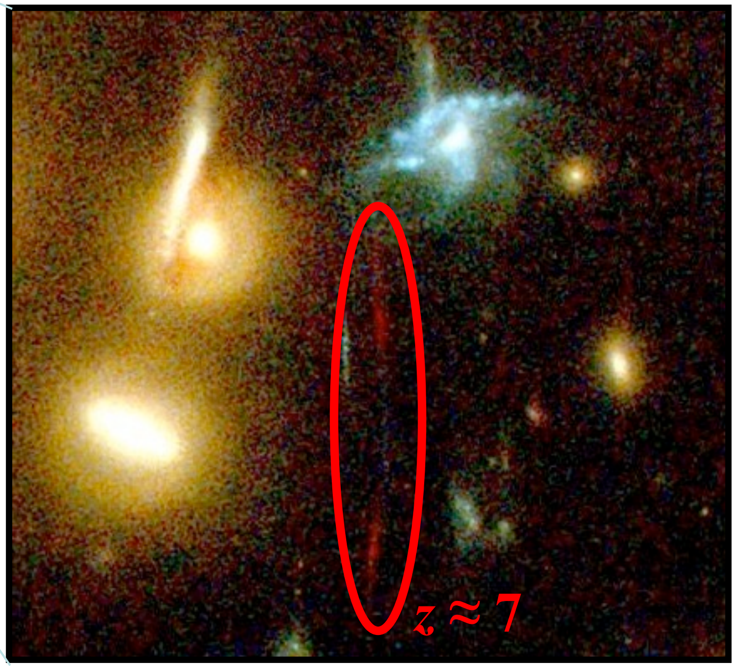

- concept
- theory
- **applications:**
    - micro-lensing
    - **strong lensing:**
        - cosmic telescopes
        - H_0 **determination**
        - missing satellite problem

- **strong lensing** – measuring H_0

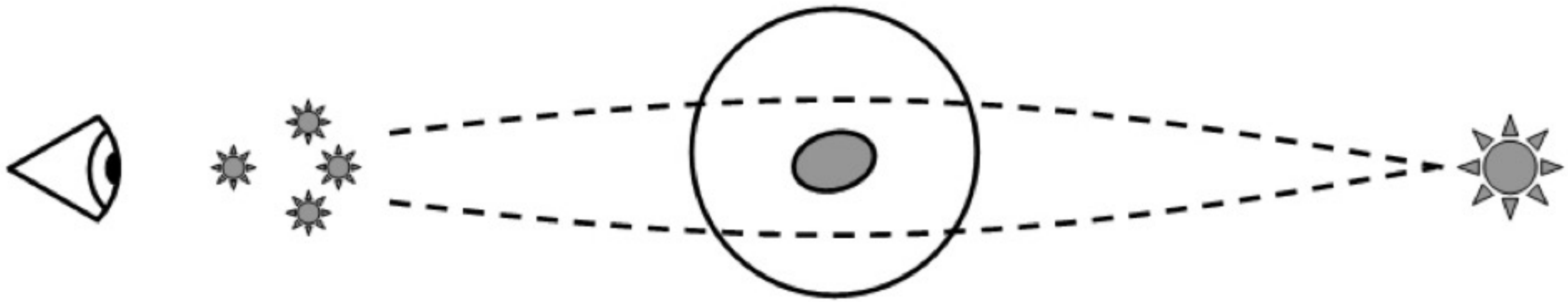

- **strong lensing** – measuring H_0

intrinsic variation of source flux

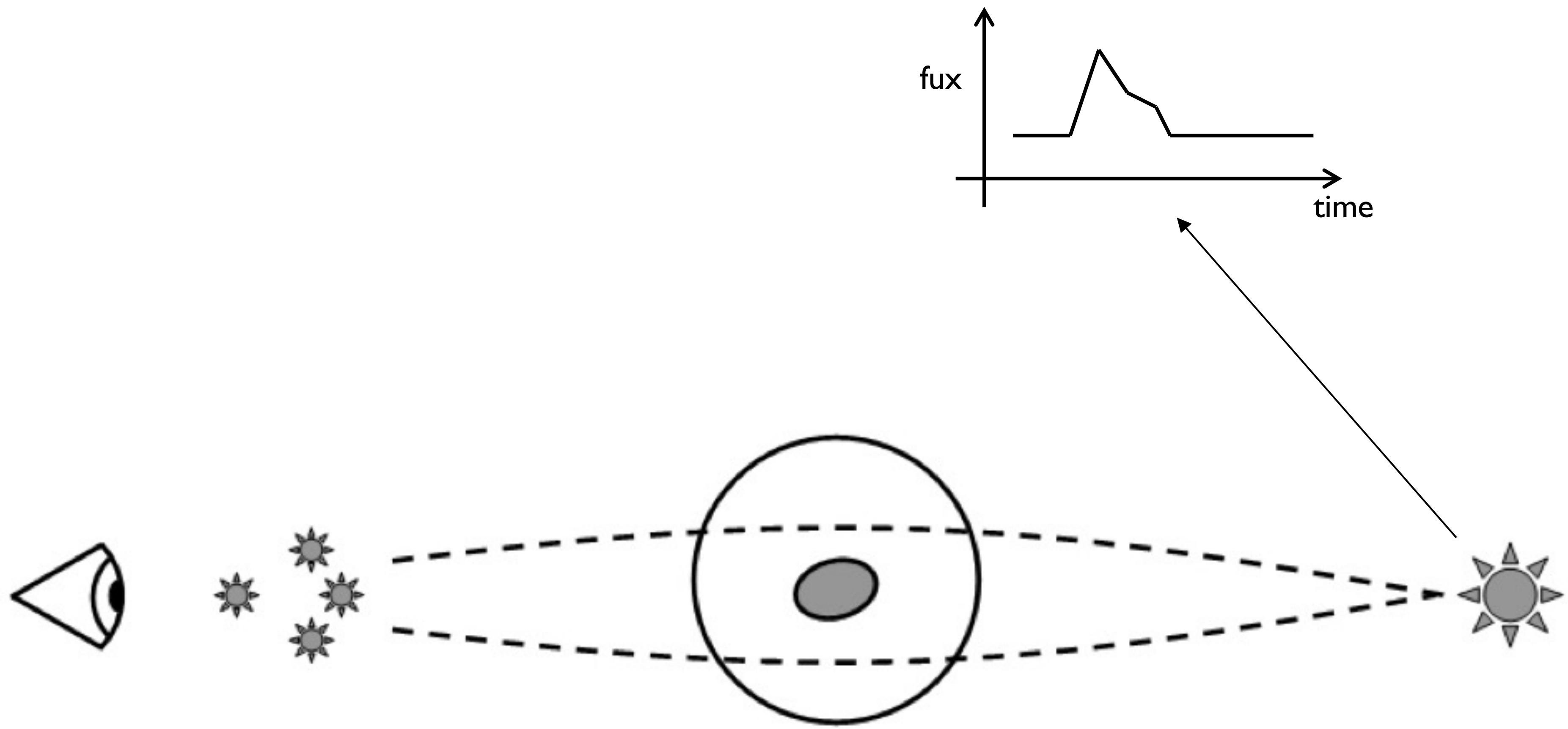

- **strong lensing** – measuring H_0

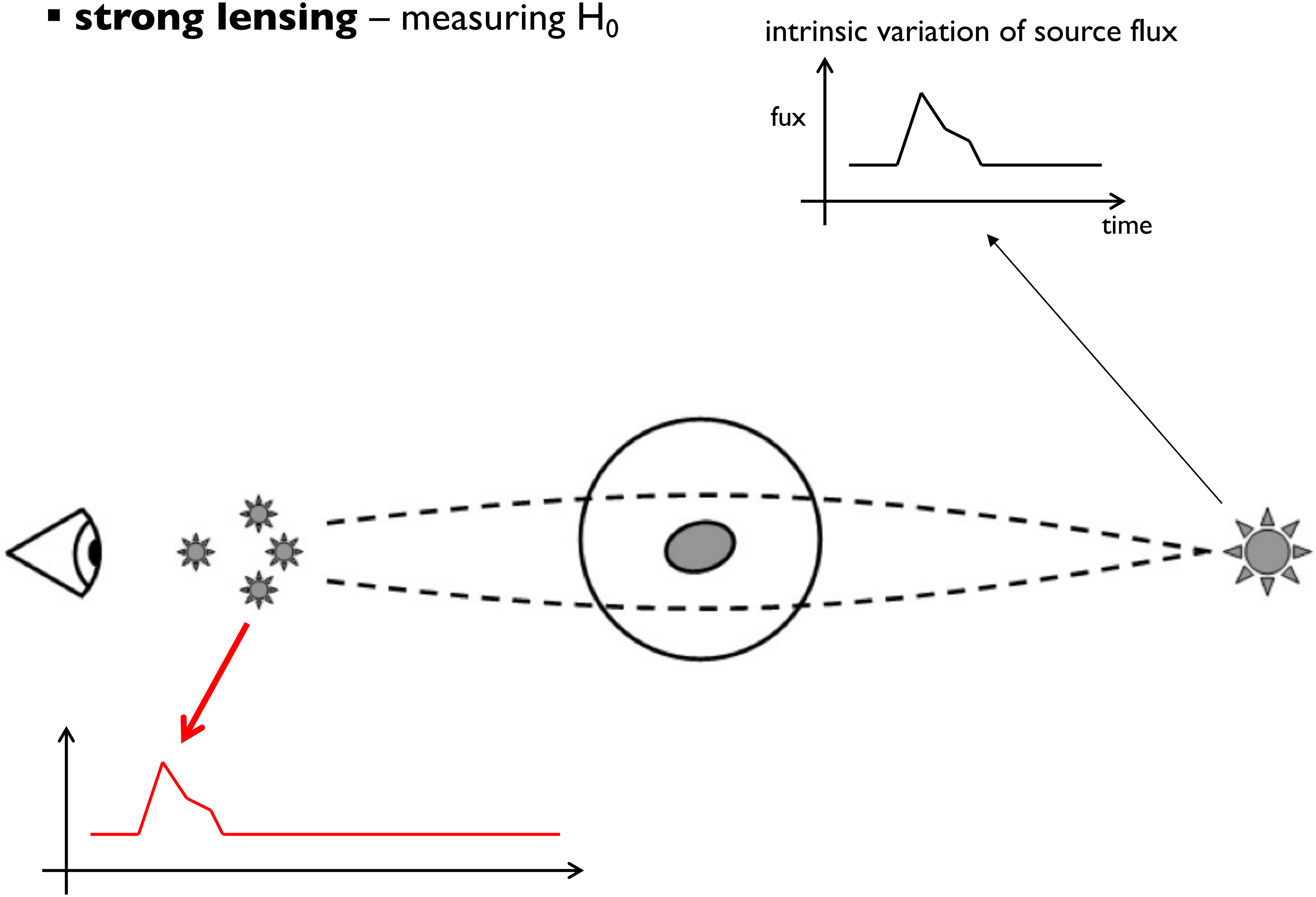

- **strong lensing** – measuring H_0

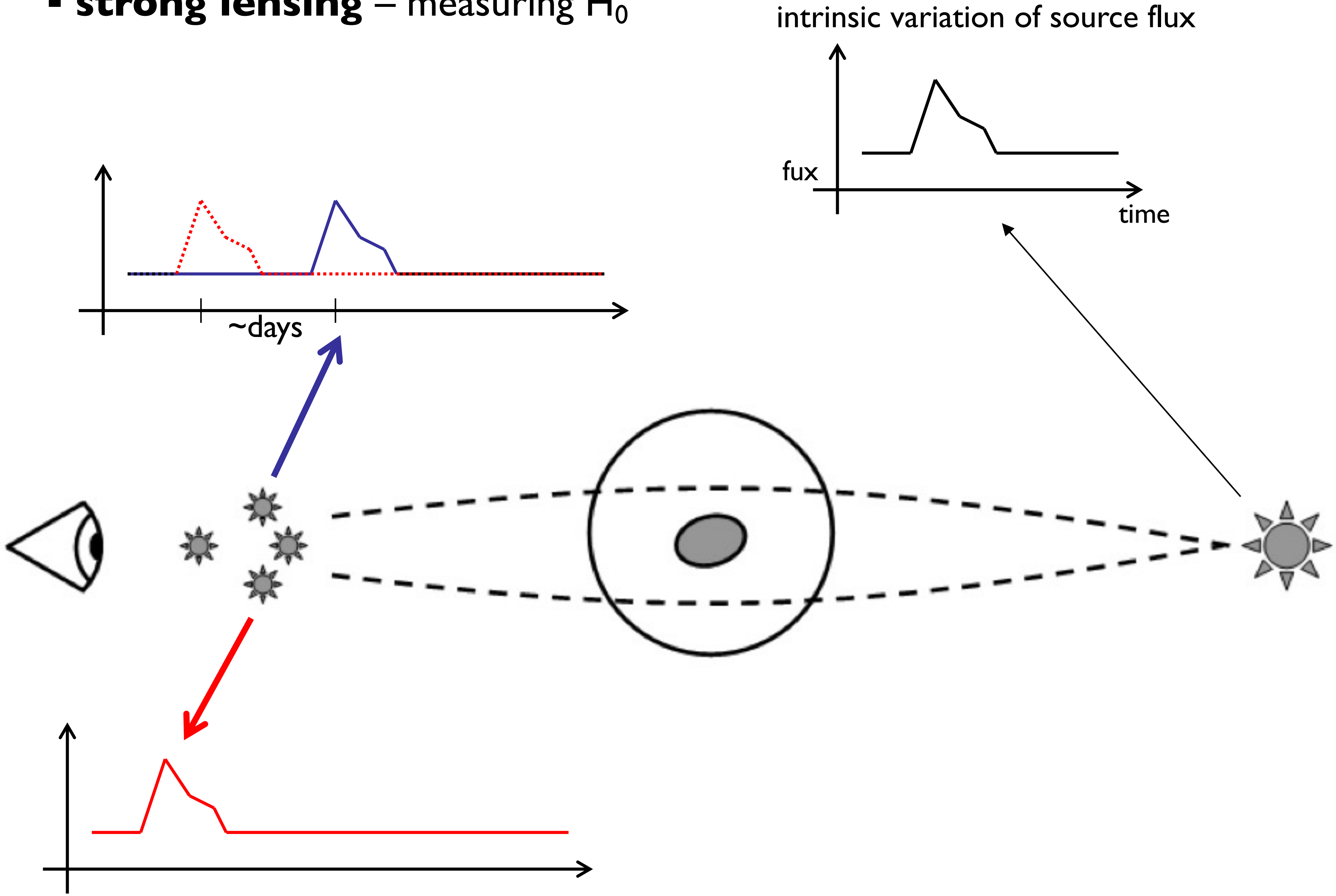

- **strong lensing** – measuring H_0

$$\Delta t \propto \frac{1}{H_0}$$

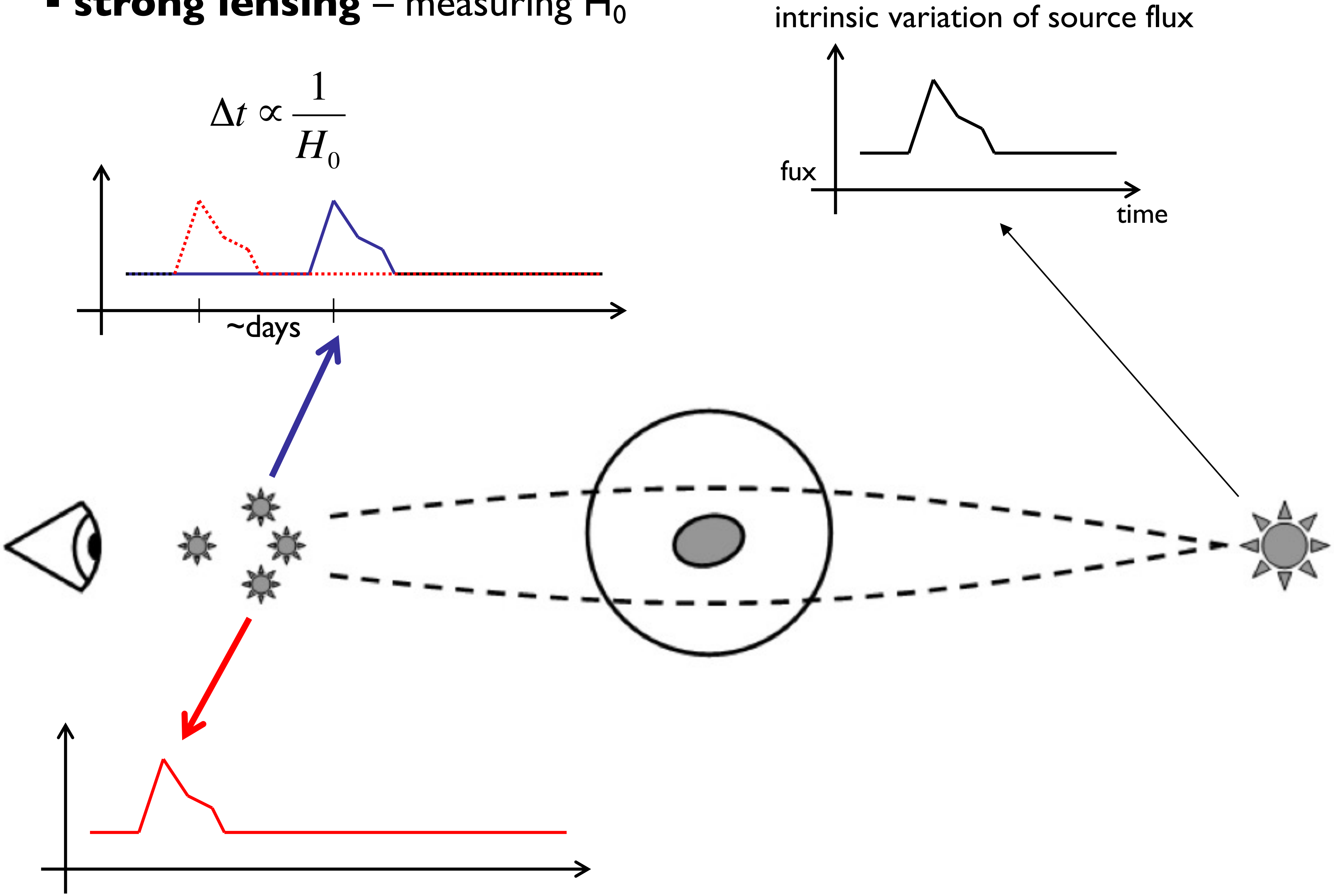

- **strong lensing** – measuring H_0

  - time delay:

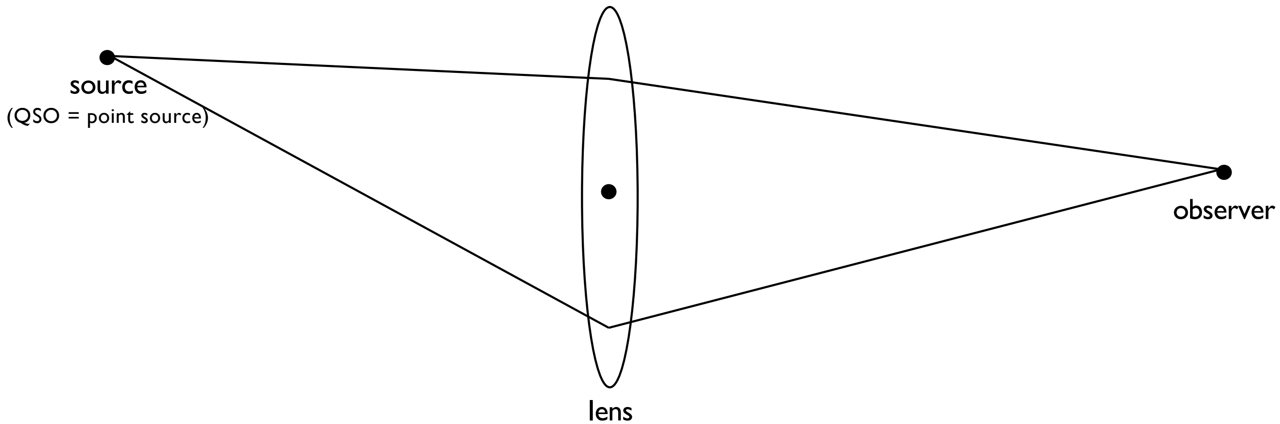

- **strong lensing** – measuring H_0

  - time delay: $$\Delta t = \Delta t_{grav} + \Delta t_{geom}$$

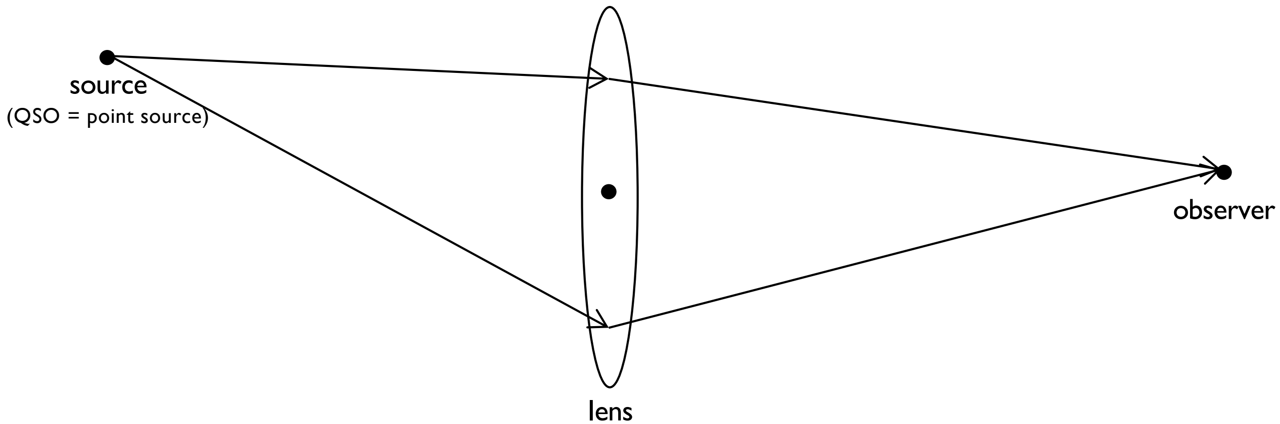

- **strong lensing** – measuring H_0
  - gravitational time delay ("Shapiro delay") Δt_{grav}

- **strong lensing** – measuring H_0

  - gravitational time delay ("Shapiro delay") Δt_{grav}

$$n = 1 - \frac{2}{c^2}\Phi \approx \frac{c}{v}$$

(cf. lecture "basics of lensing")

- **strong lensing** – measuring H_0

  - gravitational time delay ("Shapiro delay") Δt_{grav}

$$\frac{c}{v} \approx 1 - \frac{2}{c^2}\Phi$$

gravitational potential effectively lowers speed of light ray…

- **strong lensing** – measuring H_0

  - gravitational time delay ("Shapiro delay") Δt_{grav}

$$\frac{c}{v} \approx 1 - \frac{2}{c^2}\Phi$$

$$\frac{c}{v} = \frac{c}{\Delta x / \Delta t} = \frac{c\Delta t}{\Delta x} = 1 - \frac{2}{c^2}\Phi \quad \Rightarrow \quad \Delta t = \frac{1}{c}\Delta x - \frac{2}{c^3}\Phi\Delta x$$

(integrate only the extra gravitational term...)

- **strong lensing** – measuring H_0

  - gravitational time delay ("Shapiro delay") Δt_{grav}

$$\frac{c}{v} \approx 1 - \frac{2}{c^2}\Phi$$

=>
lens frame

$$\Delta t_{grav} = \frac{2}{c^3}\int_{source}^{observer} |\Phi| dl$$

- **strong lensing** – measuring H_0

  - gravitational time delay ("Shapiro delay") Δt_{grav}

$$\frac{c}{v} \approx 1 - \frac{2}{c^2}\Phi$$

=> lens frame

$$\Delta t_{grav} = \frac{2}{c^3}\int_{source}^{observer} |\Phi| dl$$

=> observers frame ($r=ax$)

$$\Delta t_{grav} = \frac{2(1+z_L)}{c^3}\int_{source}^{observer} |\Phi| dl$$

- **strong lensing** – measuring H_0

  - gravitational time delay ("Shapiro delay") Δt_{grav}

$$\frac{c}{v} \approx 1 - \frac{2}{c^2}\Phi$$

=> lens frame

$$\Delta t_{grav} = \frac{2}{c^3}\int_{source}^{observer} |\Phi| dl$$

=> observers frame

$$\Delta t_{grav} = \frac{2(1+z_L)}{c^3}\int_{source}^{observer} |\Phi| dl$$

introducing the lensing potential $\varphi(\theta) = \frac{2}{c^2}\int \frac{D_{LS}}{D_S D_L}\Phi(\theta,z)dz$

$$\Delta t_{grav} = -\frac{(1+z_L)}{c}\frac{D_S D_L}{D_{LS}}\varphi(\theta)$$

- **strong lensing** – measuring H_0

  - time delay: $$\Delta t = \Delta t_{grav} + \Delta t_{geom}$$

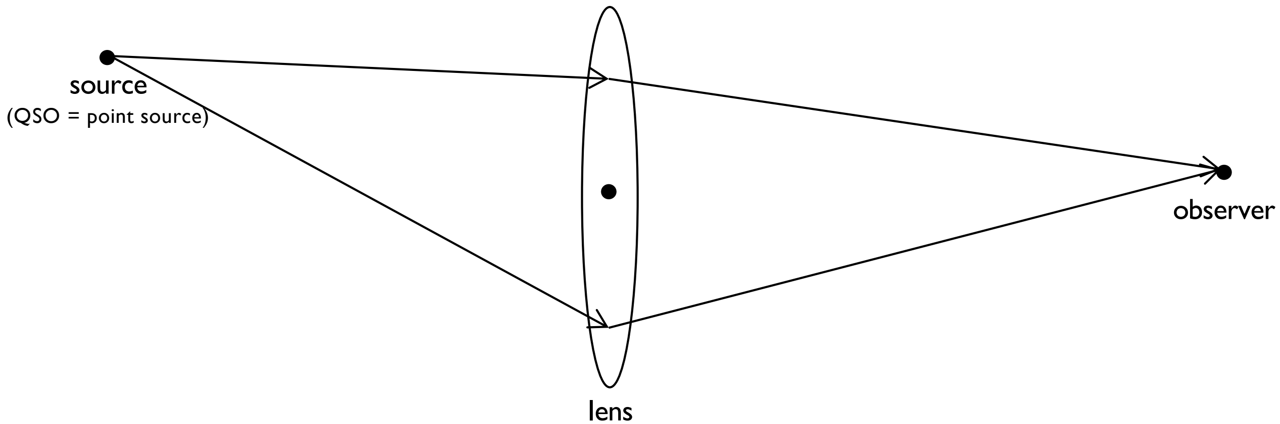

$$\Delta t_{grav} = -\frac{(1+z_L)}{c}\frac{D_S D_L}{D_{LS}}\varphi(\theta)$$

- **strong lensing** – measuring H_0

  - time delay:

$$\Delta t = \Delta t_{grav} + \Delta t_{geom}$$

?

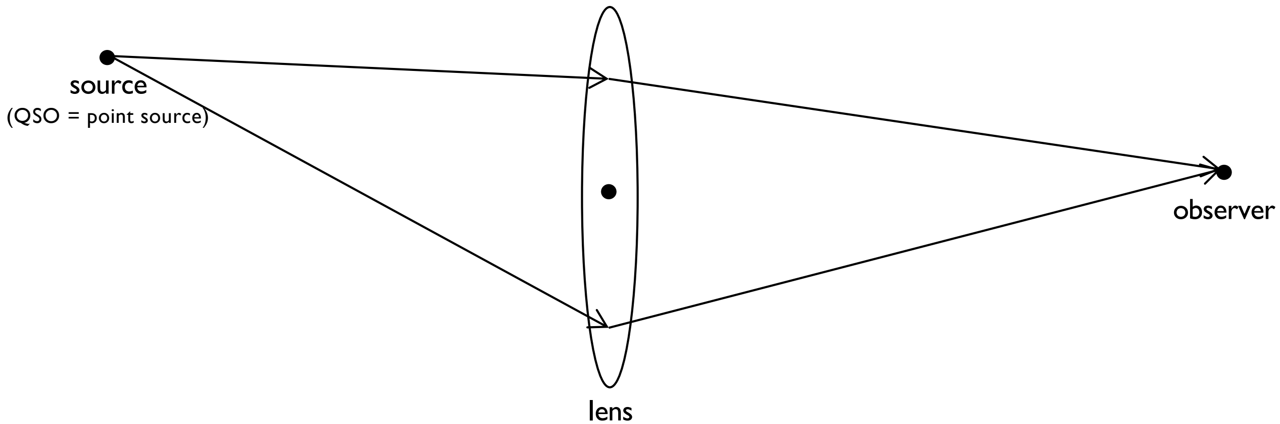

$$\Delta t_{grav} = -\frac{(1+z_L)}{c}\frac{D_S D_L}{D_{LS}}\varphi(\theta)$$

- **strong lensing** – measuring H_0
  - geometrical time delay (between lensed and un-lensed image) Δt_{geom}

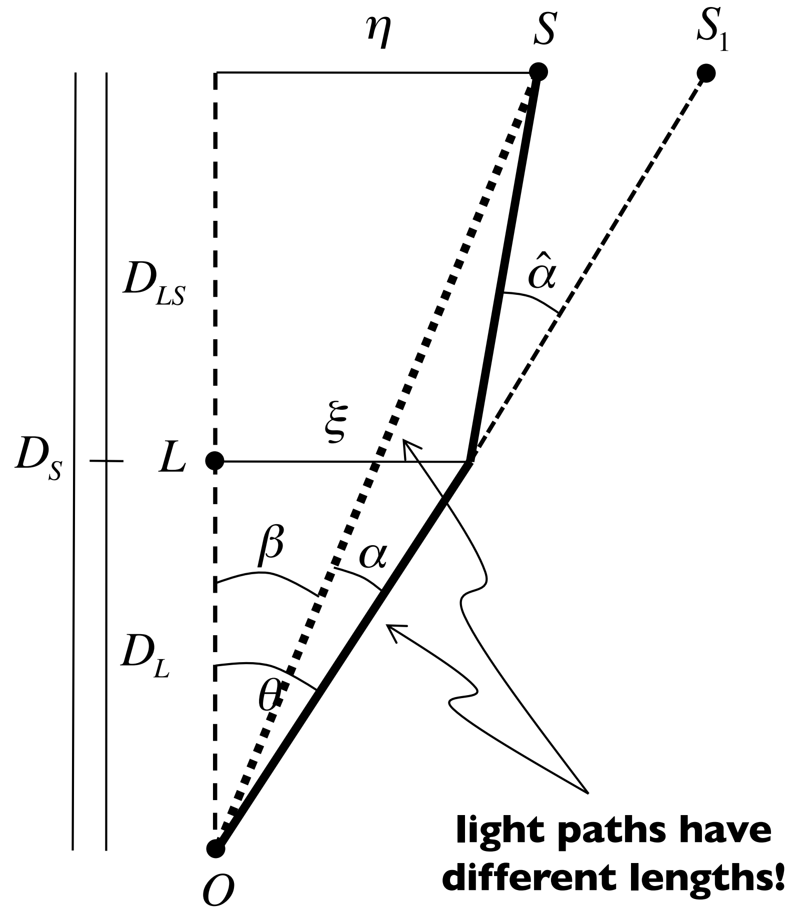

- **strong lensing** – measuring H_0
  - geometrical time delay (between lensed and un-lensed image) Δt_{geom}

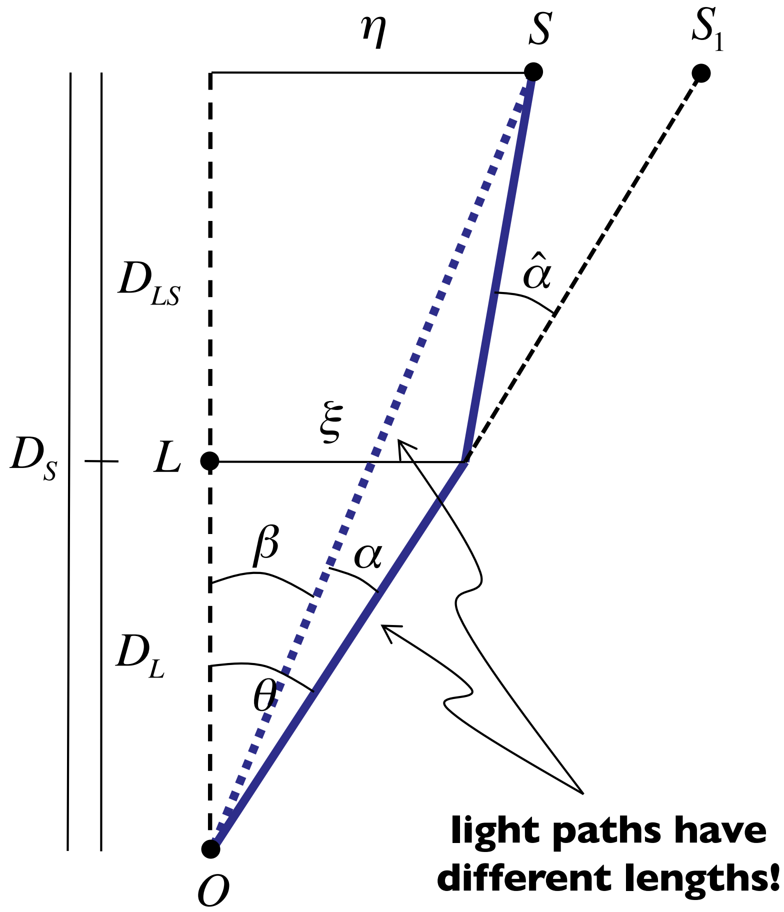

- **strong lensing** – measuring H_0
    - geometrical time delay (between lensed and un-lensed image) Δt_{geom}

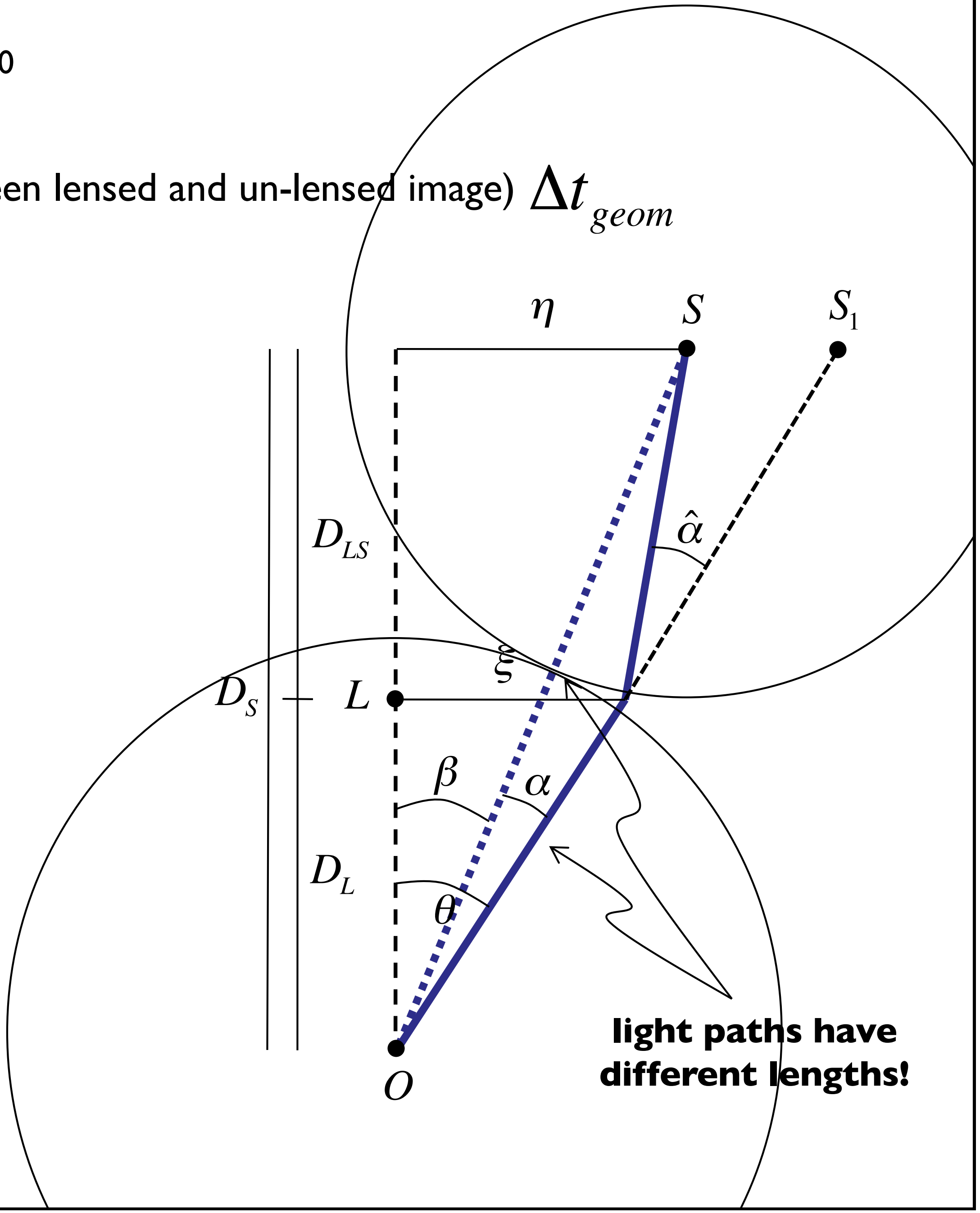

- **strong lensing** – measuring H_0
  - geometrical time delay (between lensed and un-lensed image) Δt_{geom}

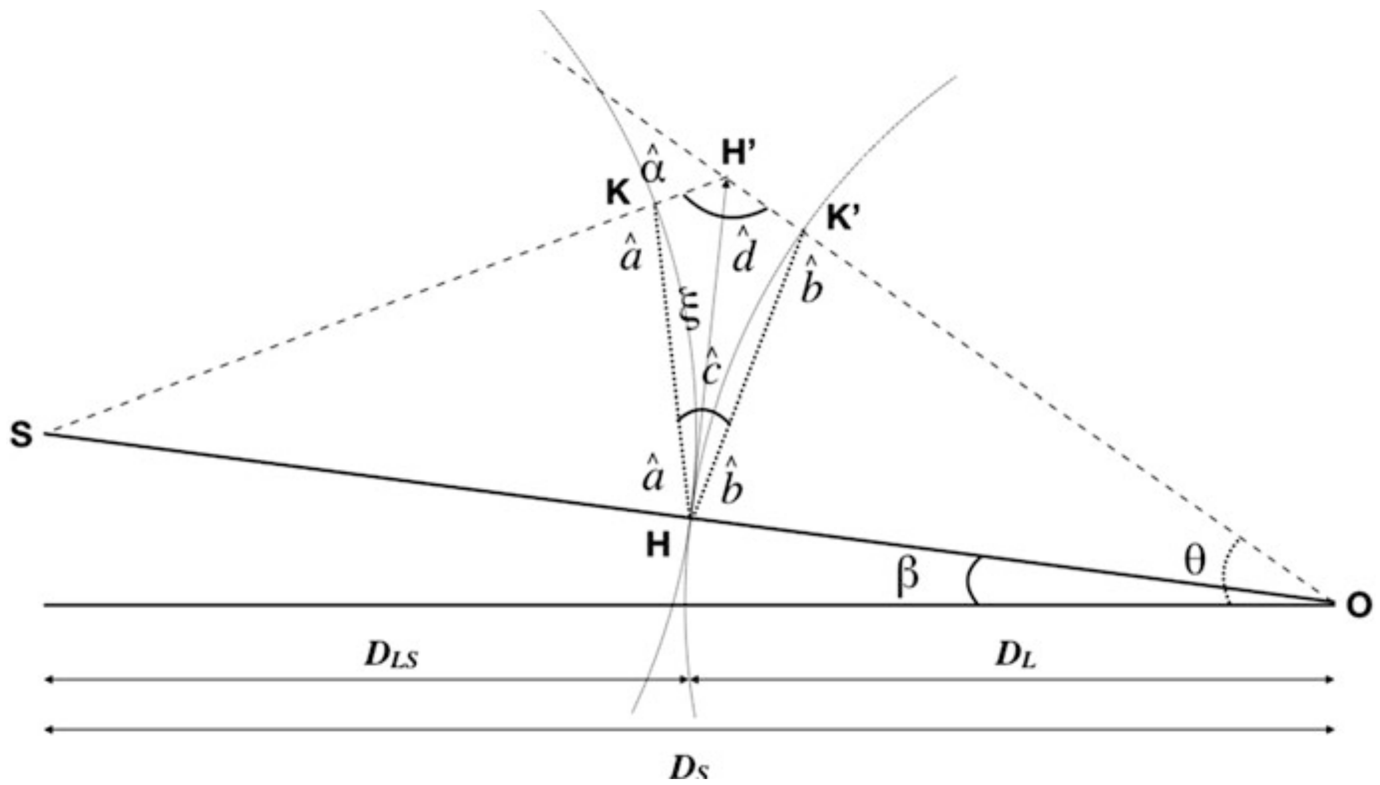

- **strong lensing** – measuring H_0

  - geometrical time delay (between lensed and un-lensed image) Δt_{geom}

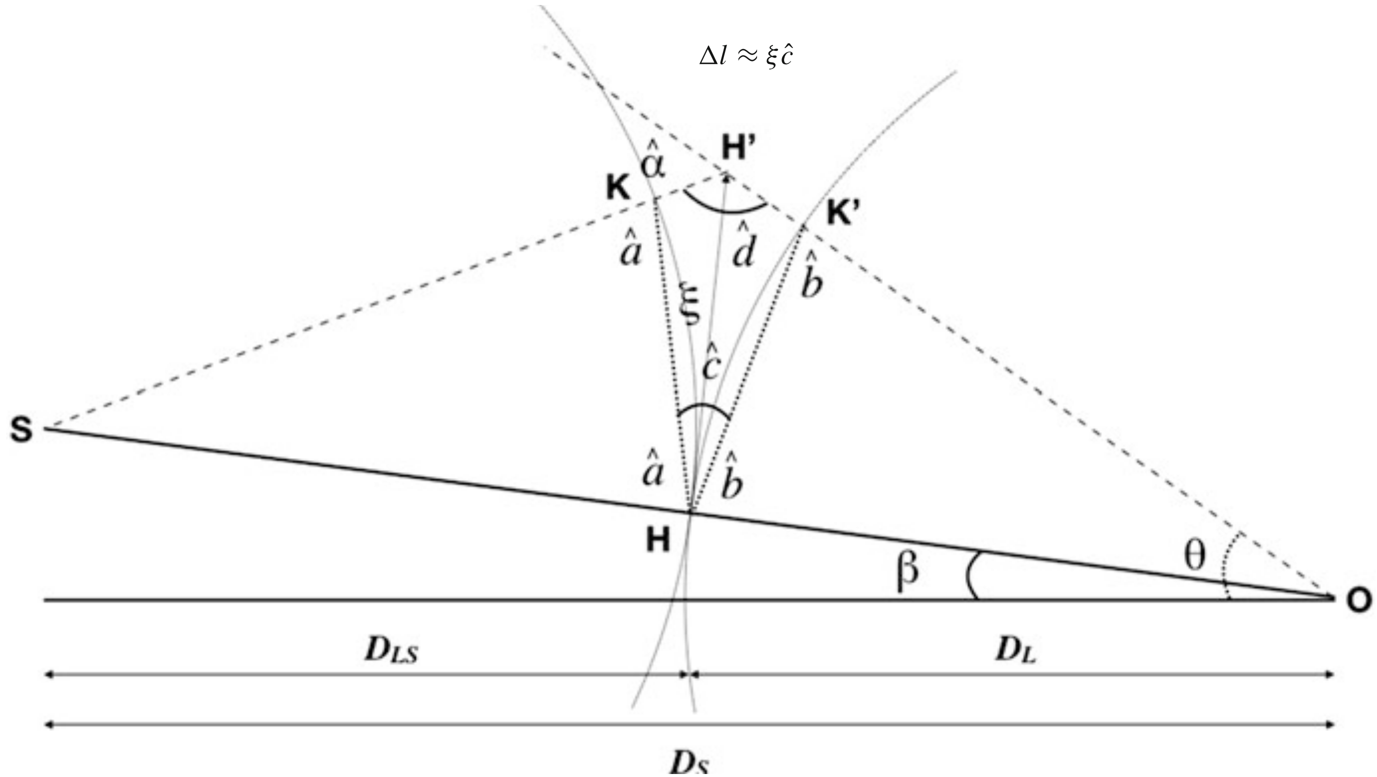

- **strong lensing** – measuring H_0

  - geometrical time delay (between lensed and un-lensed image) Δt_{geom}

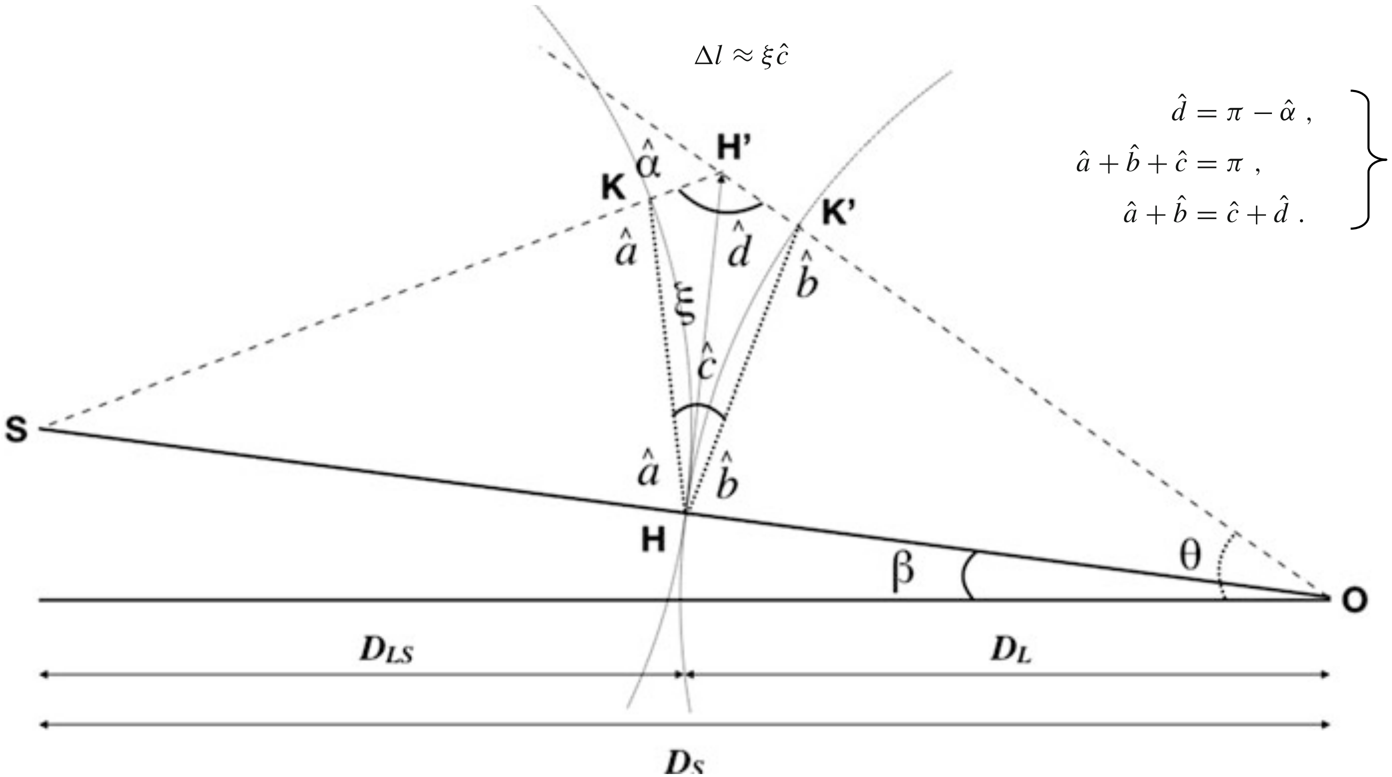

$$\left.\begin{aligned} \hat{d} &= \pi - \hat{\alpha}\ , \\ \hat{a} + \hat{b} + \hat{c} &= \pi\ , \\ \hat{a} + \hat{b} &= \hat{c} + \hat{d}\ . \end{aligned}\right\} \quad \hat{c} = \frac{\hat{\alpha}}{2}$$

- **strong lensing** – measuring H_0
  - geometrical time delay (between lensed and un-lensed image) Δt_{geom}

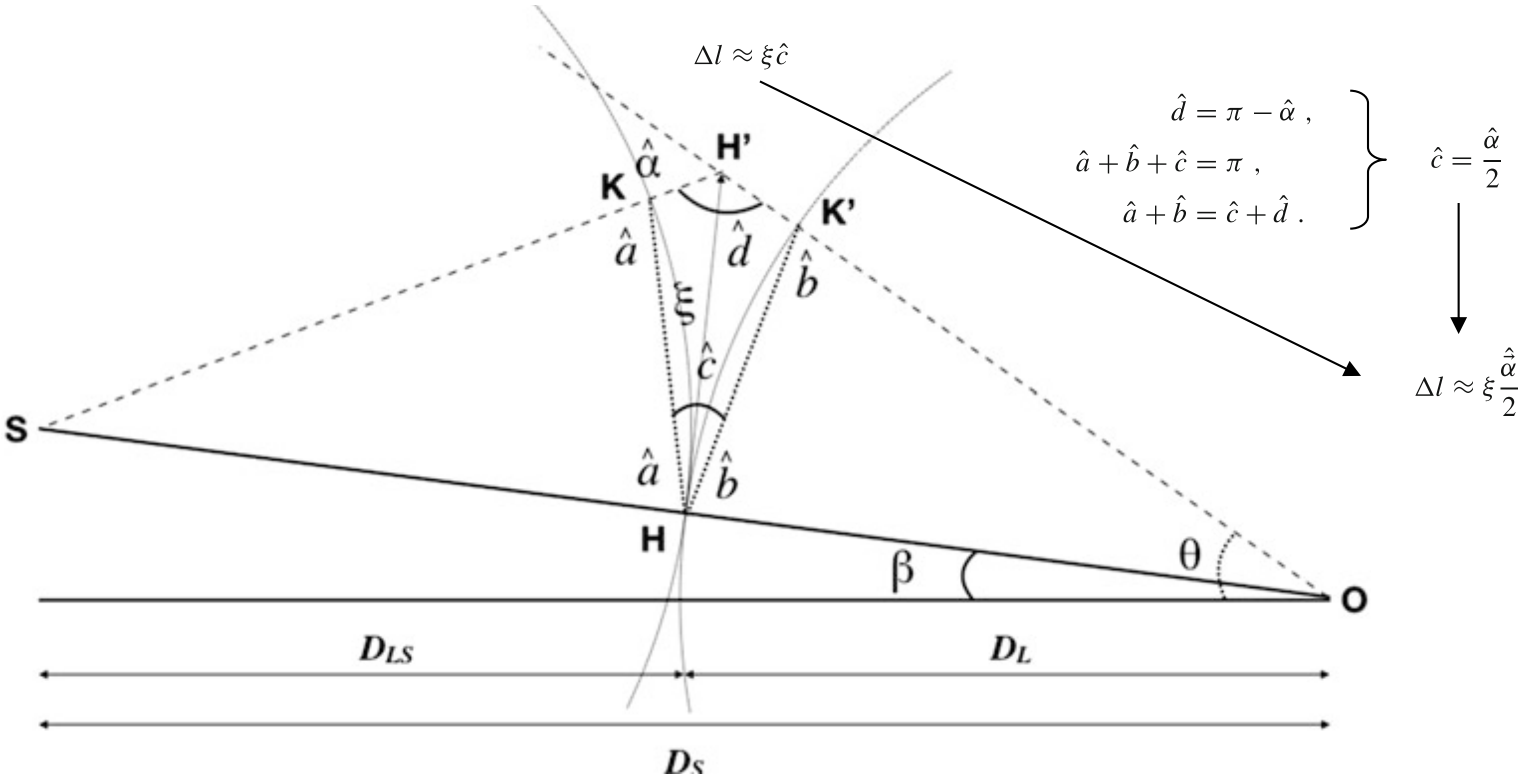

- **strong lensing** – measuring H_0

  - geometrical time delay (between lensed and un-lensed image) Δt_{geom}

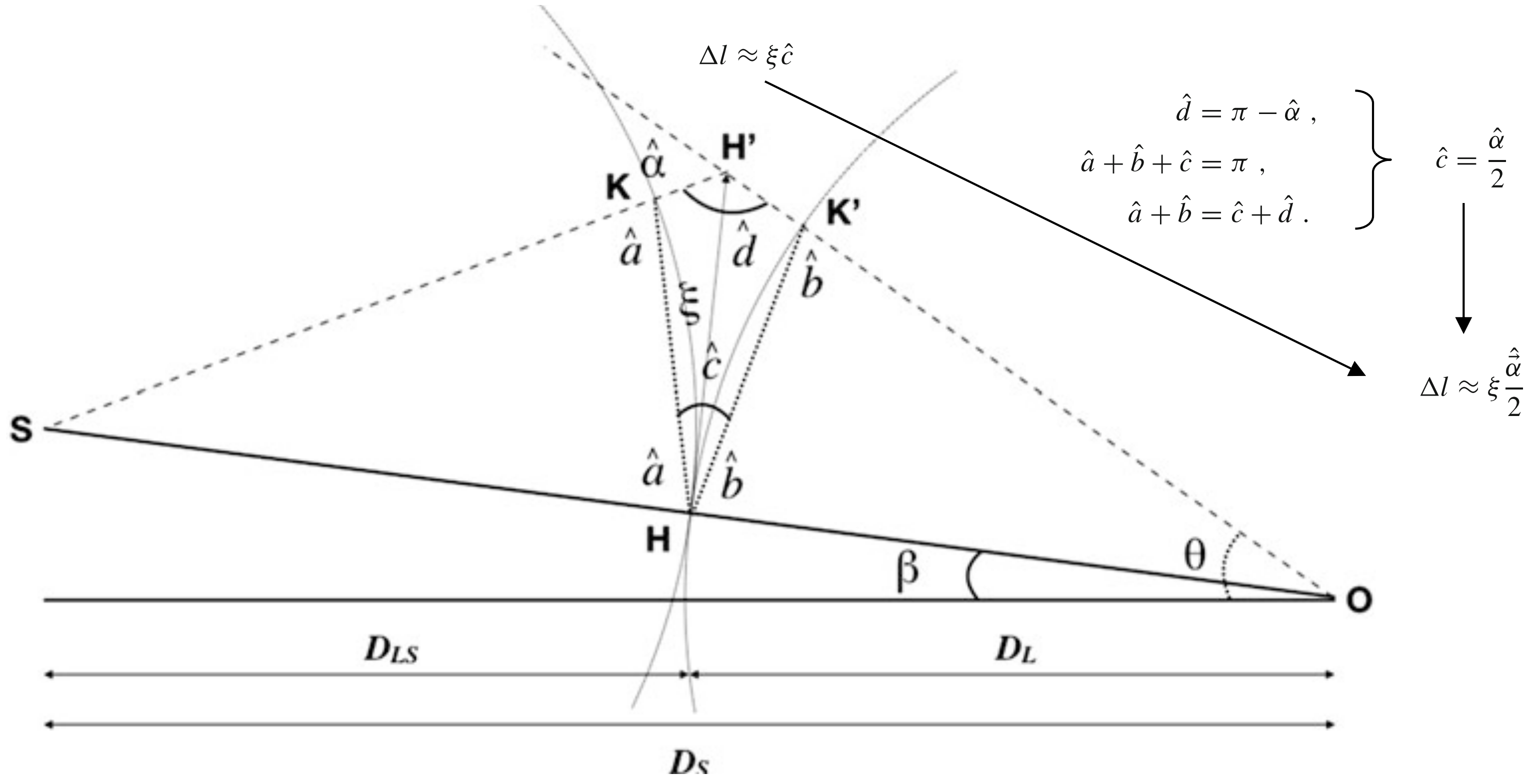

$$\Delta t_{geom} = \frac{(1 + z_L)\xi \Delta l}{c}$$

- **strong lensing** – measuring H_0
  - geometrical time delay (between lensed and un-lensed image) Δt_{geom}

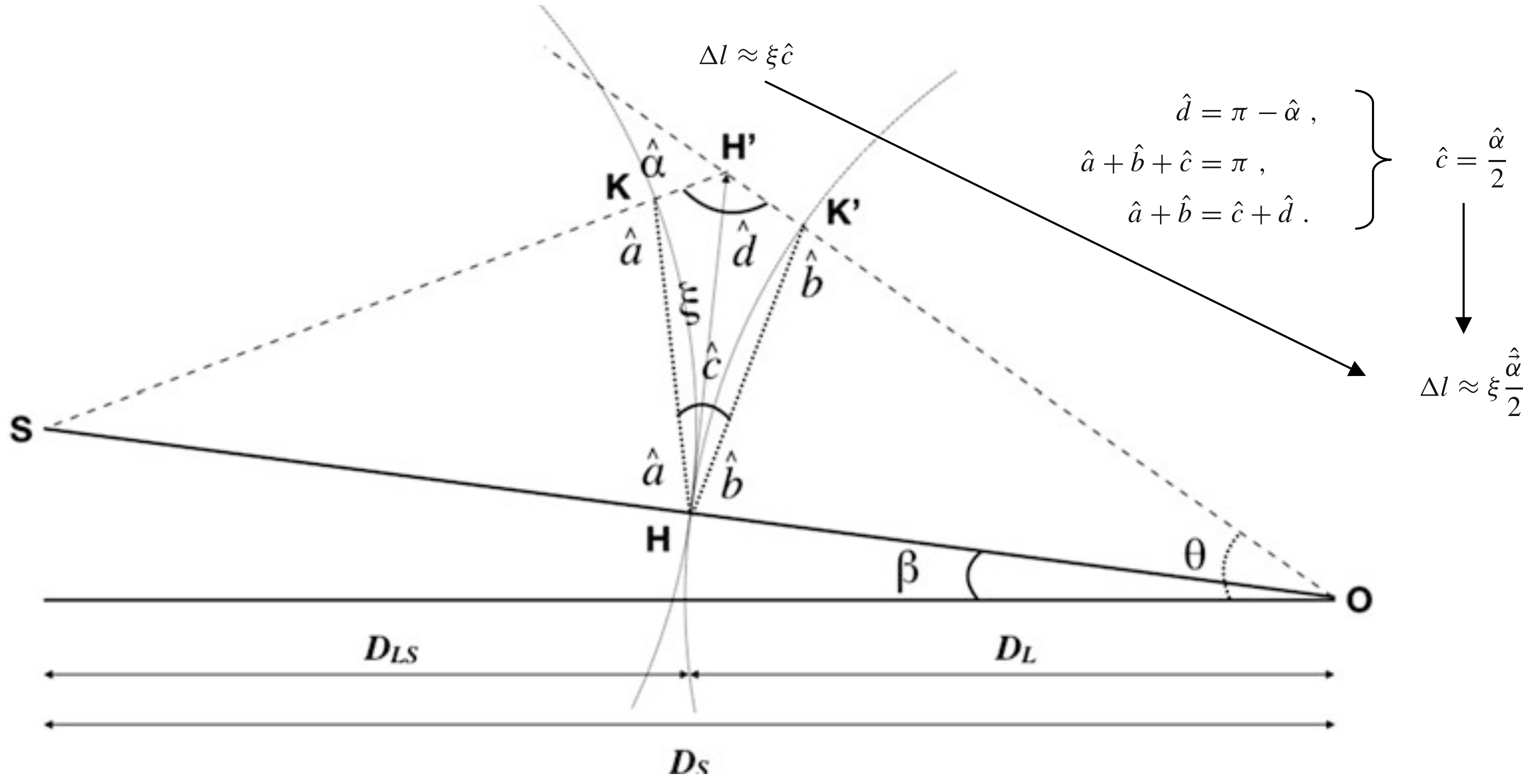

$$\Delta t_{geom} = \frac{(1+z_L)\xi\Delta l}{c} = \frac{1}{2c}\xi\hat{\alpha} = \frac{(1+z_L)}{2c}\frac{D_L D_S}{D_{LS}}\alpha(\theta-\beta) = \frac{(1+z_L)}{2c}\frac{D_L D_S}{D_{LS}}(\theta-\beta)^2$$

- **strong lensing** – measuring H_0

  - time delay: $$\Delta t = \Delta t_{grav} + \Delta t_{geom}$$

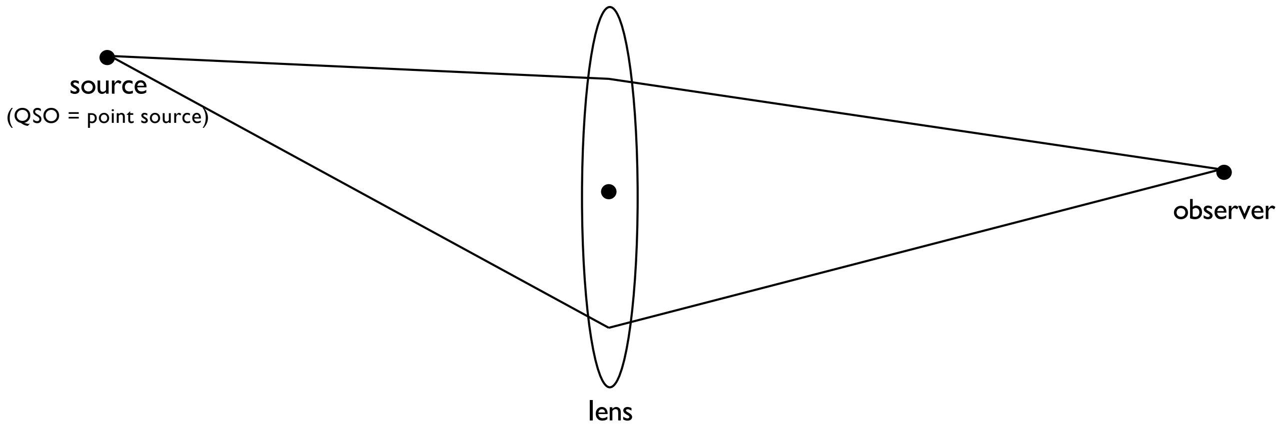

$$\Delta t_{grav} = -\frac{(1+z_L)}{c}\frac{D_S D_L}{D_{LS}}\varphi(\theta)$$

$$\Delta t_{geom} = \frac{1+z_L}{2c}\frac{D_S D_L}{D_{LS}}\left(\theta-\beta\right)^2$$

- **strong lensing** – measuring H_0

  - time delay: $$\Delta t = \Delta t_{grav} + \Delta t_{geom}$$

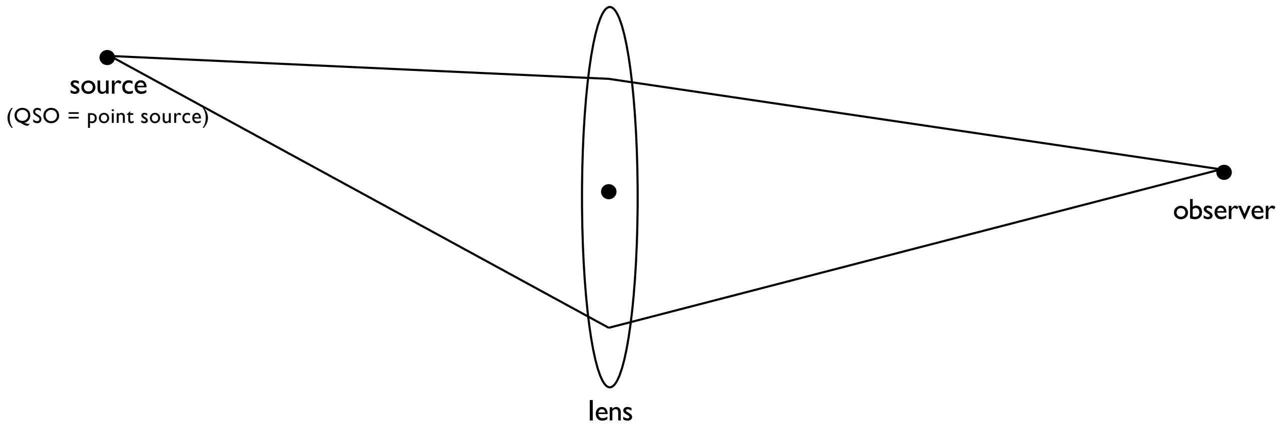

$$\Delta t = \frac{1+z_L}{2c}\frac{D_S D_L}{D_{LS}}(\theta-\beta)^2 - \frac{1+z_L}{c}\frac{D_S D_L}{D_{LS}}\varphi$$

$$= \frac{1+z_L}{c}\frac{D_S D_L}{D_{LS}} \left(\frac{1}{2}(\theta-\beta)^2 - \varphi\right)$$

- **strong lensing** – measuring H_0

  - time delay:

$$\Delta t = \frac{1+z_L}{c}\frac{D_S D_L}{D_{LS}}\left(\frac{1}{2}(\theta-\beta)^2-\varphi\right)$$

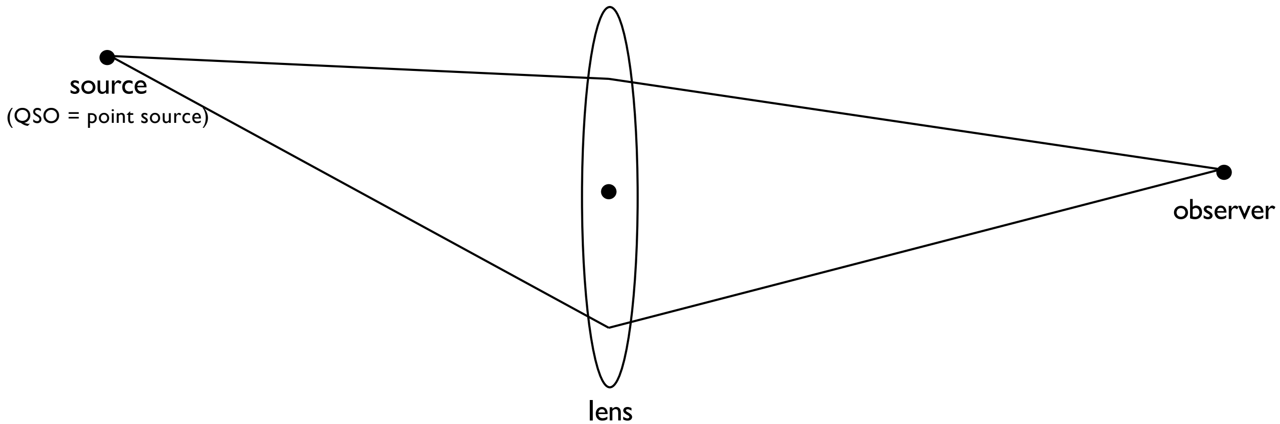

- **strong lensing** – measuring H_0

  - time delay: $$\Delta t = \underbrace{\frac{1+z_L}{c}\frac{D_S D_L}{D_{LS}}}_{\textbf{cosmology}} \underbrace{\left(\frac{1}{2}(\theta-\beta)^2 - \varphi\right)}_{\textbf{lens}}$$

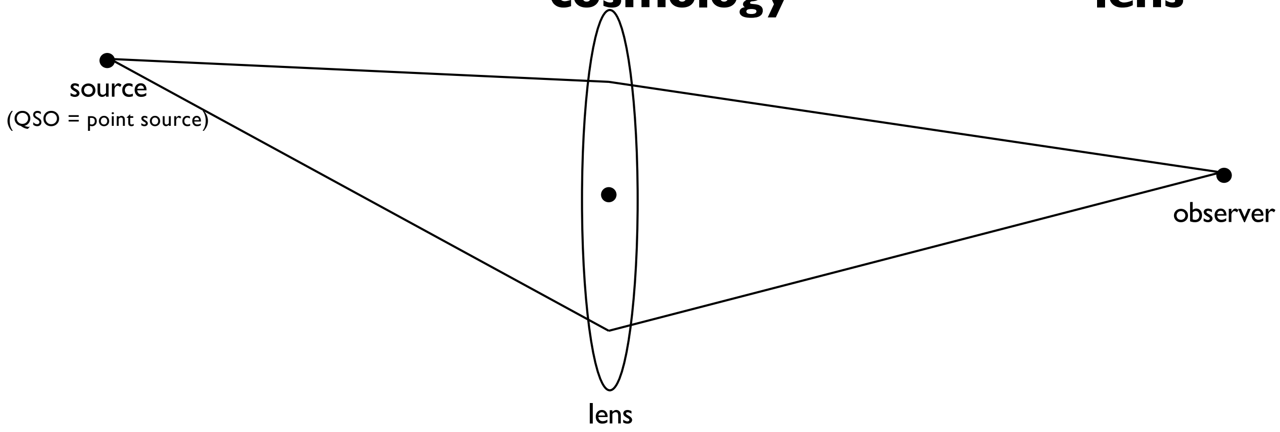

- **strong lensing** – measuring H_0

  - time delay:

$$\Delta t = \underbrace{\frac{1+z_L}{c}\frac{D_S D_L}{D_{LS}}}_{\textbf{cosmology}} \underbrace{\left(\frac{1}{2}(\theta-\beta)^2-\varphi\right)}_{\textbf{lens}}$$

...let's measure cosmological distances!

- **strong lensing** – measuring H_0

  - time delay:

$$\Delta t = \underbrace{\frac{1+z_L}{c}\frac{D_S D_L}{D_{LS}}}_{\textbf{cosmology}} \underbrace{\left(\frac{1}{2}(\theta-\beta)^2-\varphi\right)}_{\textbf{lens}}$$

- angular diameter distances*

$$D_S = d_A(0, z_S)$$

$$D_L = d_A(0, z_L)$$

$$D_{LS} = d_A(z_L, z_S)$$

*because they ensure that the lens equation is fulfilled (as they are defined that way…)

- **strong lensing** – measuring H_0

  - time delay:

$$\Delta t = \underbrace{\frac{1+z_L}{c}\frac{D_S D_L}{D_{LS}}}_{\textbf{cosmology}} \underbrace{\left(\frac{1}{2}\left(\theta-\beta\right)^2-\varphi\right)}_{\textbf{lens}}$$

- angular diameter distances

$$D_S = d_A(0, z_S)$$

$$D_L = d_A(0, z_L)$$

$$D_{LS} = d_A(z_L, z_S)$$

$$d_A(z_1,z_2) = \frac{c}{H_0}\frac{1}{1+z_2}\frac{\mathrm{sinn}(\sqrt{|\Omega_k|}E(z_1,z_2))}{\sqrt{|\Omega_k|}}$$

$$\mathrm{sinn}(u) = \begin{cases} \sin(u) & ;\ \Omega_k < 0 \\ u & ;\ \Omega_k = 0 \\ \sinh(u) & ;\ \Omega_k > 0 \end{cases}$$

$$E(z_1,z_2) = \int_{z_1}^{z_2} \frac{dz}{\sqrt{\Omega_0(1+z)^3 + \Omega_k(1+z)^2 + \Omega_{de}(1+z)^{3(1+w)}}}$$

$$p_{de} = w\rho_{de}$$

- **strong lensing** – measuring H_0

  - time delay:

$$\Delta t = \underbrace{\frac{1+z_L}{c}\frac{D_S D_L}{D_{LS}}}_{\textbf{cosmology}} \underbrace{\left(\frac{1}{2}(\theta-\beta)^2-\varphi\right)}_{\textbf{lens}}$$

- angular diameter distances

$$D_S = d_A(0, z_S) \approx \frac{1}{H_0}$$

$$D_L = d_A(0, z_L) \approx \frac{1}{H_0}$$

$$D_{LS} = d_A(z_L, z_S) \approx \frac{1}{H_0}$$

$$d_A(z_1, z_2) = \frac{c}{H_0}\frac{1}{1+z_2}\frac{\mathrm{sinn}(\sqrt{|\Omega_k|}E(z_1,z_2))}{\sqrt{|\Omega_k|}}$$

$$\mathrm{sinn}(u) = \begin{cases} \sin(u) & ;\ \Omega_k < 0 \\ u & ;\ \Omega_k = 0 \\ \sinh(u) & ;\ \Omega_k > 0 \end{cases}$$

$$E(z_1, z_2) = \int_{z_1}^{z_2} \frac{dz}{\sqrt{\Omega_0(1+z)^3 + \Omega_k(1+z)^2 + \Omega_{de}(1+z)^{3(1+w)}}}$$

$$p_{de} = w\rho_{de}$$

- **strong lensing** – measuring H_0

  - time delay:

$$\Delta t = \underbrace{\frac{1+z_L}{c}\frac{D_S D_L}{D_{LS}}}_{\textbf{cosmology}} \underbrace{\left(\frac{1}{2}(\theta-\beta)^2-\varphi\right)}_{\textbf{lens}}$$

- angular diameter distances

$$D_S = d_A(0,z_S) \approx \frac{1}{H_0}$$

$$D_L = d_A(0,z_L) \approx \frac{1}{H_0}$$

$$D_{LS} = d_A(z_L,z_S) \approx \frac{1}{H_0}$$

$$d_A(z_1,z_2) = \frac{c}{H_0}\frac{1}{1+z_2}\frac{\mathrm{sinn}(\sqrt{|\Omega_k|}E(z_1,z_2))}{\sqrt{|\Omega_k|}}$$

$$\mathrm{sinn}(u) = \begin{cases} \sin(u) & ;\ \Omega_k < 0 \\ u & ;\ \Omega_k = 0 \\ \sinh(u) & ;\ \Omega_k > 0 \end{cases}$$

$$E(z_1,z_2) = \int_{z_1}^{z_2} \frac{dz}{\sqrt{\Omega_0(1+z)^3 + \Omega_k(1+z)^2 + \Omega_{de}(1+z)^{3(1+w)}}}$$

$$p_{de} = w\rho_{de}$$

- **strong lensing** – measuring H_0

  - time delay:

$$\Delta t = \underbrace{\frac{1}{H_0}\,E}_{\textbf{cosmology}} \underbrace{\left(\frac{1}{2}(\theta-\beta)^2 - \varphi\right)}_{\textbf{lens}}$$

- **strong lensing** – measuring H_0

  - time delay:

$$\Delta t = \underbrace{\frac{1}{H_0} E}_{\textbf{cosmology}} \underbrace{\left(\frac{1}{2}(\theta - \beta)^2 - \varphi\right)}_{\textbf{lens}}$$

direct dependence on H_0

indirect (and weak) dependence on Ω_0, Ω_k, Ω_{de}, w

- **strong lensing** – measuring H_0

B0218+357

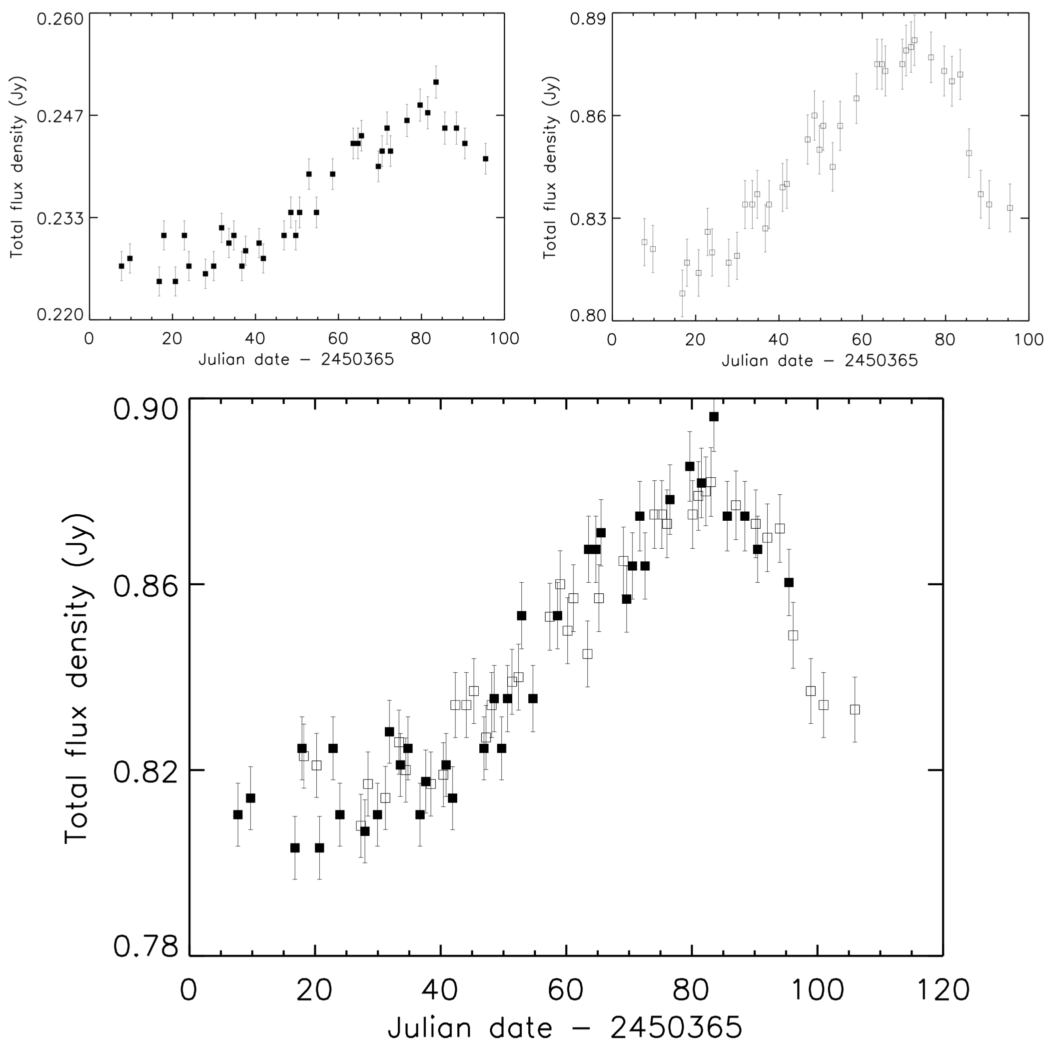

Δt = 10.5 days

H_0 = 69 km/sec/Mpc (isothermal ellipsoid)

Biggs et al. (1999)

- **strong lensing** – measuring H_0

lens	Δt
RXJ0911+0551	146
Q0957+561	417
PG1115+080	12
SBS1520+530	129
B1600+434	51
PKS1830–211	26
HE2149–2745	103

H_0 = 51 km/sec/Mpc (isothermal ellipsoid)

Kochanek et al. (2002)

- **strong lensing** – measuring H_0

B0218+357

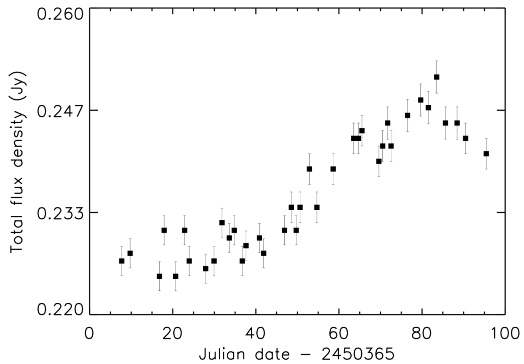

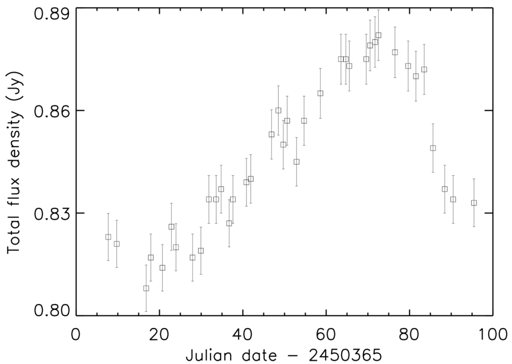

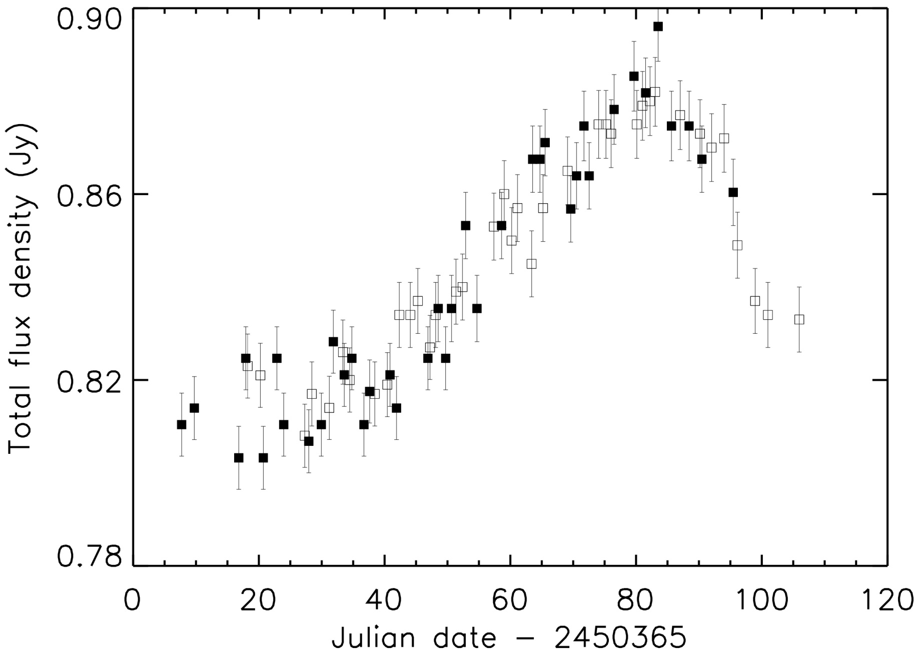

Δt = 10.5 days

H_0 = 78 km/sec/Mpc (isothermal sphere)

Wucknitz et al. (2004)

- **strong lensing** – measuring H_0

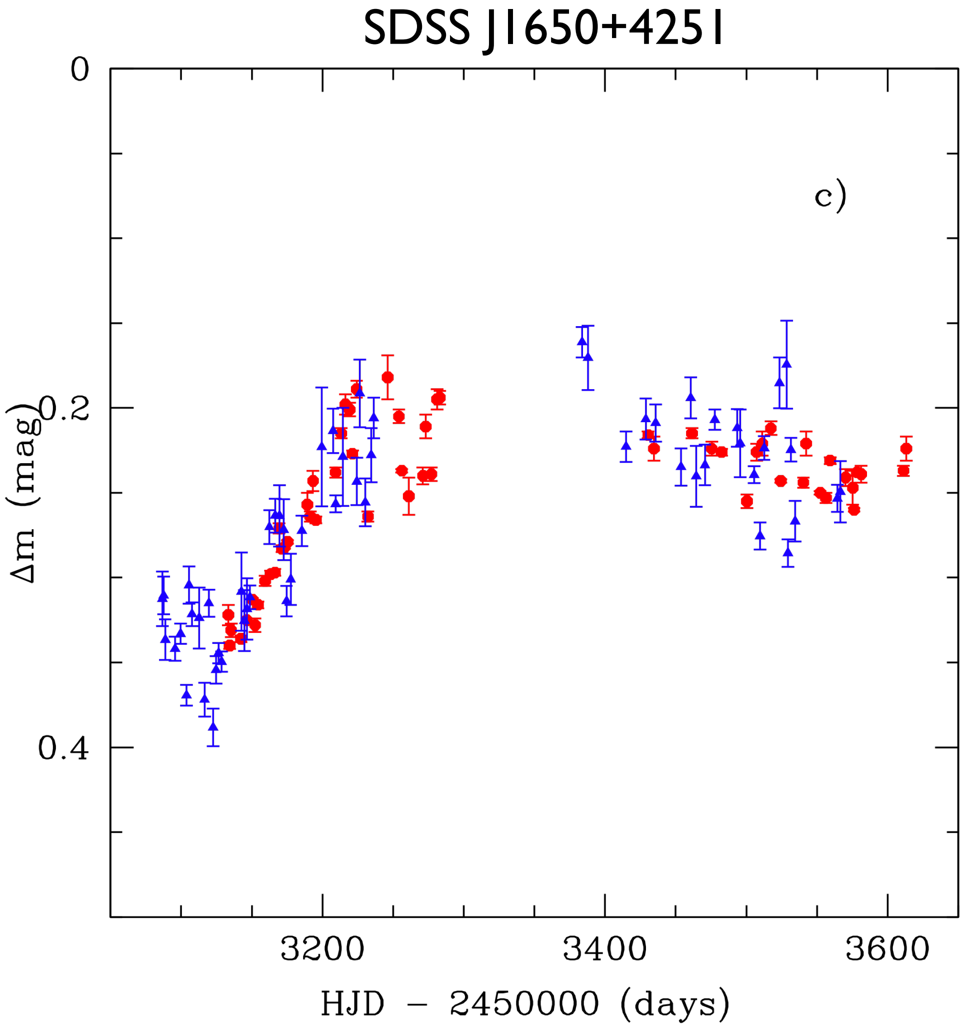

Δt = 46.7 days

H_0 = 52 km/sec/Mpc (isothermal sphere)

H_0 = 72 km/sec/Mpc (de Vaucouleur)

Vuissoz et al. (2007)

- **strong lensing** – measuring H_0

method	H_0 [km/sec/Mpc]	reference
CMB	73	(Spergel et al. 2007)
SN Type Ia	62	(Sandage et al. 2006)
SN Type Ia	73	(Riess et al. 2005)
SZ effect	66	(Jones et al. 2005)
lensing	68	(Oguri et al. 2007, 16 lenses)
lensing	72	(Saha et al. 2007, 10 lenses)

Coles et al. (2008)

- **strong lensing** – measuring H_0

method	H_0 [km/sec/Mpc]	reference
CMB	73	(Spergel et al. 2007)
SN Type Ia	62	(Sandage et al. 2006)
SN Type Ia	73	(Riess et al. 2005)
SZ effect	66	(Jones et al. 2005)
lensing	68	(Saha et al. 2007, 10 lenses)

check COSMOGRAIL & H0LiCOW for latest developments (http://cosmograil.epfl.ch & https://shsuyu.github.io/H0LiCOW/site)

Coles et al. (2008)

- **strong lensing** – measuring H_0

Remember the tension for H0 measurements:
- local (Cepheids method) vs CMB measurements

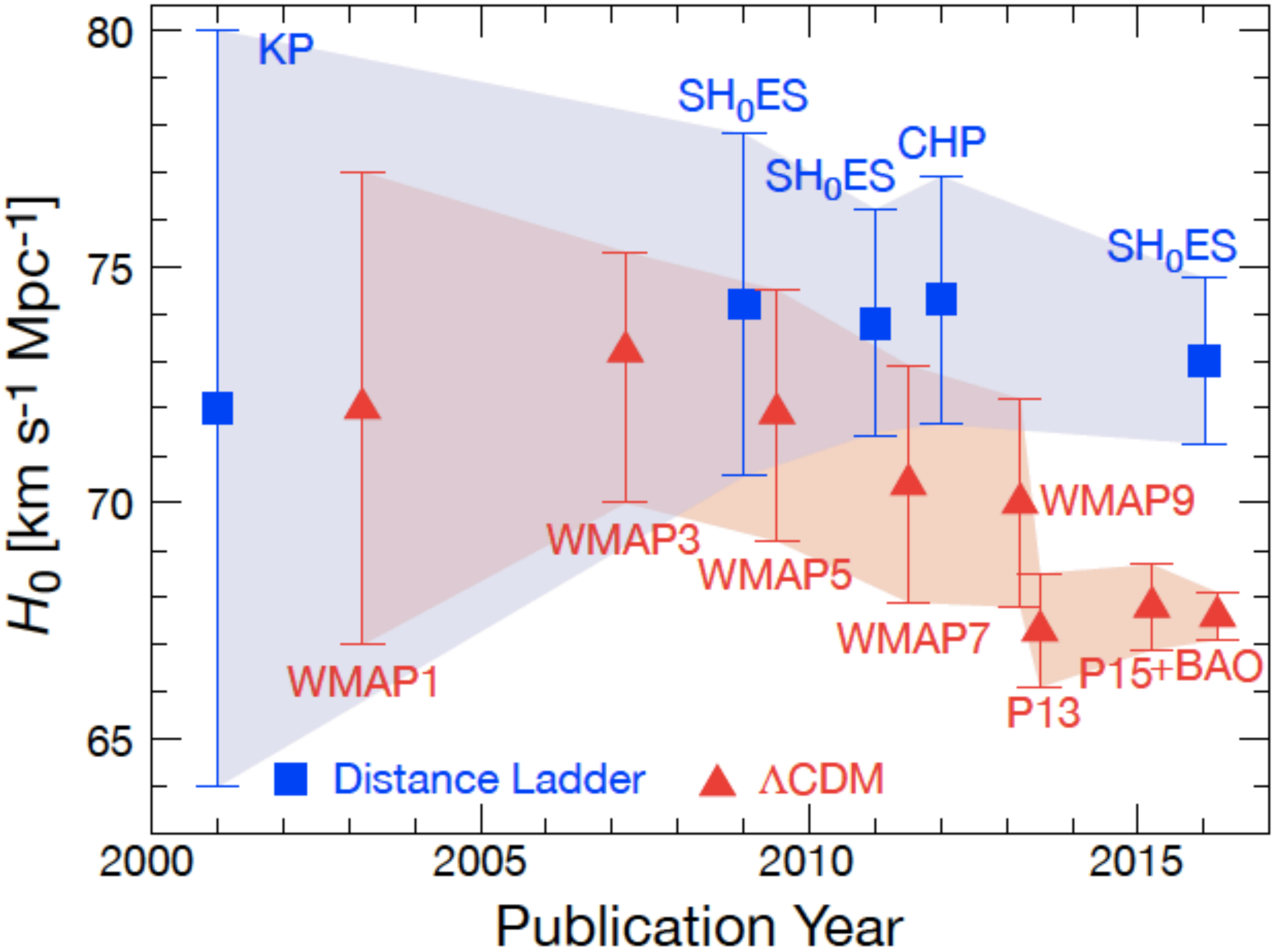

Freedman (2017)

- **strong lensing** – measuring H_0

Remember the tension for H0 measurements:
- local (Cepheids method) vs CMB measurements

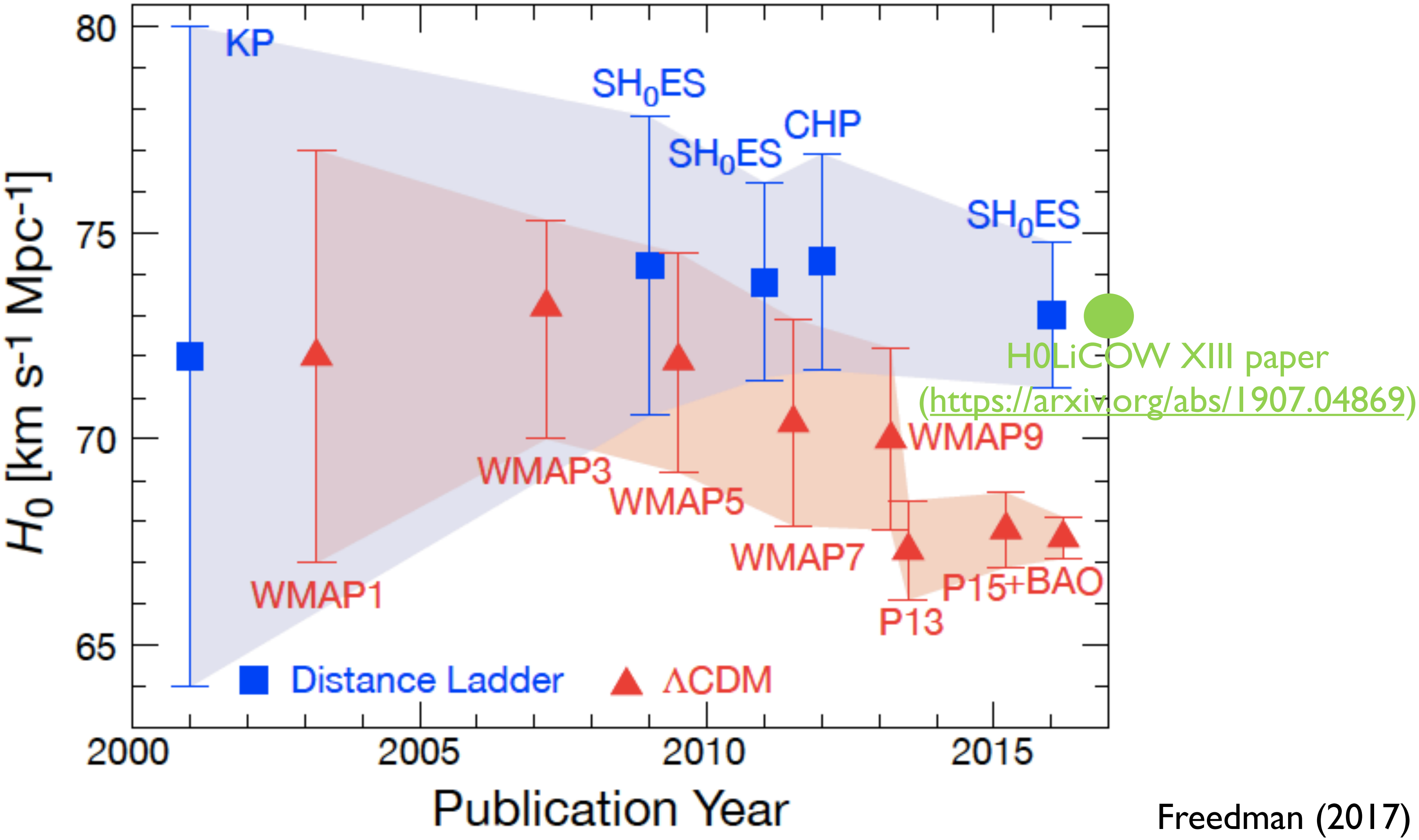

Freedman (2017)

- concept
- theory
- **applications:**
    - micro-lensing
    - **strong lensing:**
        - cosmic telescopes
        - H_0 determination
        - **missing satellite problem**

- **strong lensing** - the "missing satellite problem"

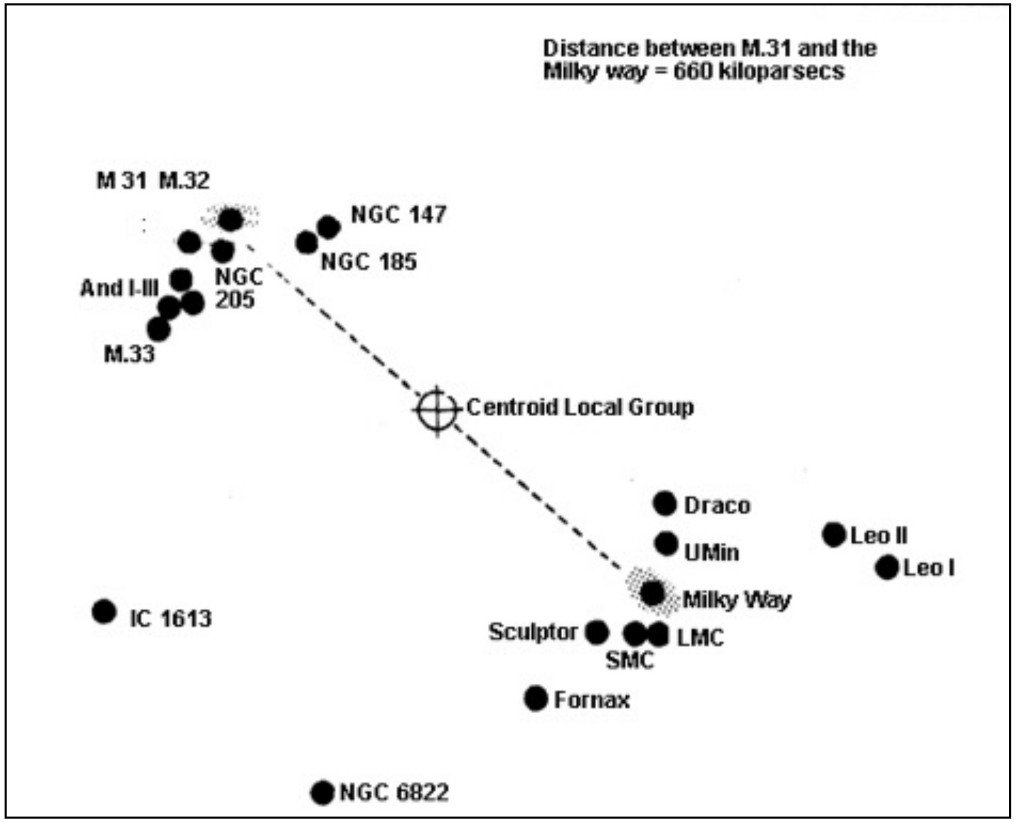

ca. 50 satellites observed

- **strong lensing** - the "missing satellite problem"

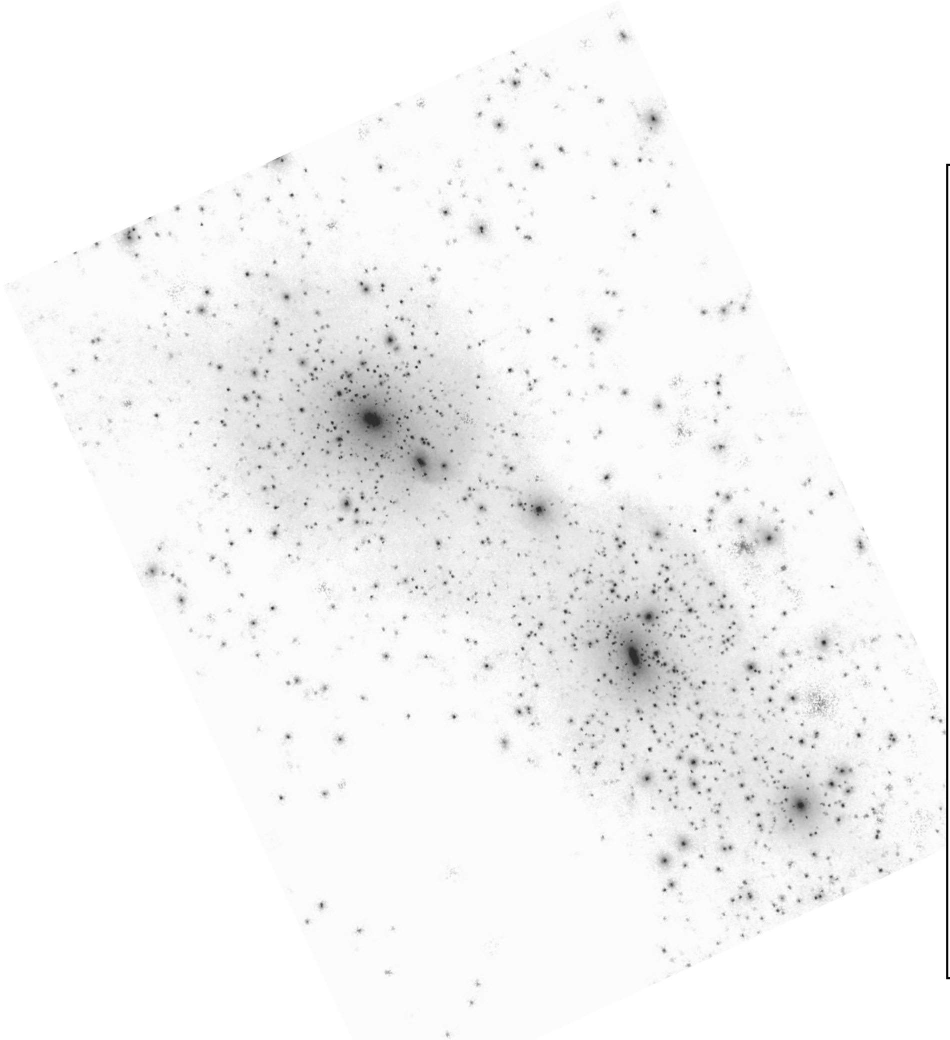

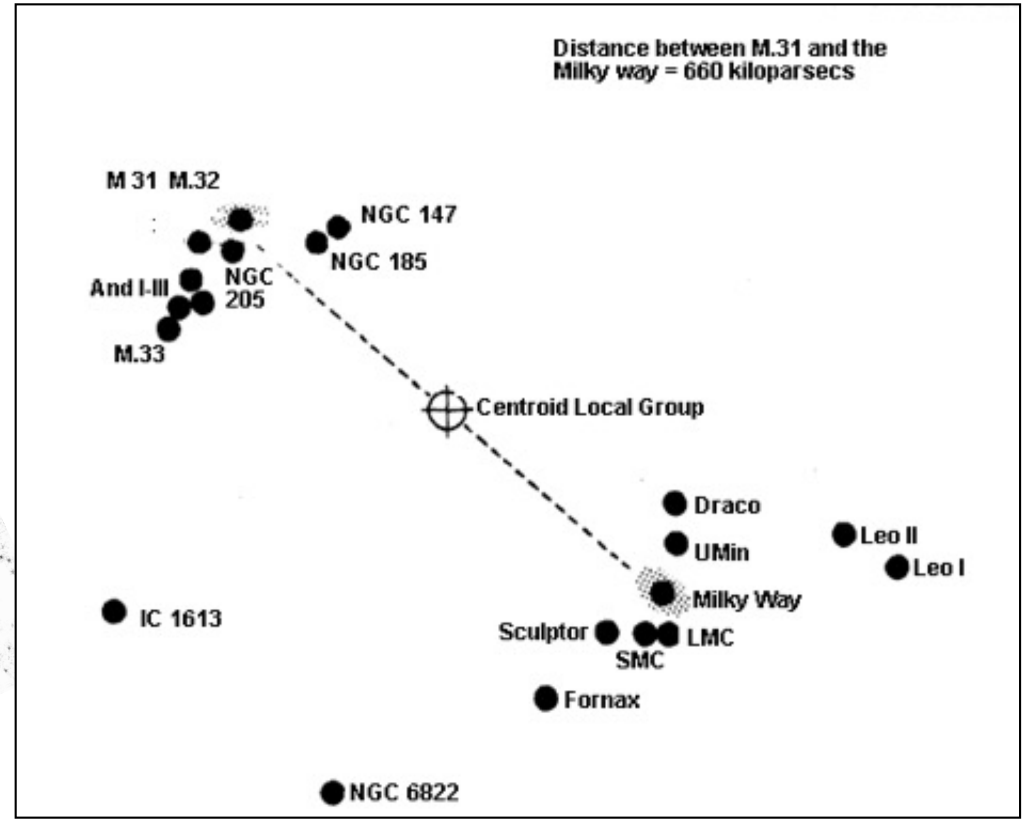

> 1000 subhaloes simulated

ca. 50 satellites observed

- **strong lensing** - the "missing satellite problem"

maybe detectable via lensing!?

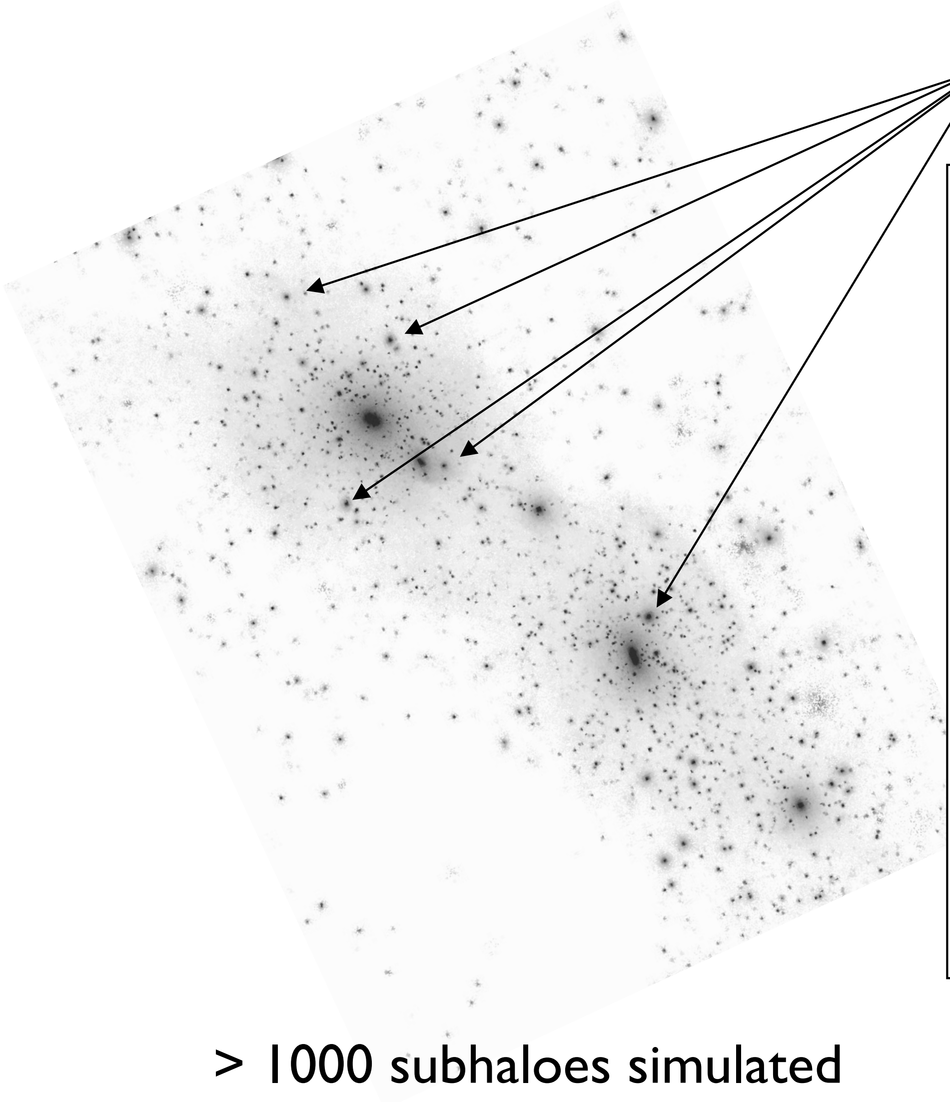

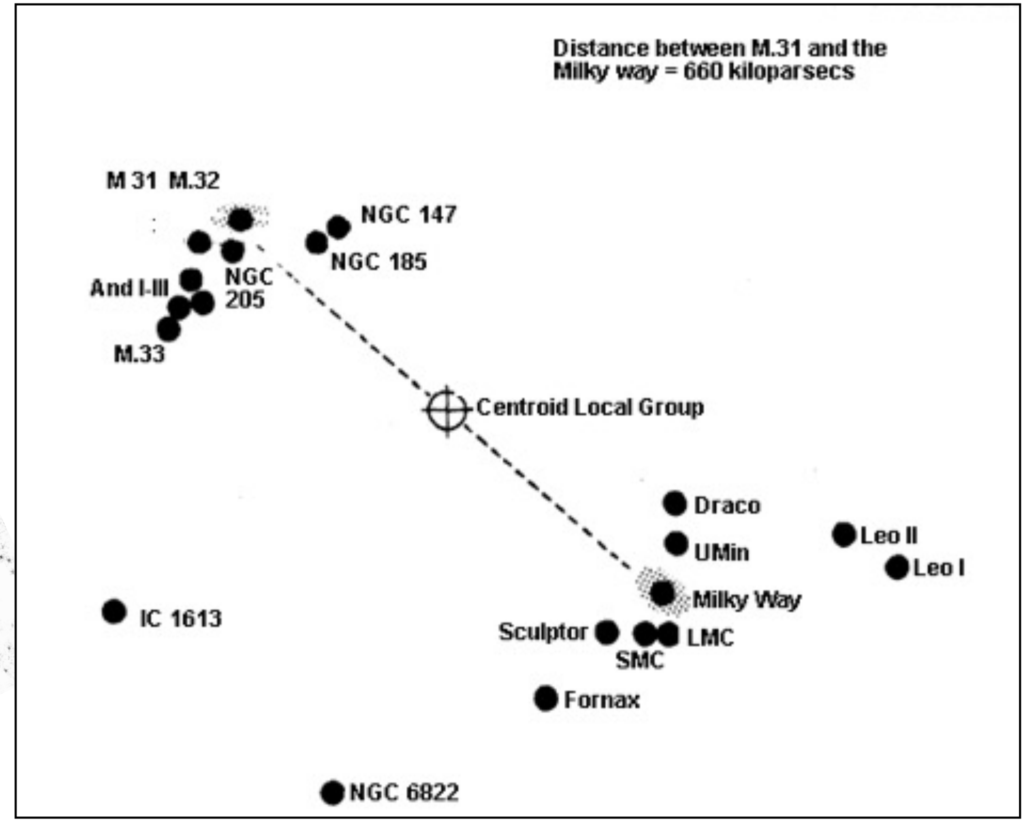

> 1000 subhaloes simulated

ca. 50 satellites observed

- **strong lensing** - the "missing satellite problem"

ray only lensed by cluster

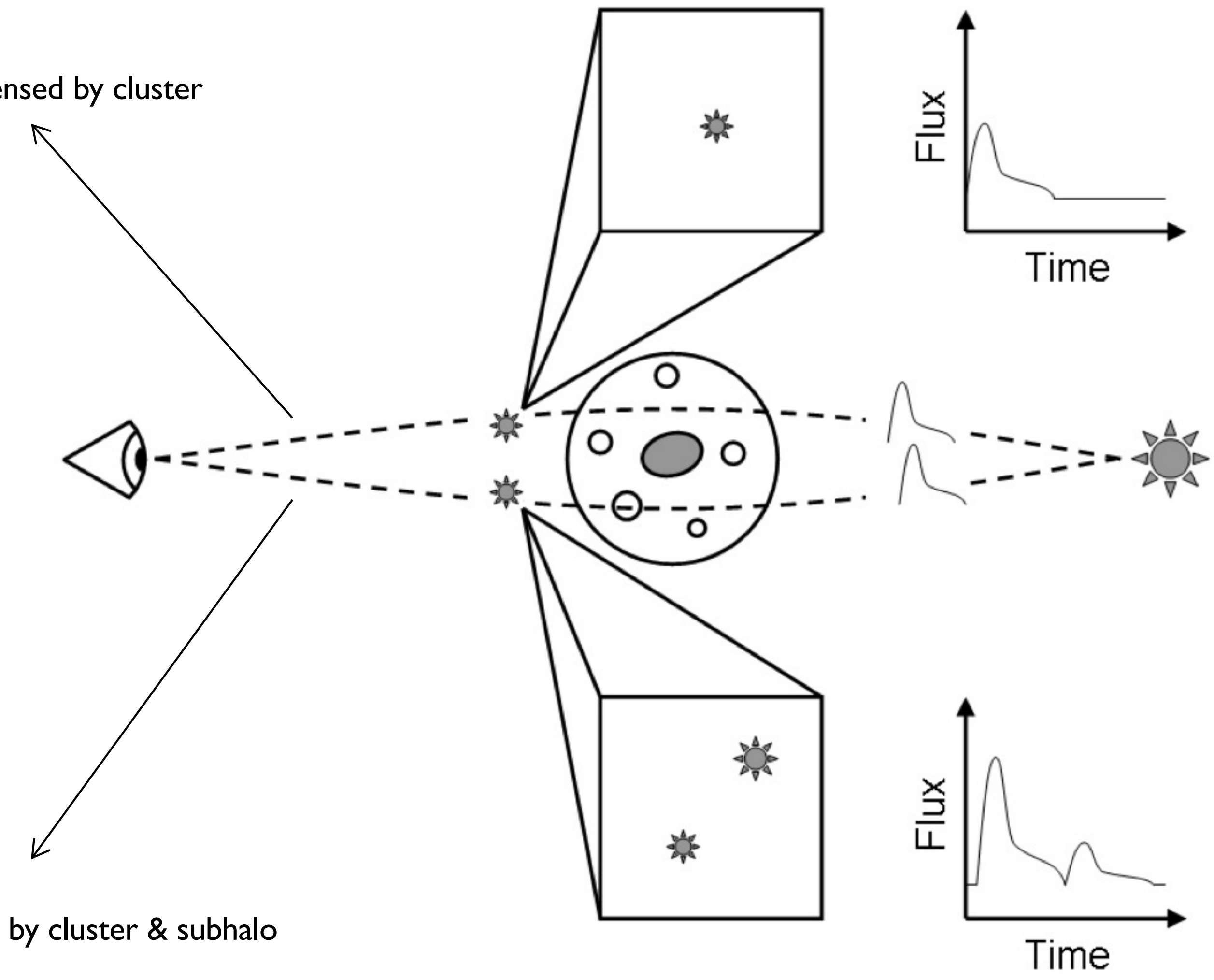

ray lensed by cluster & subhalo

Zackrisson & Riehm (2009)

- **strong lensing** - the "missing satellite problem"

  - presence of substructure can cause…

    …flux ratio anomalies

    …astrometric effects

    …time-delay effects

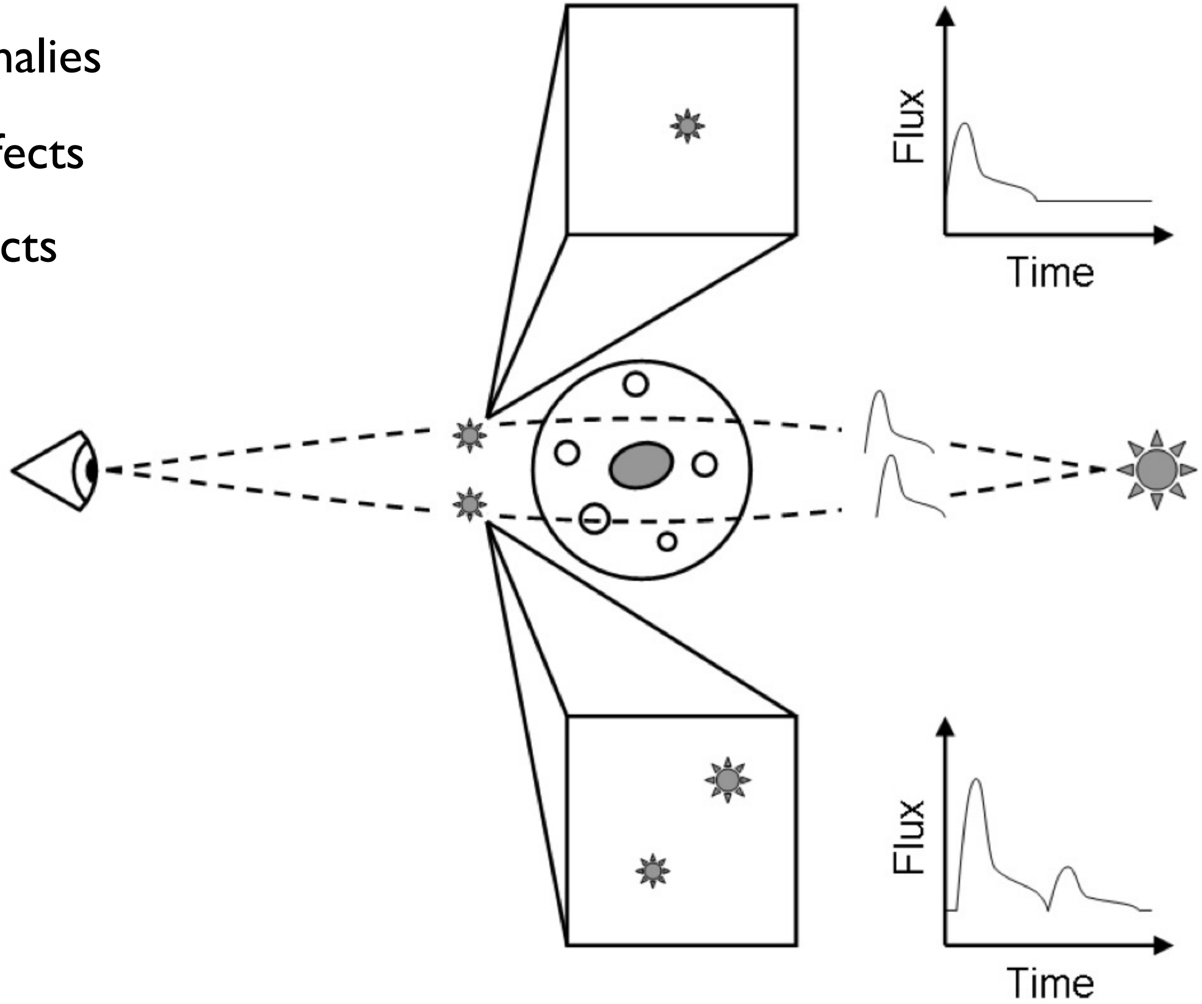

Zackrisson & Riehm (2009)

- **strong lensing** - the "missing satellite problem"
  - presence of substructure can cause…

    …flux ratio anomalies

    …astrometric effects

    …time-delay effects

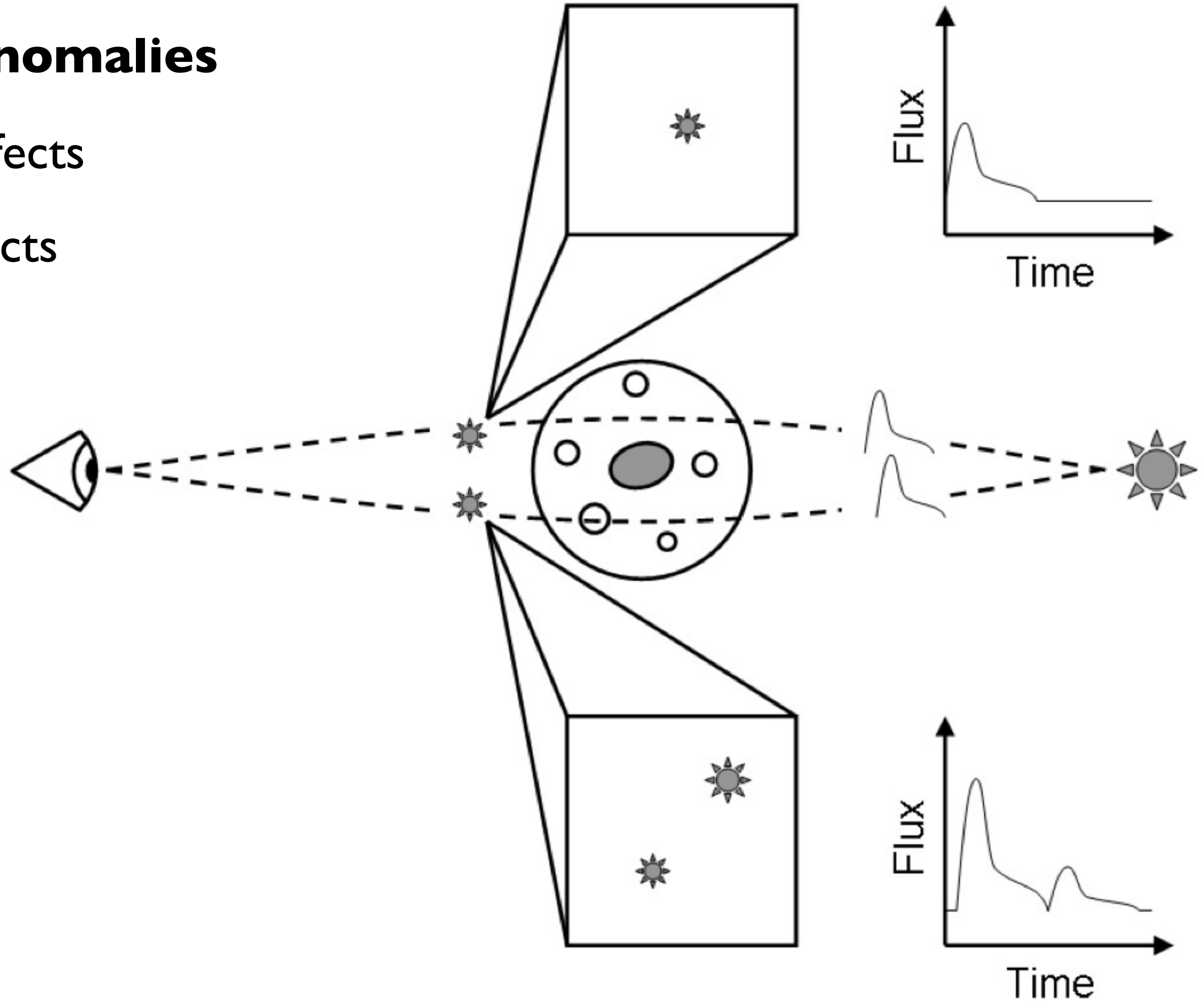

Zackrisson & Riehm (2009)

- **strong lensing** - the "missing satellite problem"
  - anomalous flux ratio are (frequently) observed…

A, B, C, and D are images of a background source

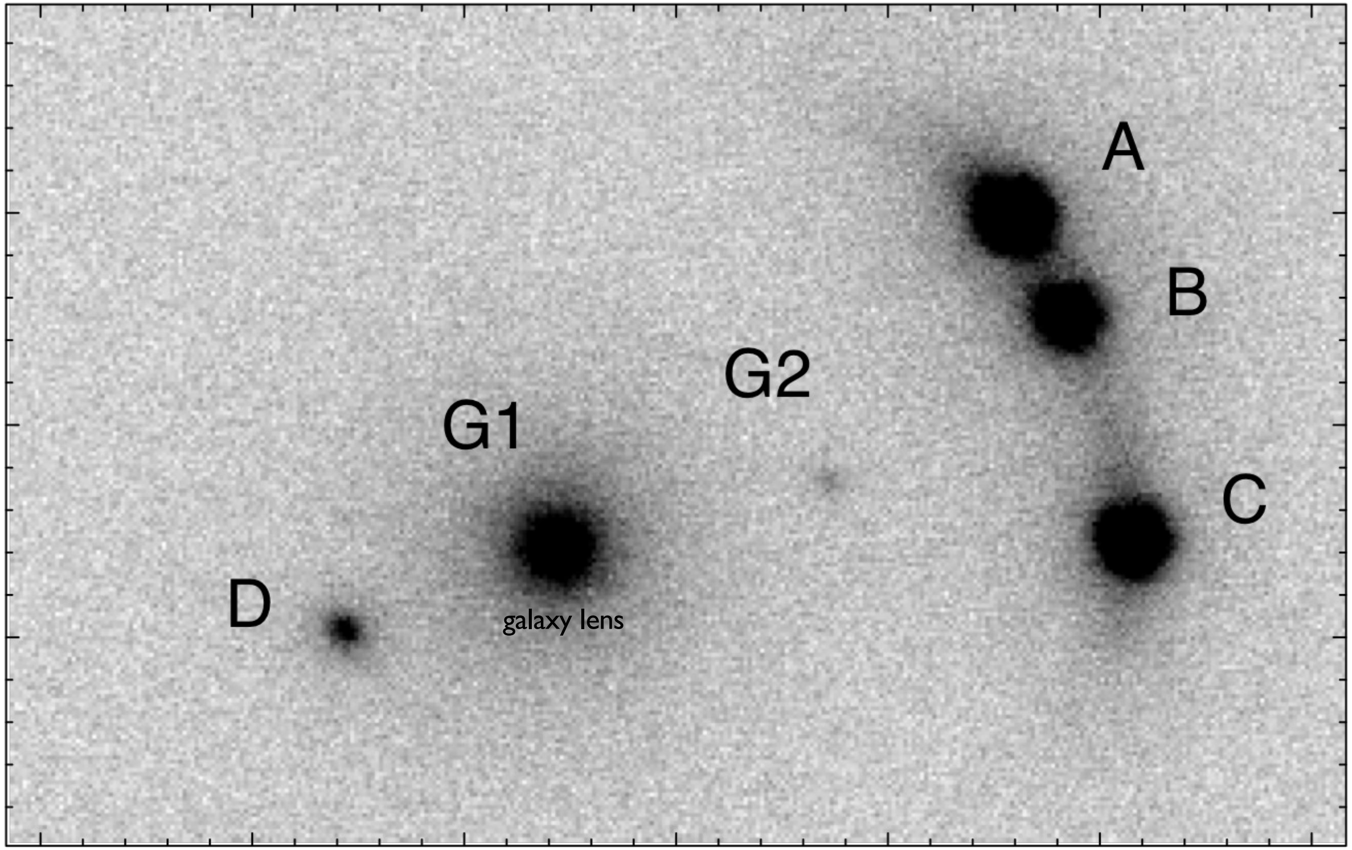

B2045+265 (McKean et al. 2007)

- **strong lensing** - the "missing satellite problem"
  - anomalous flux ratio are (frequently) observed…

A, B, C, and D are images of a background source, but...

...image A is brighter than B, even though a smooth lens model predicts the opposite

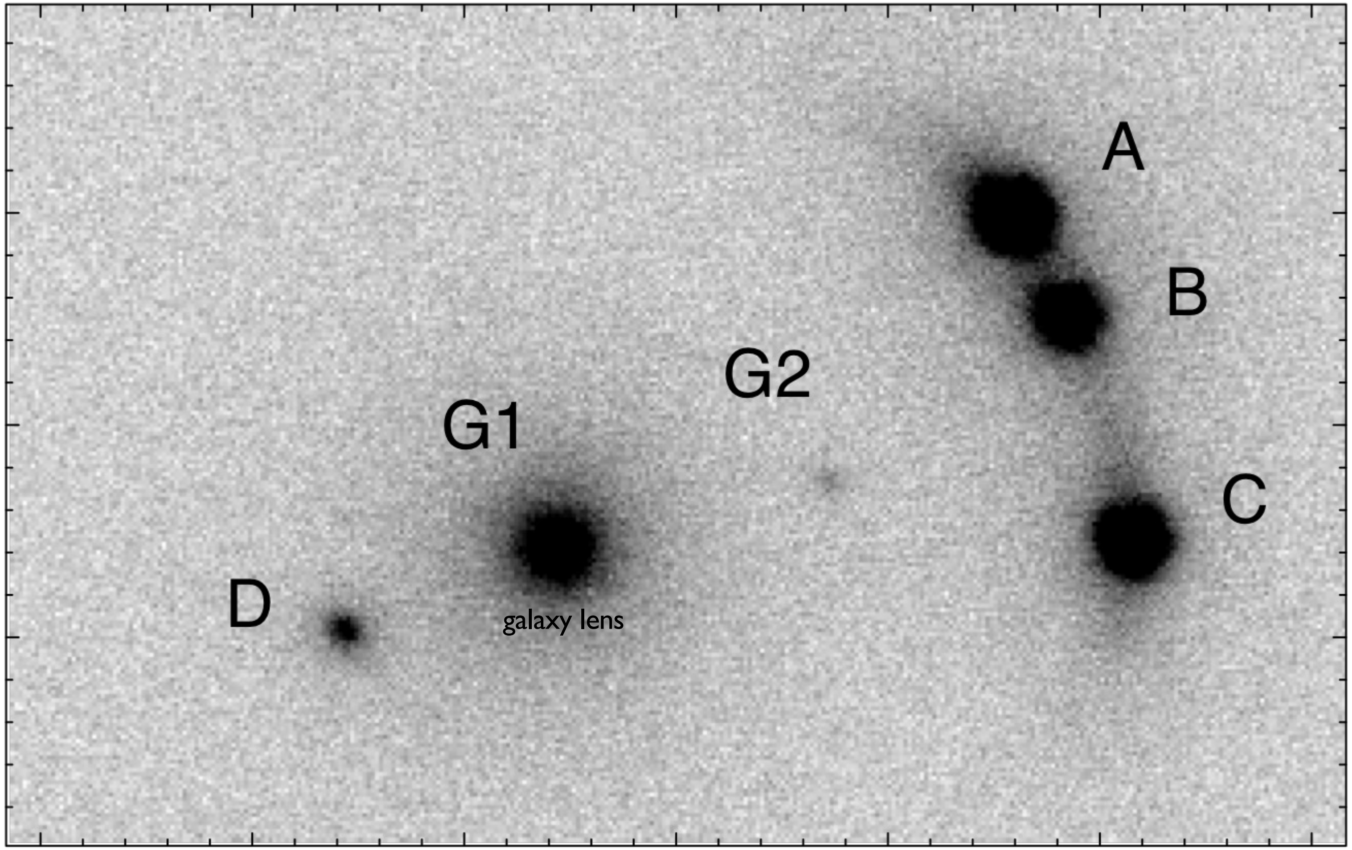

B2045+265 (McKean et al. 2007)

- **strong lensing** - the "missing satellite problem"
  - anomalous flux ratio are (frequently) observed…

A, B, C, and D are images of a background source, but...

...image A is brighter than B, even though a smooth lens model predicts the opposite

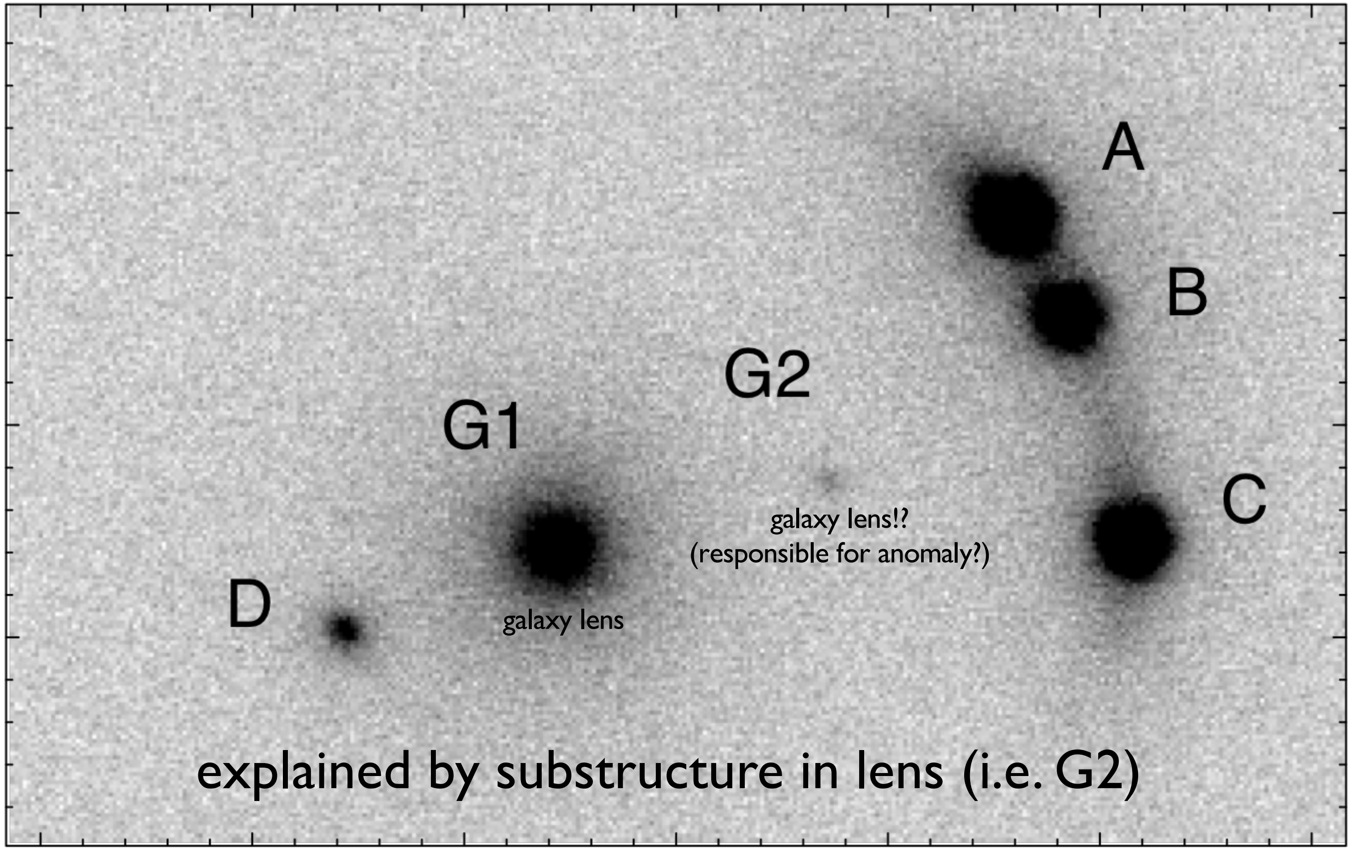

B2045+265 (McKean et al. 2007)

- **strong lensing** - the "missing satellite problem"

  • anomalous flux ratio are (frequently) observed, but in general…

…there are too few subhaloes (in the central region) to explain the observed signal!?

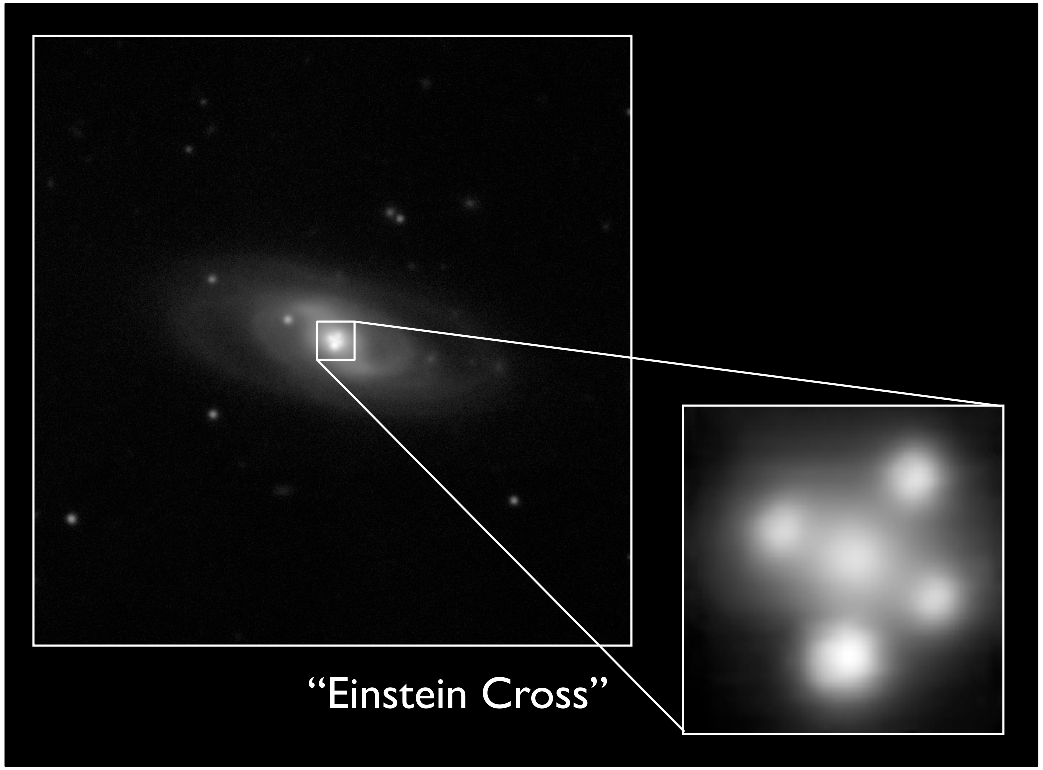

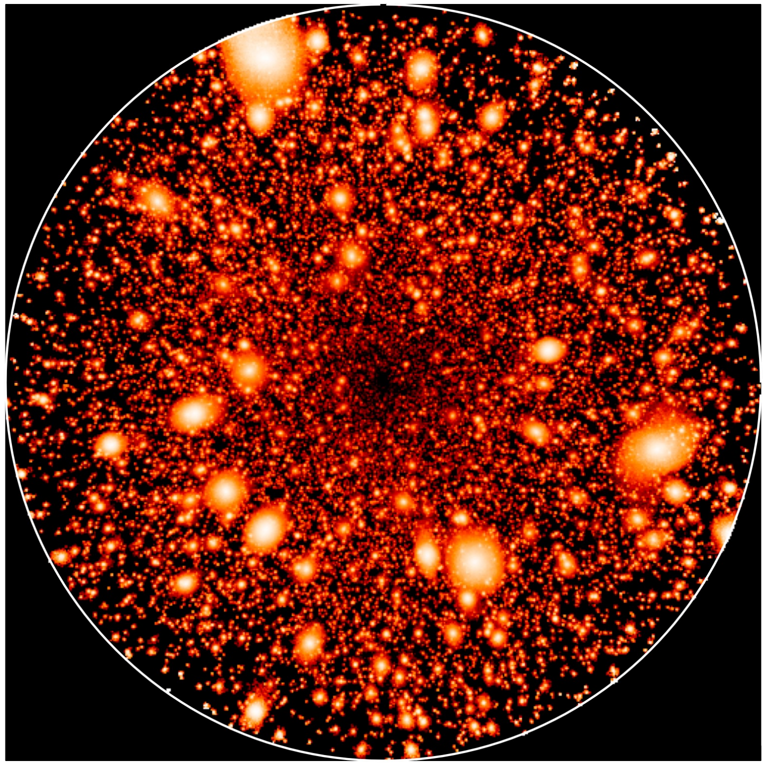

Xu et al., astro-ph/0903.4559 (Aquarius simulation)

▪ **strong le**

• anomal … general…

…there … l region)

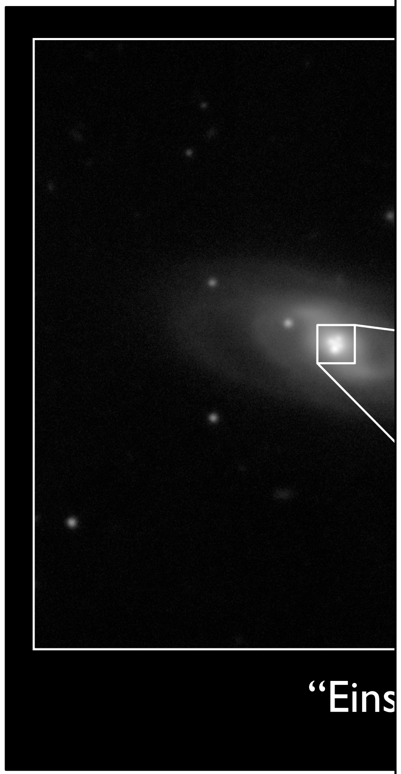

Meneghetti et al. (2020)

COSMOLOGY

An excess of small-scale gravitational lenses observed in galaxy clusters

Massimo Meneghetti[1,2,3]*, Guido Davoli[1,4], Pietro Bergamini[1], Piero Rosati[5,1], Priyamvada Natarajan[6], Carlo Giocoli[1,5,7], Gabriel B. Caminha[8], R. Benton Metcalf[7], Elena Rasia[9,10], Stefano Borgani[9,10,11,12], Francesco Calura[1], Claudio Grillo[13,14], Amata Mercurio[15], Eros Vanzella[1]

Cold dark matter (CDM) constitutes most of the matter in the Universe. The interplay between dark and luminous matter in dense cosmic environments, such as galaxy clusters, is studied theoretically using cosmological simulations. Observations of gravitational lensing are used to characterize the properties of substructures—the small-scale distribution of dark matter—in clusters. We derive a metric, the probability of strong lensing events produced by dark-matter substructure, and compute it for 11 galaxy clusters. The observed cluster substructures are more efficient lenses than predicted by CDM simulations, by more than an order of magnitude. We suggest that systematic issues with simulations or incorrect assumptions about the properties of dark matter could explain our results.

In the standard cosmological model, the matter content of the Universe is dominated by cold dark matter (CDM), collisionless particles that interact with ordinary matter (baryons) only through gravity. Gravitationally bound dark-matter halos form hierarchically, with the most massive systems forming through mergers of smaller ones. As structure assembles in this fashion, large dark-matter halos contain smaller-scale substructure in the form of embedded subhalos.

The most massive dark-matter halos at the present time are galaxy clusters, with masses of $\sim 10^{14}$ to $\sim 10^{15}$ solar masses ($M_\odot$, one solar mass is $\sim 2 \times 10^{30}$ kg). Galaxy clusters contain about a thousand member galaxies that are hosted in subhalos. The detailed spatial distribution of dark matter in galaxy clusters can be mapped by observing gravitational lensing of distant background galaxies. When distant background galaxies are in near perfect alignment with the massive foreground cluster, strong gravitational lensing occurs. Strong lensing—nonlinear effects produced by the deflection of light—results in multiple distorted images of individual background galaxies that can be detected in Hubble Space Telescope (HST) imaging.

The probability and strength of these nonlinear strong lensing effects can be predicted theoretically from simulations of structure formation (*1*). We test these predictions using observations of galaxy clusters, combining lensing data from the HST with spectroscopic data from the Very Large Telescope (VLT). Our observed sample of lensing clusters is split into three sets for this analysis: (i) a reference sample comprising three clusters with well-constrained mass distributions (mass models): MACS J1206.2-0847 (MACSJ1206) at redshift $z = 0.439$, MACS J0416.1-2403 (MACSJ0416) at $z = 0.397$, and Abell S1063 (AS1063) at $z = 0.348$ (*2*–*6*); (ii) a sample that includes the publicly available mass models for four Hubble Frontier Fields clusters [HFF, (*7*)], namely Abell 2744 at $z = 0.308$, Abell 370 at $z = 0.375$, MACS J1149.5+2223 (MACSJ1149) at $z = 0.542$, and MACS J0717.5+3745 (MACSJ0717) at $z = 0.545$; and (iii) four clusters from the Cluster Lensing and Supernova Survey with Hubble [CLASH, (*8*)] project, with recent mass reconstructions [(*9*), their "Gold" sample]: RX J2129.7+0005 (RXJ2129) at $z = 0.234$, MACS J1931.8-2635 (MACSJ1931) at $z = 0.352$, MACS J0329.7-0211 (MACSJ0329) at $z = 0.450$, and MACS J2129.4-0741 (MACSJ2129) at $z = 0.587$. A color-composite image of MACSJ1206, one of the clusters in our reference sample (i), is shown in Fig. 1. Images of the other clusters are shown in figs. S1 to S3.

Owing to their large masses, all these galaxy clusters act as strong lenses, producing multiple images of numerous background galaxies. To reconstruct their mass distributions, we combine the images with available spectroscopic data (*3*, *10*). For each cluster, the membership of hundreds of galaxies is confirmed spectroscopically, and their redshifts have been measured. The spectroscopy has also allowed identification of tens of multiply imaged background sources per cluster.

Mass models for the reference cluster sample were constructed by using the publicly available parametric lens inversion code LENSTOOL (*11*) and published previously (*6*). Clusters were modeled as a superposition of large-scale components to account for the large-scale cluster dark-matter halos, and small-scale components that describe the substructure. We associate the spatial positions of cluster member galaxies with the locations of dark-matter substructure. The detailed mass distribution in these cluster galaxies is constrained using stellar kinematics measurements of cluster member galaxies from the VLT spectroscopy.

The mass models for the clusters in the other two samples are built similarly (*12*); however, unlike the reference sample, the mass distribution in the cluster member galaxies is not constrained using data from stellar kinematics. For the HFF sample, a suite of lensing mass models constructed independently by several groups are publicly available from the Mikulski Archive for Space Telescopes (MAST); we used only those built using LENSTOOL for consistency [e.g., (*13*, *14*)]. For the "Gold" sample, we use published models (*9*) that were also built with LENSTOOL.

The multiple images of distant sources lensed by foreground galaxy clusters have angular separations of several tens of arcseconds. The most distorted gravitational arcs occur near lines that enclose the inner regions of the cluster, referred to as critical lines, which delineate the region where strong lensing occurs. The size of the critical lines depends on the redshifts of the background sources. Substructures within each cluster act as smaller-scale gravitational lenses embedded within the larger lens. If these substructures are massive enough and compact enough, they can also produce additional local strong lensing events on much smaller scales with separations of less than a few arcseconds. These small-scale features are expected to appear around the critical lines produced by individual cluster galaxies. We refer to these localized features as Galaxy-Galaxy Strong Lensing (GGSL) events. Sufficiently high-resolution mass reconstructions are necessary to recover these smaller-scale critical lines. For example, Fig. 1 shows the network of critical lines in MACSJ1206 for two possible source redshifts, $z = 1$ and $z = 7$. The cluster produces a large-scale critical line extending to 15 to 30 arc sec and many smaller-scale critical lines around individual substructures, as shown in the insets. The presence of secondary critical lines indicates that the substructures are centrally concentrated and massive enough to act as individual strong lenses.

[1]Osservatorio di Astrofisica e Scienza dello Spazio di Bologna, Istituto Nazionale di Astrofisica Via Gobetti 93/3, I-40129, Bologna, Italy. [2]National Institute for Nuclear Physics, viale Berti Pichat 6/2, I-40127 Bologna, Italy. [3]Division of Physics, Mathematics, and Astronomy, California Institute of Technology, Pasadena, CA 91125, USA. [4]Centro Euro-Mediterraneo sui Cambiamenti Climatici (CMCC), viale Berti Pichat 6/2, I-40127 Bologna, Italy. [5]Dipartimento di Fisica e Scienza della Terra, Università di Ferrara, via Saragat 1, I-44122 Ferrara, Italy. [6]Department of Astronomy, 52 Hillhouse Avenue, Steinbach Hall, Yale University, New Haven, CT 06511, USA. [7]Dipartimento di Fisica e Astronomia, Università di Bologna, via Gobetti 93/2, 40129 Bologna, Italy. [8]Kapteyn Astronomical Institute, University of Groningen, Postbus 800, 9700 AV Groningen, Netherlands. [9]Osservatorio Astronomico di Trieste, Istituto Nazionale di Astrofisica, Via Tiepolo, 11, I-34131 Trieste, Italy. [10]Institute for Fundamental Physics of the Universe, Via Beirut 2, 34014 Trieste, Italy. [11]Department of Physics, University of Trieste, via Tiepolo 11, I-34131 Trieste, Italy. [12]National Institute for Nuclear Physics, Via Valerio 2, I-34127 Trieste, Italy. [13]Dipartimento di Fisica, Università degli Studi di Milano, via Celoria 16, I-20133 Milano, Italy. [14]Niels Bohr Institute, University of Copenhagen, Lyngbyvej 2, 4. sal 2100 Copenhagen, Denmark.
***Corresponding author. Email: massimo.meneghetti@inaf.it**

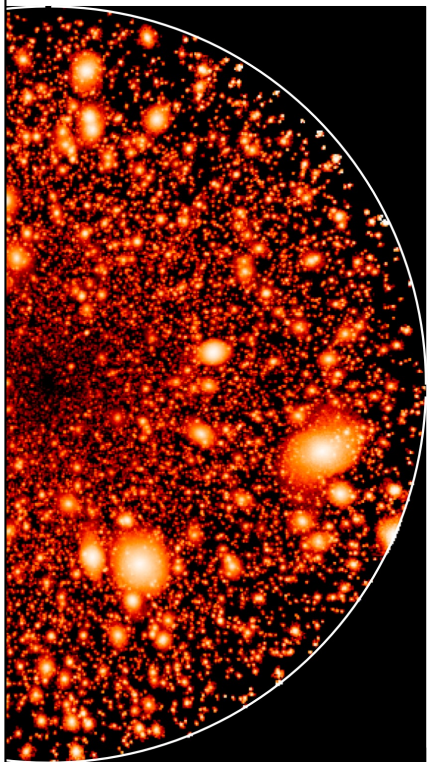

Xu et al., astro-ph/0903.4559 (Aquarius simulation)

- **strong lensing** - the "missing satellite problem"

  - presence of substructure can cause…

    …flux ratio anomalies

    …astrometric effects

    …time-delay effects

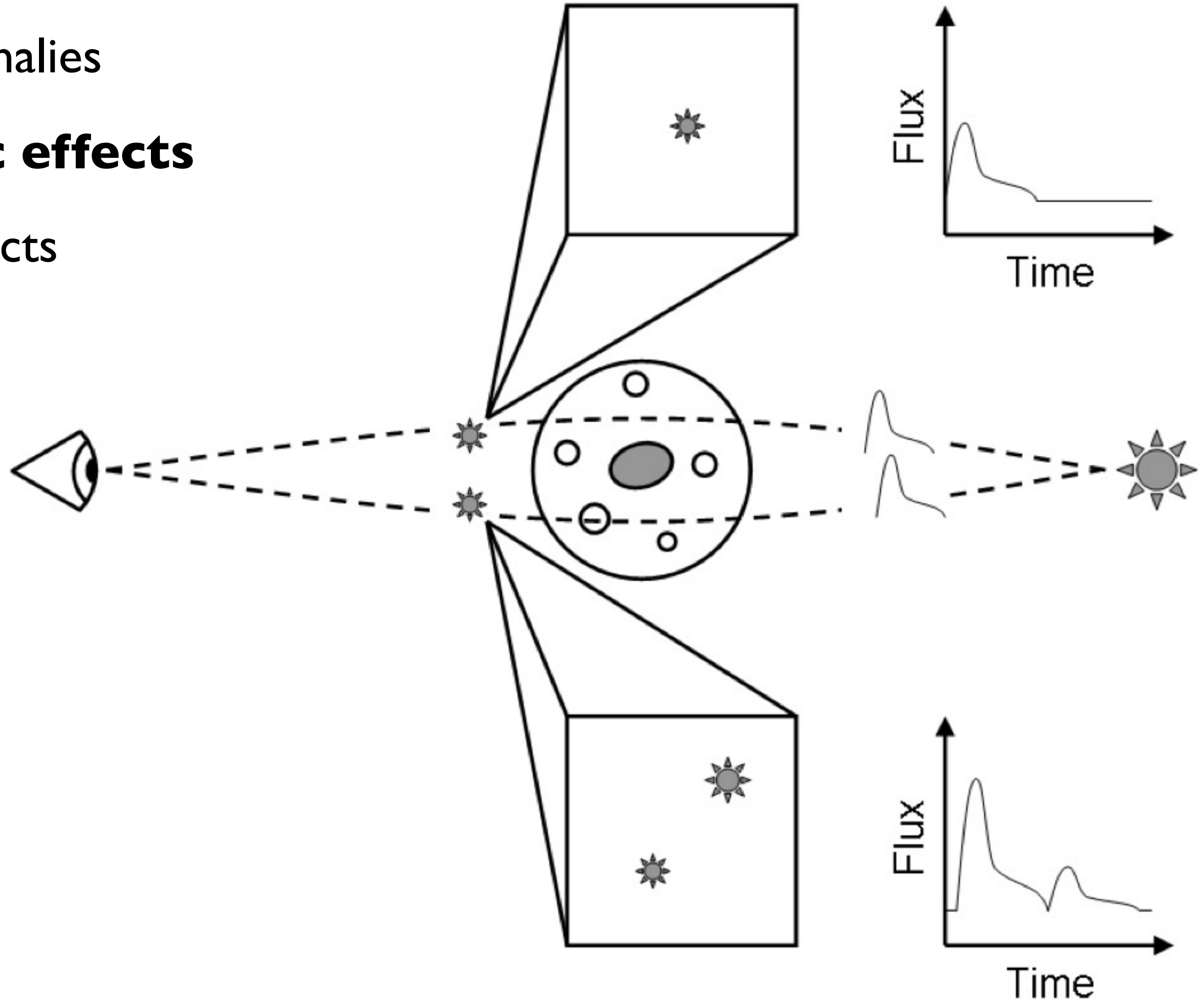

Zackrisson & Riehm (2009)

- **strong lensing** - the "missing satellite problem"

  - astrometric effects…

…produce deflections of a few tens of milliarcsec
(and are therefore difficult to detect!)

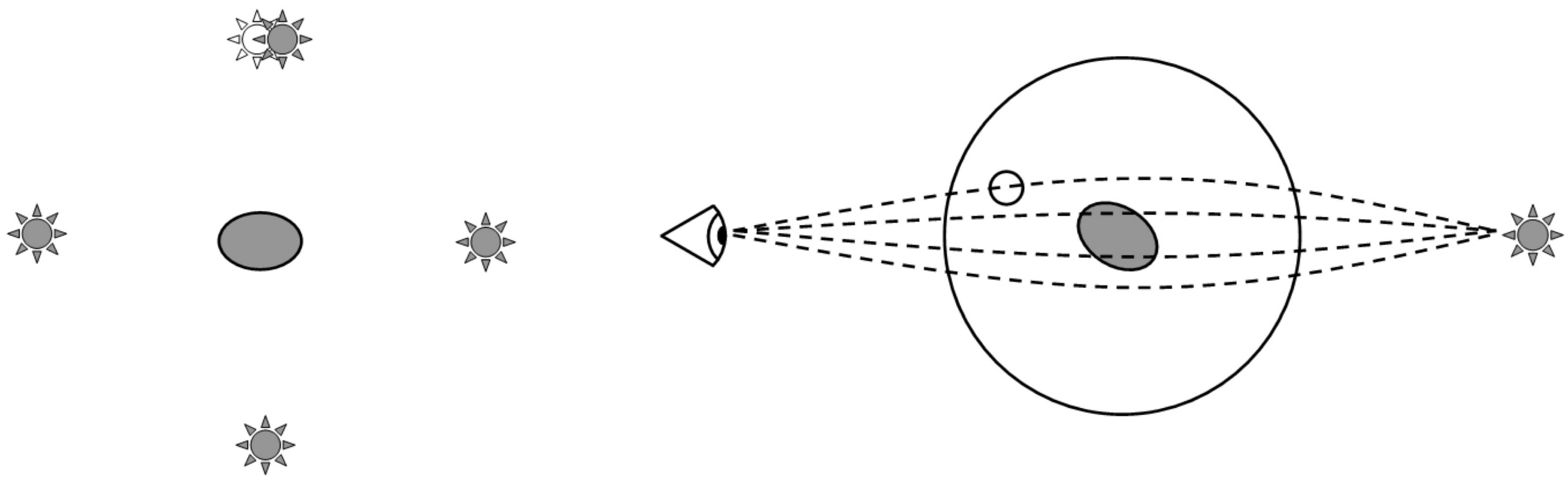

Zackrisson & Riehm (2009)

- **strong lensing** - the "missing satellite problem"

  - presence of substructure can cause…

    …flux ratio anomalies

    …astrometric effects

    …time-delay effects

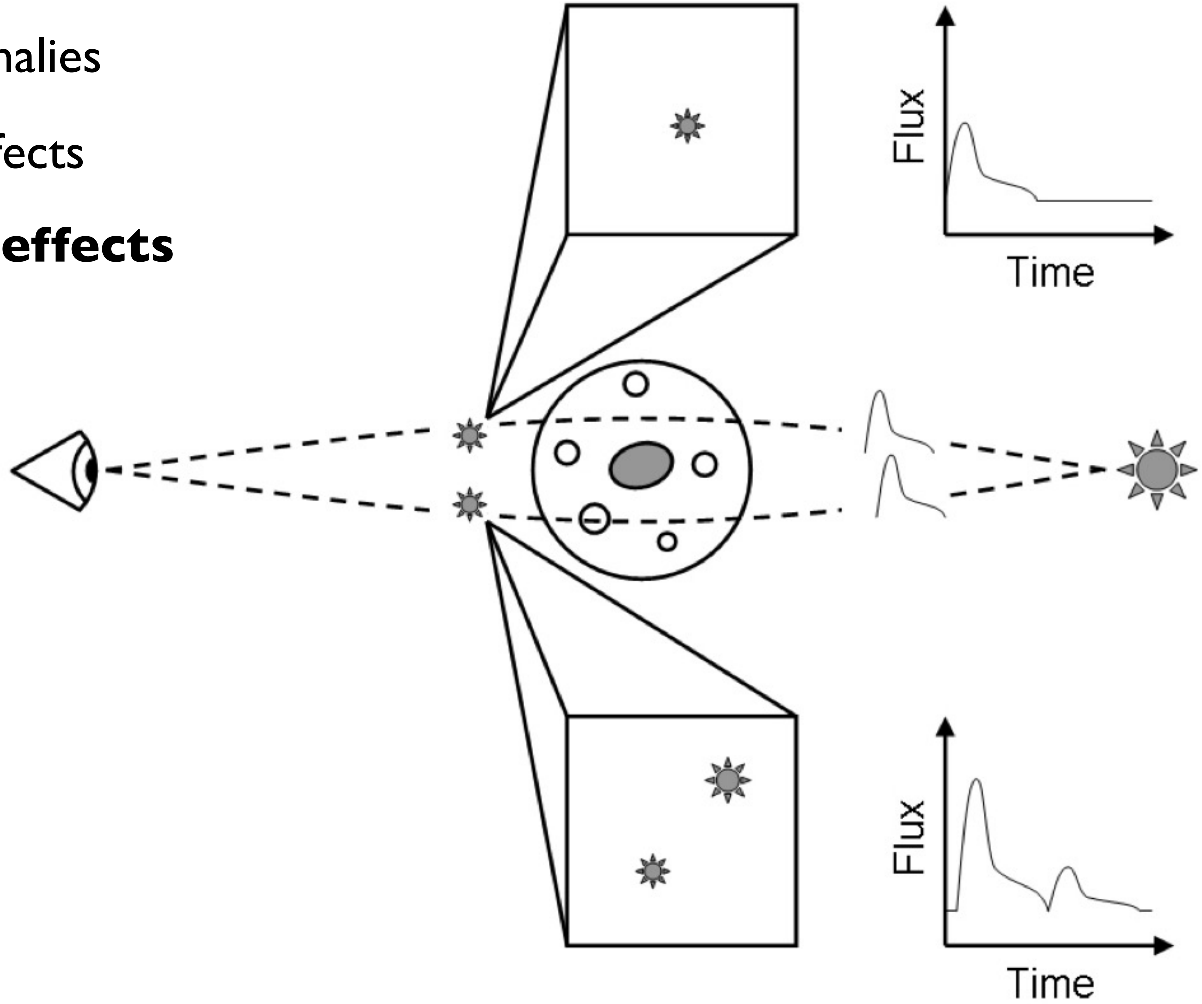

Zackrisson & Riehm (2009)

- **strong lensing** - the "missing satellite problem"

  - time-delay

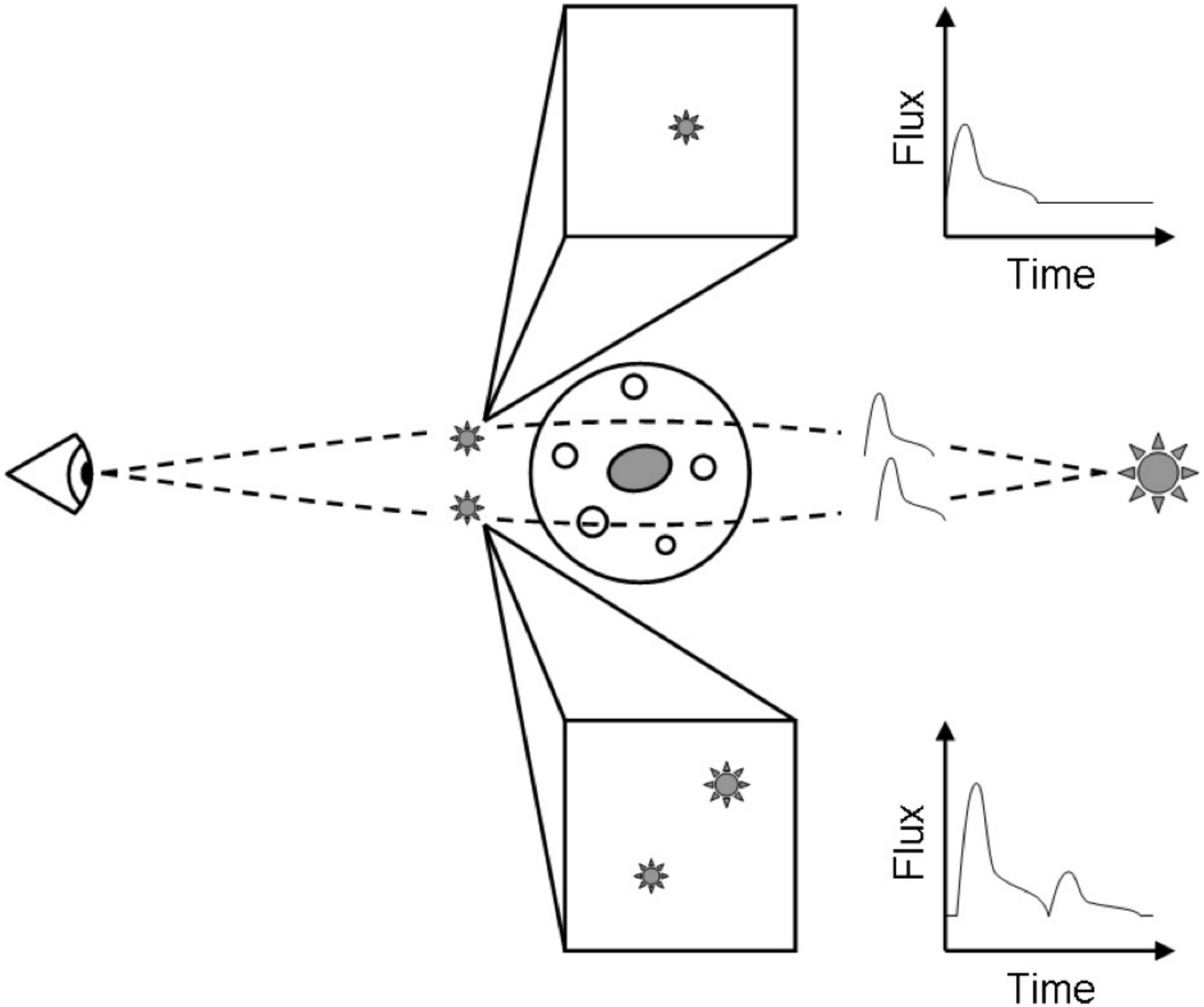

Zackrisson & Riehm (2009)

- **strong lensing** - the "missing satellite problem"
  - time-ordering reversals…

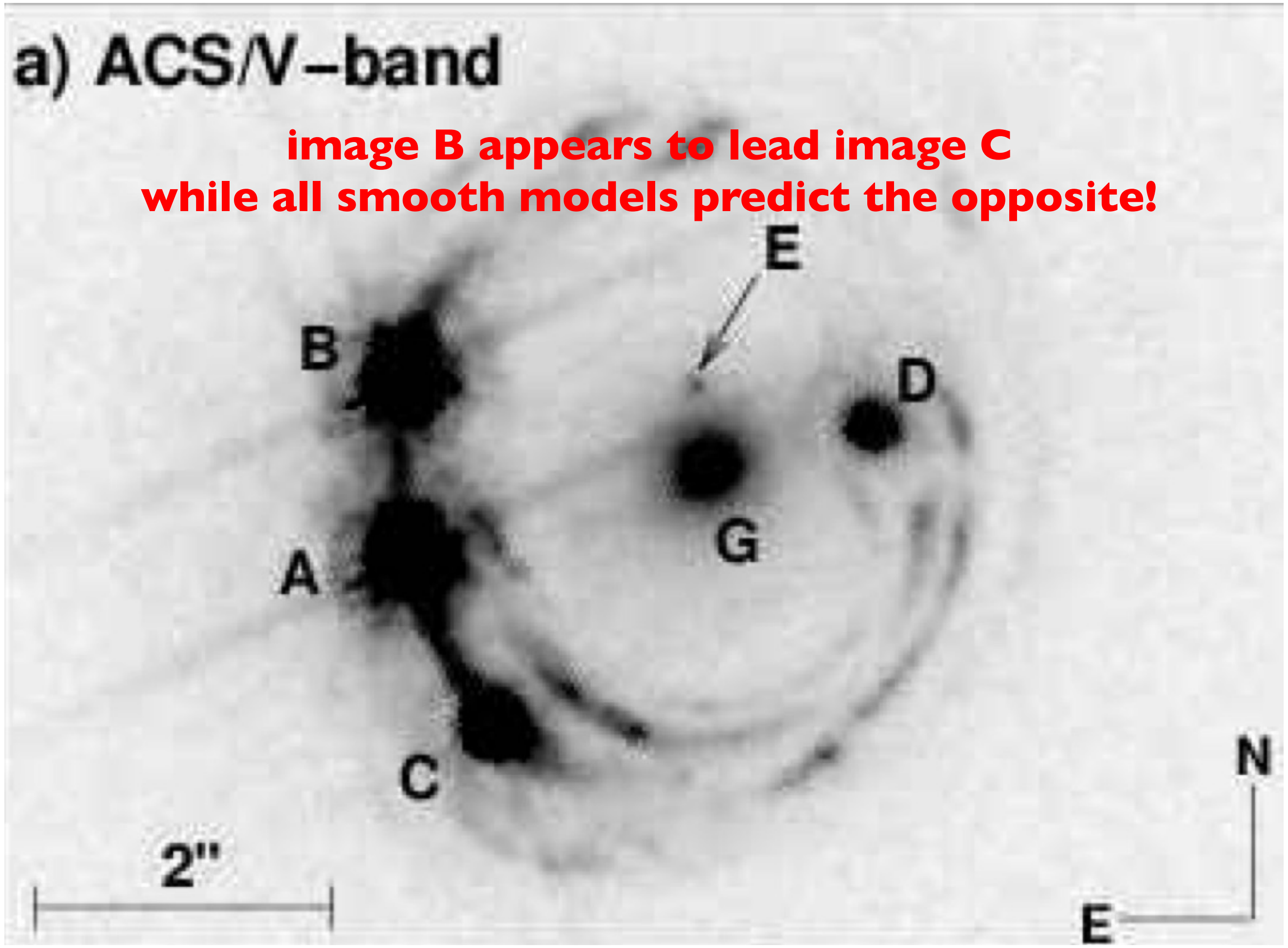

Morgan et al., astro-ph/0605321

- **strong lensing** - the "missing satellite problem"

  - time-ordering reversals…

  …may be explained by the presence of a substructure population

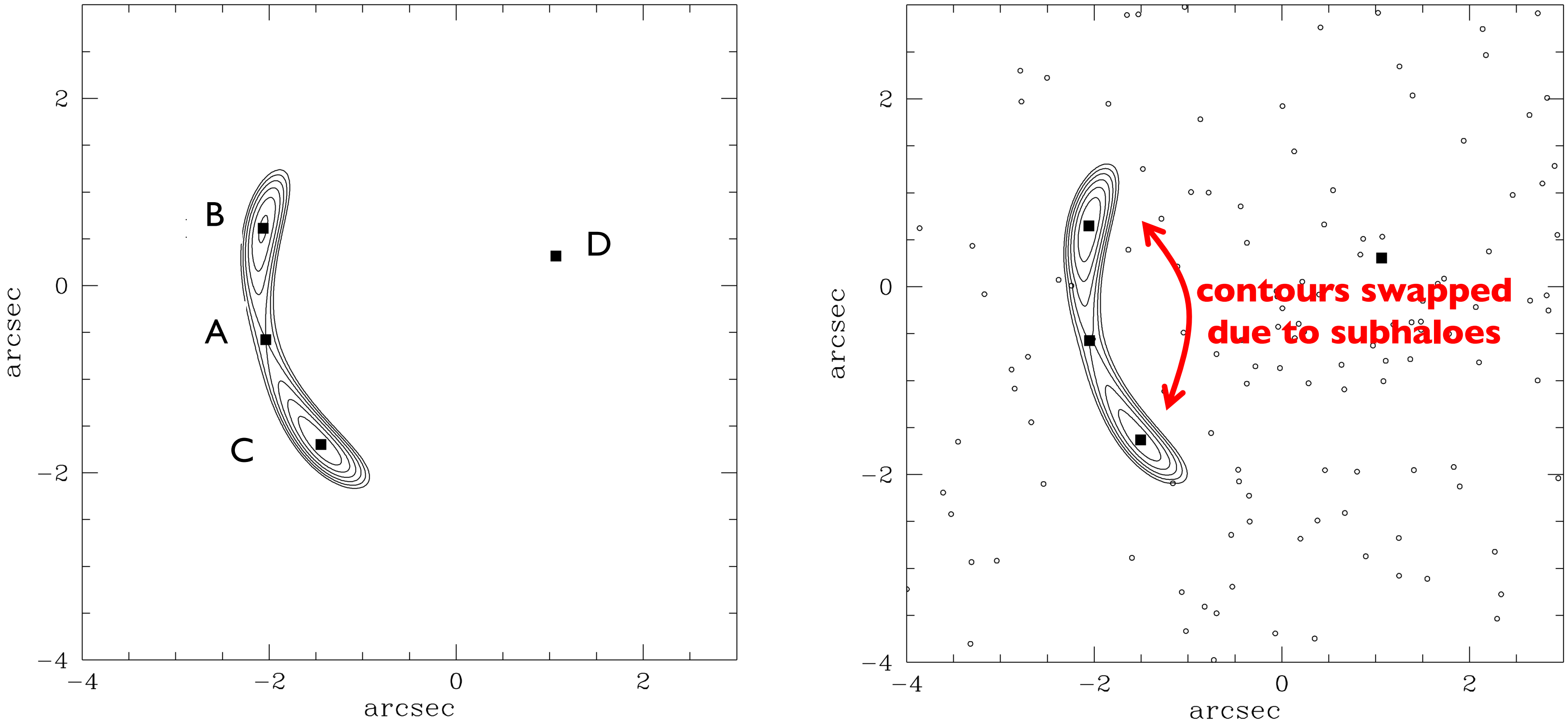

Keeton & Moustakas, astro-ph/0805.0309

- **strong lensing** - the “missing satellite problem”

• flux ratio anomalies	unclear (possibly no?)
• image splitting	upcoming…
• time ordering reversals	possibly

- is all about (resolved) images:

  1. lens mass distribution: *determines type of images*
  2. source location: *determines position of images (and their number)*

- has application in:

  - search for dark matter (substructure)
  - planet detection
  - determination of H_0
  - mass modelling of lens' mass distrribution
  - ...

Alexander Knebe, *Universidad Autonoma de Madrid*